

UNCLASSIFIED

AD NUMBER

AD219888

LIMITATION CHANGES

TO:

**Approved for public release; distribution is
unlimited.**

FROM:

**Distribution authorized to U.S. Gov't. agencies
and their contractors;
Administrative/Operational Use; JUN 1958. Other
requests shall be referred to Army Engineer
Waterways Experimental Station, Vicksburg, MS.**

AUTHORITY

USAEWES ltr 19 Mar 1973

THIS PAGE IS UNCLASSIFIED

UNCLASSIFIED

AZ15888

Armed Services Technical Information Agency

**ARLINGTON HALL STATION
ARLINGTON 12 VIRGINIA**

**FOR
MICRO-CARD
CONTROL ONLY**

11 OF 3

**NOTICE: WHEN GOVERNMENT OR OTHER DRAWINGS, SPECIFICATIONS OR OTHER DATA
ARE USED FOR ANY PURPOSE OTHER THAN IN CONNECTION WITH A DEFINITELY RELATED
GOVERNMENT PROCUREMENT OPERATION, THE U. S. GOVERNMENT THEREBY INCURS
NO RESPONSIBILITY, NOR ANY OBLIGATION WHATSOEVER; AND THE FACT THAT THE
GOVERNMENT MAY HAVE FORMULATED, FURNISHED, OR IN ANY WAY SUPPLIED THE
SAID DRAWINGS, SPECIFICATIONS, OR OTHER DATA IS NOT TO BE REGARDED BY
IMPLICATION OR OTHERWISE AS IN ANY MANNER LICENSING THE HOLDER OR ANY OTHER
PERSON OR CORPORATION, OR CONVEYING ANY RIGHTS OR PERMISSION TO MANUFACTURE,
USE OR SELL ANY PATENTED INVENTION THAT MAY IN ANY WAY BE RELATED THERETO.**

UNCLASSIFIED

CONFIDENTIAL

TO - Unclassified - PER AUTHORITY LISTED IN

ASTIA TAB NO. - U59-18 -

DATE - 15, Sept. 59

R

AD No. 301367

ASTIA FILE copy

This document is the property of the United States
Government. It is furnished for the duration of the contract and
shall be returned when no longer required, or upon
recall by ASTIA to the following address:

Armed Services Technical Information Agency, Arlington Hall Station,
Arlington 12, Virginia

**NOTICE: THIS DOCUMENT CONTAINS INFORMATION AFFECTING THE
NATIONAL DEFENSE OF THE UNITED STATES WITHIN THE MEANING
OF THE ESPIONAGE LAWS, TITLE 18, U.S.C., SECTIONS 793 AND 794.
THE TRANSMISSION OR THE REVELATION OF ITS CONTENTS IN
ANY MANNER TO AN UNAUTHORIZED PERSON IS PROHIBITED BY LAW.**

AD-219888

~~CONFIDENTIAL~~

CRATERING EFFECTS OF SURFACE AND BURIED HE CHARGES IN LOESS AND CLAY



TECHNICAL REPORT NO. 2-482

June 1958

.....
• Regraded UNCLASSIFIED by 1st Ind .
• fm OCE (ENGNB) dtd 9 June 1959 .
• to WES Bsc ltr of 1 June 1959. .
• subject: "Declassification of .
• Report, 'Cratering Effects of .
• Surface and Buried HE Charges' .
• (U)." *DR 9/16/59* .
.....

U. S. Army Engineer Waterways Experiment Station
CORPS OF ENGINEERS
Vicksburg, Mississippi

ARMY MRC VICKSBURG - MISS.

~~CONFIDENTIAL~~

This document has been approved
for public release and sale; its
distribution is unlimited.

W34
No. 2-482
Cop. 3

~~CONFIDENTIAL~~

ii Blank

iii

Preface

The data reported herein were obtained during the experimental phase of a study authorized by the Office, Chief of Engineers (OCE), as a part of R&D Project 8-12-10-C01, "Effects of Nuclear Weapons on Terrain and Engineering Structures" (fiscal year 1957). During fiscal year 1958 it is anticipated that these data, in a more extensive form, will be applied by Mr. C. W. Livingston, of Barodynamics, Inc., to his empirical approach to the cratering problem and that the conclusions reached by Mr. Livingston will be published later. In order to make the test results available at an earlier date, it is believed desirable to publish them in a form considered more or less conventional for presenting cratering-type research.

The experimental tests, along with the data reduction, were accomplished during the period March 1956-May 1957 by personnel of the Hydraulics Division, U. S. Army Engineer Waterways Experiment Station (USAEWES), under the general supervision of Messrs. E. P. Fortson, Jr., and F. R. Brown. The study was made by personnel of the Special Investigations Section under the direction of Mr. G. L. Arbuthnot, Jr., assisted by Mr. J. N. Strange. Test operations and data analysis were performed by Messrs. J. M. Pinkston, Jr., and S. E. Bartlett.

The comments and suggestions of Mr. C. W. Livingston, during the early phase of the test program, are gratefully acknowledged.

33048

~~CONFIDENTIAL~~

Contents

	<u>Page</u>
Preface	iii
Notations	vii
Summary	ix
Introduction	1
Test Conditions	1
Properties of the loess and clay materials	1
Test charges	2
Test Procedures	3
Test Data	3
Discussion of Test Results	9
Variables that affect cratering	9
Effect of soil type	9
Effect of charge position on cratering	10
Effect of charge position on camouflet	13
Investigation of the Permanent Radial Displacement	15
Conclusions	16
List of References	18
Tables 1-4	
Plates 1-47	

Notations

d_a	Apparent crater depth, ft
d'_a	$d_a/W^{1/3}$, ft/lb $^{1/3}$
d_t	True crater depth, ft
d'_t	$d_t/W^{1/3}$, ft/lb $^{1/3}$
$d'_{t\text{lc}}$	$d_t/W^{1/3}$ in loess or clay, ft/lb $^{1/3}$
$d'_{t\text{sg}}$	$d_t/W^{1/3}$ in sand and gravel, ft/lb $^{1/3}$
D	Diameter of charge, ft
D_c	Average diameter of camouflet, ft
D'_c	$D_c/W^{1/3}$, ft/lb $^{1/3}$
D_h	Horizontal diameter of camouflet, ft
D'_h	$D_h/W^{1/3}$, ft/lb $^{1/3}$
D_v	Vertical diameter of camouflet, ft
D'_v	$D_v/W^{1/3}$, ft/lb $^{1/3}$
H	Height of charge, ft
V_c	Volume of camouflet, cu ft
V'_c	V_c/W , cu ft/lb
V_t	Volume of true crater, cu ft
V'_t	V_t/W , cu ft/lb
w_a	Apparent crater width, ft
w'_a	$w_a/W^{1/3}$, ft/lb $^{1/3}$
w_t	True crater width, ft
w'_t	$w_t/W^{1/3}$, ft/lb $^{1/3}$
$w'_{t\text{lc}}$	$w_t/W^{1/3}$ in loess or clay, ft/lb $^{1/3}$
$w'_{t\text{sg}}$	$w_t/W^{1/3}$ in sand and gravel, ft/lb $^{1/3}$
W	Weight of charge, lb

- Z Depth of burial of charge, ft
δ Radial displacement along ground surface, ft
 δ' Reduced radial displacement, $\text{ft/lb}^{1/3}$
 λ Reduced horizontal distance from ground zero, $\text{ft/w}^{1/3}$
 λ_c $\text{Z/w}^{1/3}$, $\text{ft/lb}^{1/3}$
 λ_o $\text{Z/w}^{1/3}$ where the true crater volume is a maximum, $\text{ft/lb}^{1/3}$

Summary

This study was made in an effort to evaluate the cratering effects of charges placed both at and below the air-ground interface, with emphasis on the deeply buried charges. Composition C-k charges of 1/8, 1/2, 1, and 8 lb were fired in homogeneous deposits of loess and clay. The resulting craters and camouflets were carefully surveyed by conventional methods. From the test results it was determined that: (a) the optimum charge depth λ occurred within a range of scaled depths of burial such that $-2.5 > \lambda > -2.75$; (b) camouflets were formed in both the loess and clay soils when the scaled depth of burial λ was below approximately -3.2; and (c) the geometry of the camouflets was essentially spherical.

CRATERING EFFECTS OF SURFACE AND BURIED HE CHARGES IN LOESS AND CLAY

Introduction

1. This study was made in an effort to determine the cratering effects of charges positioned both at and below the air-ground interface, with emphasis on the deeply buried charges. A total of 85 shots were fired. The charges were buried at various depths within the range $0 > \lambda_c > -14$. In addition, the permanent radial displacements at the ground surface were also measured.

2. The cratering tests were made in two types of homogeneous soils: loess and clay. The tests in the loess soil were conducted in an area in the northeast portion of the WES reservation. The loess deposits in this locale are extensive and unusually homogeneous. Similar tests in clay^{3*} were accomplished at the WES Big Black test site located about 10 miles southeast of Vicksburg, Mississippi.

Test Conditions

Properties of the loess and clay materials

3. The following tabulation presents the average properties of the loess and clay materials as determined from a number of similar samples. The Atterberg limits were obtained from a total of eight samples, three from the clay material and five from the loess material. Density and moisture-content samples were taken before each shot at a depth corresponding to the depth of burial of the charge. The values listed are the averages of the individual observations:

	Density lb/cu ft	Moisture Content %	Atterberg Limits		
			LL	PL	PI
Clay	117	20.8	43.0	23.0	20.0
Loess	113	19.0	44.8	24.3	20.5

* Raised numerals refer to items in the list of references that follows the text of this report.

The two materials manifested only small variations within the respective test areas. The density samples exhibited a scatter of approximately $\pm 5\%$, while the moisture-content samples showed about 10% variation.

4. The results of mechanical analyses are shown in fig. 1 for both the loess and clay materials. The similarity of grain size is apparent; however, as the plot indicates, the loess is the finer grained of the two materials.

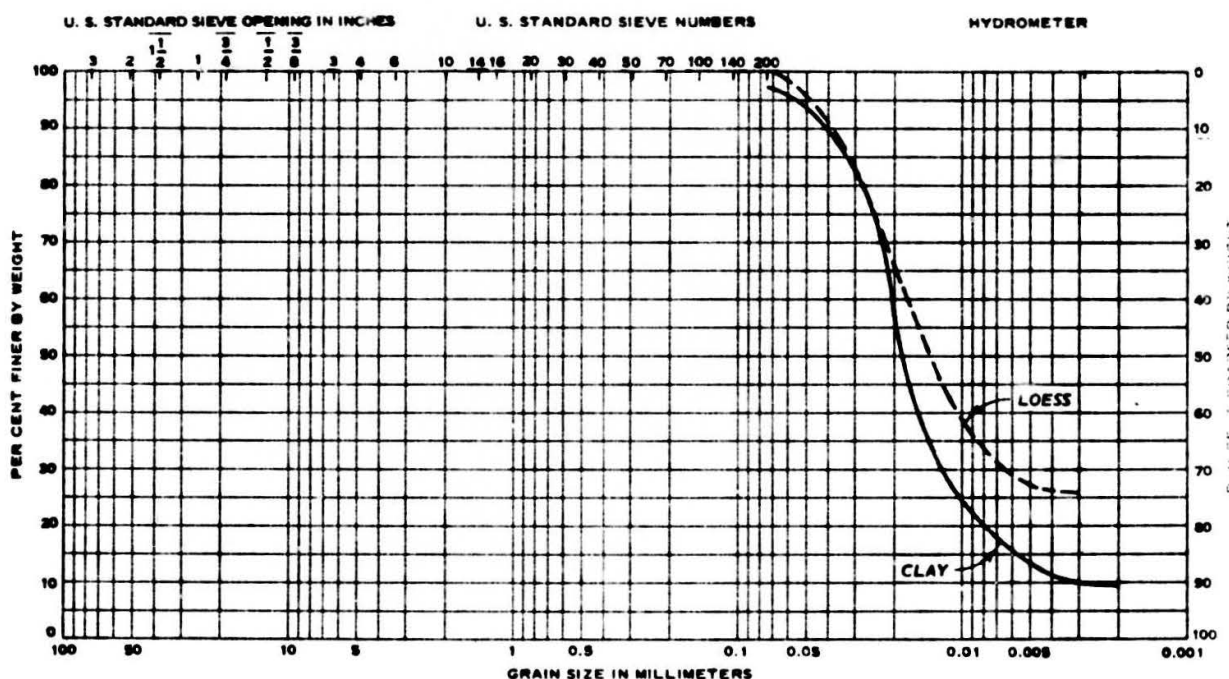


Fig. 1. Gradation of loess and clay soils

Test charges

5. A total of 59 shots were fired in the loess material and 26 in the clay material. All charges were cylindrically shaped and were hand-packed from bulk supply of composition C-4. The various weights and dimensions are described in the following tabulation:

<u>Charge Weight, lb</u>	<u>Dimensions of Charge, ft</u>	
	<u>Height, H</u>	<u>Diameter, D</u>
1/8	0.12	0.12
1/2	0.19	0.19
1	0.24	0.24
8	0.47	0.47

These charges were positioned at reduced depths which varied from $\lambda_c = 0$ to $\lambda_c = -14.0$, the minus sign denoting positions below the air-ground interface.

Test Procedures

6. The holes in the respective materials, in which the charges were placed, were bored to the proper depth ($Z + 1/2 H$) by means of earth augers of various sizes (diameter slightly larger than the corresponding charge diameter). After the charges were placed, the access holes were carefully backfilled by hand-tamping the material to about the same density as the surrounding soil. The charges were then fired using a Corps of Engineers special electric blasting cap as the detonator.

7. Sounding of the resulting crater or camouflet* boundary was accomplished by carefully cutting a trench along a diameter of the crater or camouflet to a depth sufficient to expose the limits of complete rupture. The various profiles (apparent crater, true crater, complete rupture limitations, or camouflet) were then sounded using conventional crater-sounding techniques. These methods have been described in detail in other WES publications.² Crater and camouflet nomenclatures are shown in plates 1 and 2.

Test Data

8. Table 1 lists the dimensions of the craters formed in loess, table 2 presents similar information for clay, and table 3 presents pertinent measurements associated with the camouflets in both loess and clay. Plots of the apparent craters, the true craters, the complete rupture zones (where definable), and the cross-sectional geometry of the camouflets (where applicable) are shown in plates 3-41. Only the half-crater profiles are shown; these, however, were derived as an average of the total profile. The boundaries of the various craters were determined by averaging the appropriate measurements obtained along a diameter of the crater/camouflet. Photographs of typical craters are presented in figs. 2-10.

* The hollow sphere formed underground when a charge is detonated sufficiently deep so that the void created does not breach the surface.

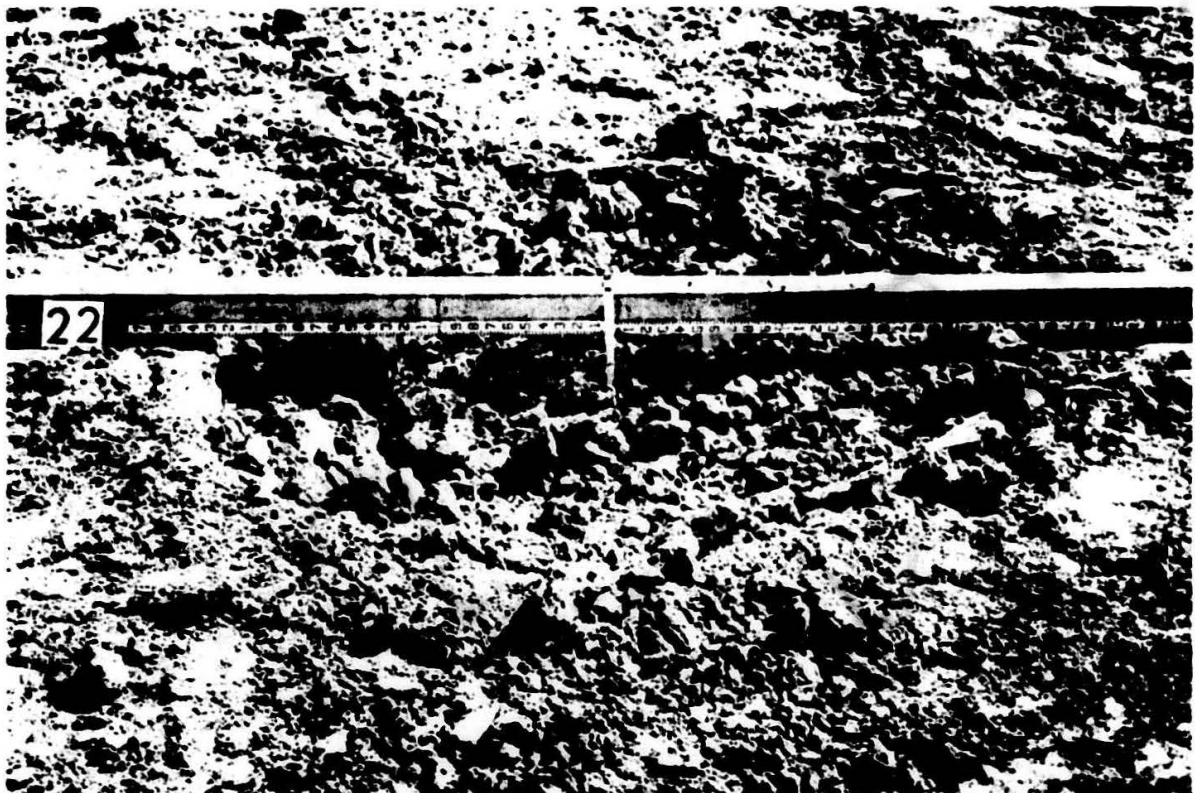


Fig. 2. Before trenching, shot 22 ($\lambda_c = -1.50$)

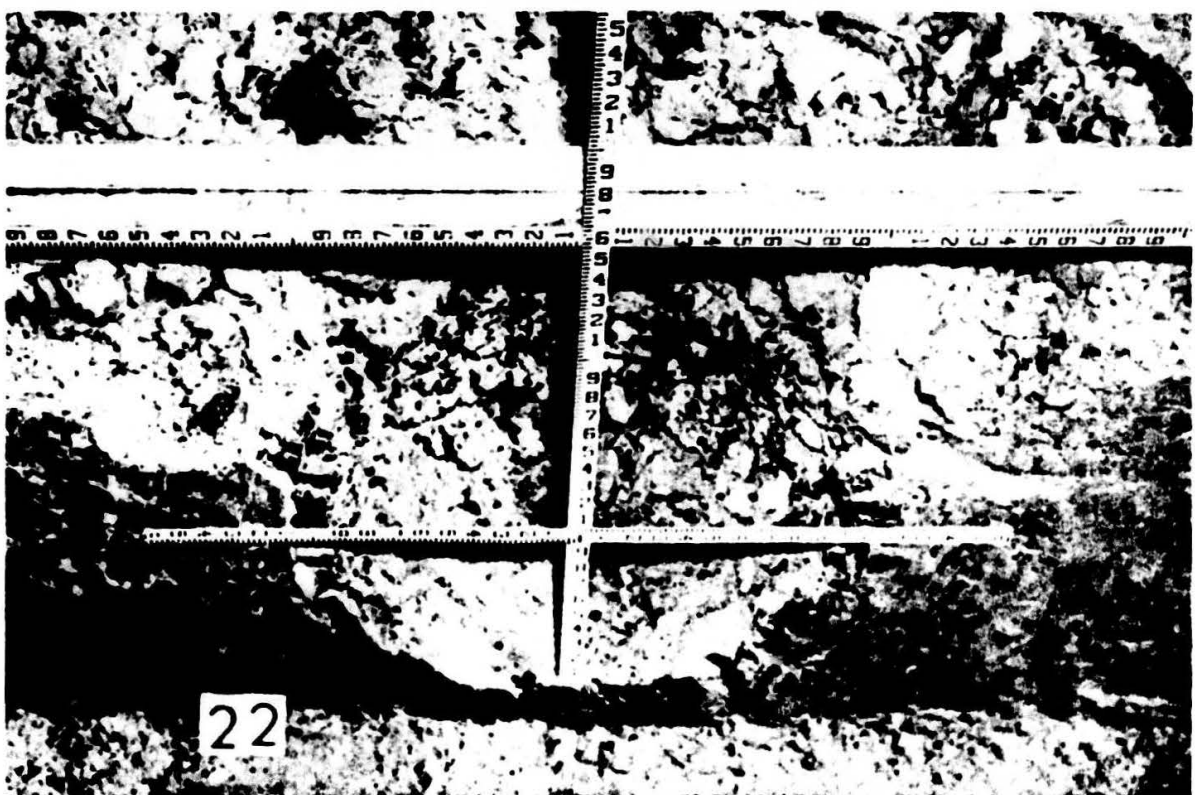


Fig. 3. After trenching, shot 22 ($\lambda_c = -1.50$)



Fig. 4. Before trenching, shot 33 ($\lambda_c = -2.75$)

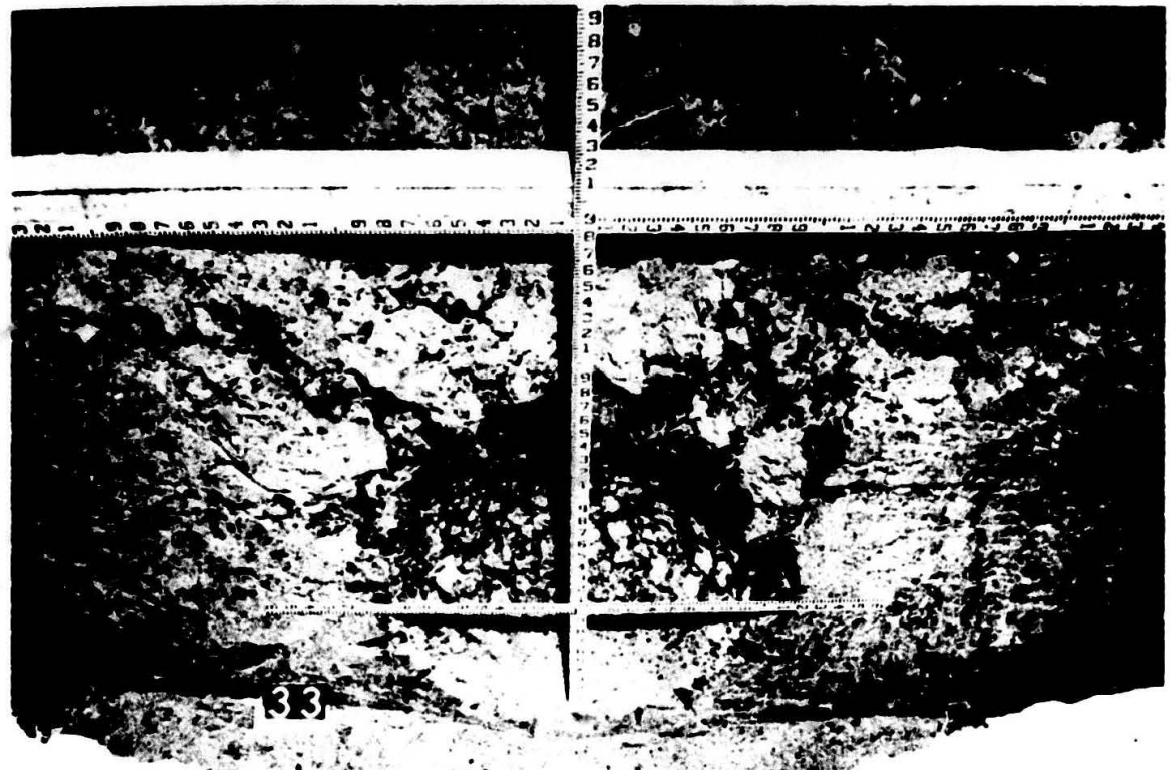


Fig. 5. After trenching, shot 33 ($\lambda_c = -2.75$)

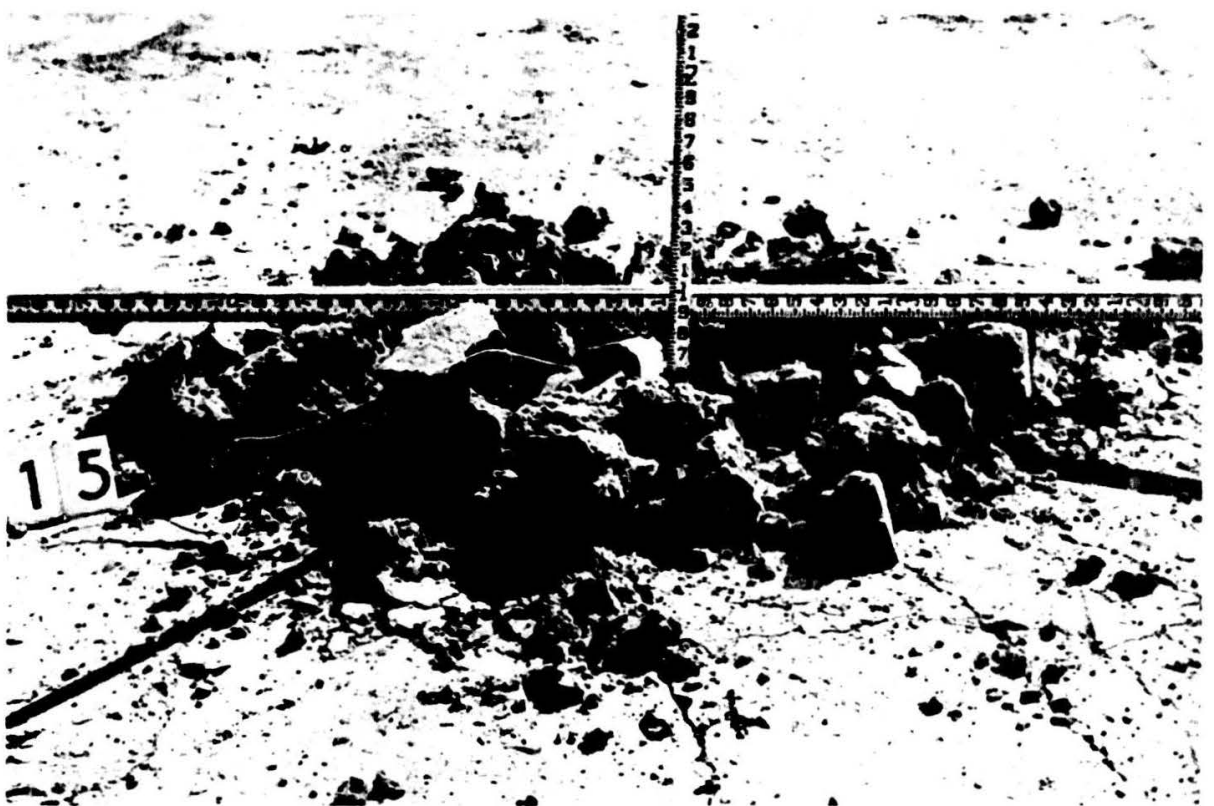


Fig. 6. Before trenching, shot 15 ($\lambda_c = -3.00$)

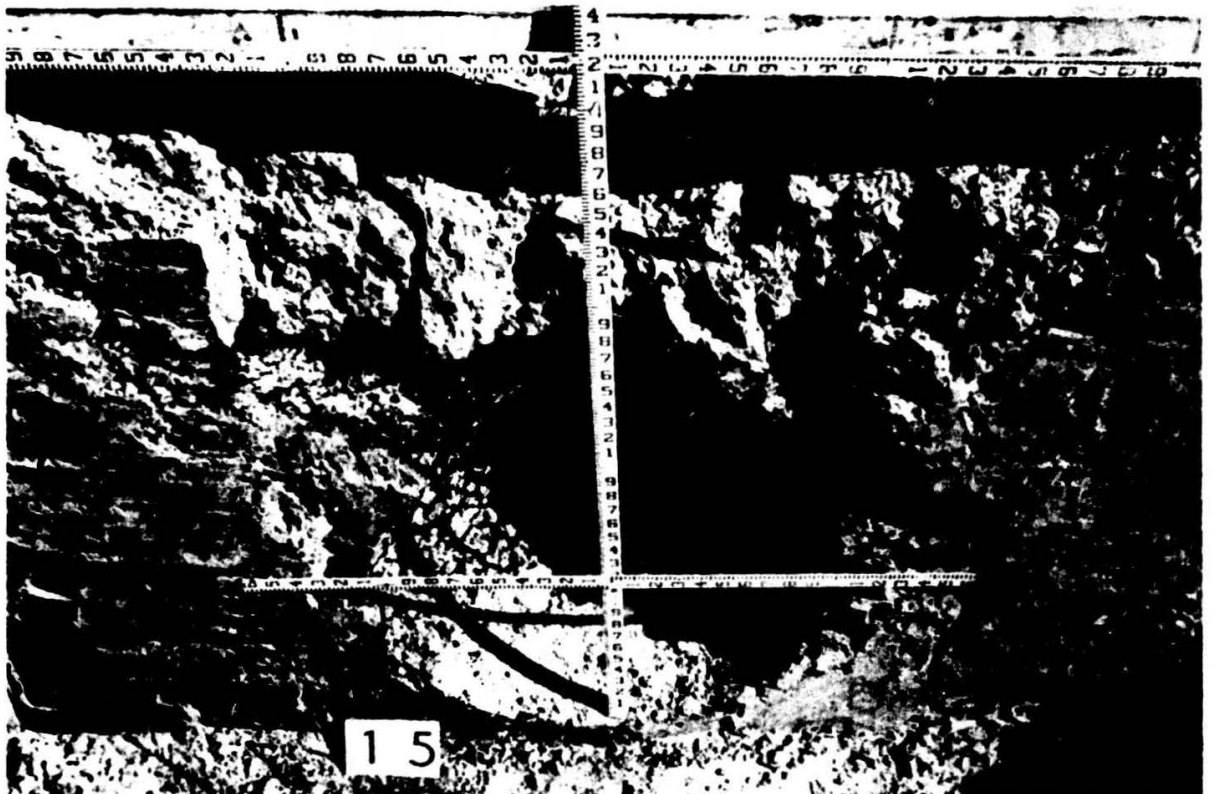


Fig. 7. After trenching, shot 15 ($\lambda_c = -3.00$)



Fig. 8. Before trenching, shot 32 ($\lambda_c = -3.25$)

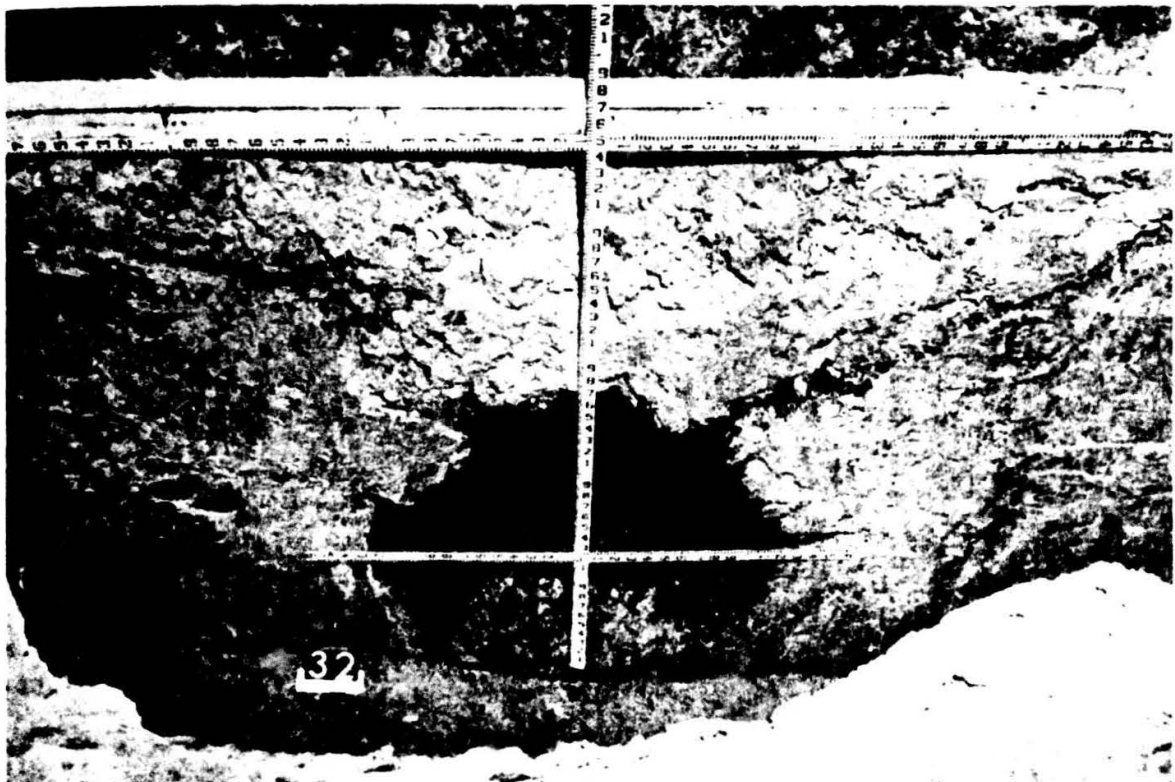


Fig. 9. After trenching, shot 32 ($\lambda_c = -3.25$)

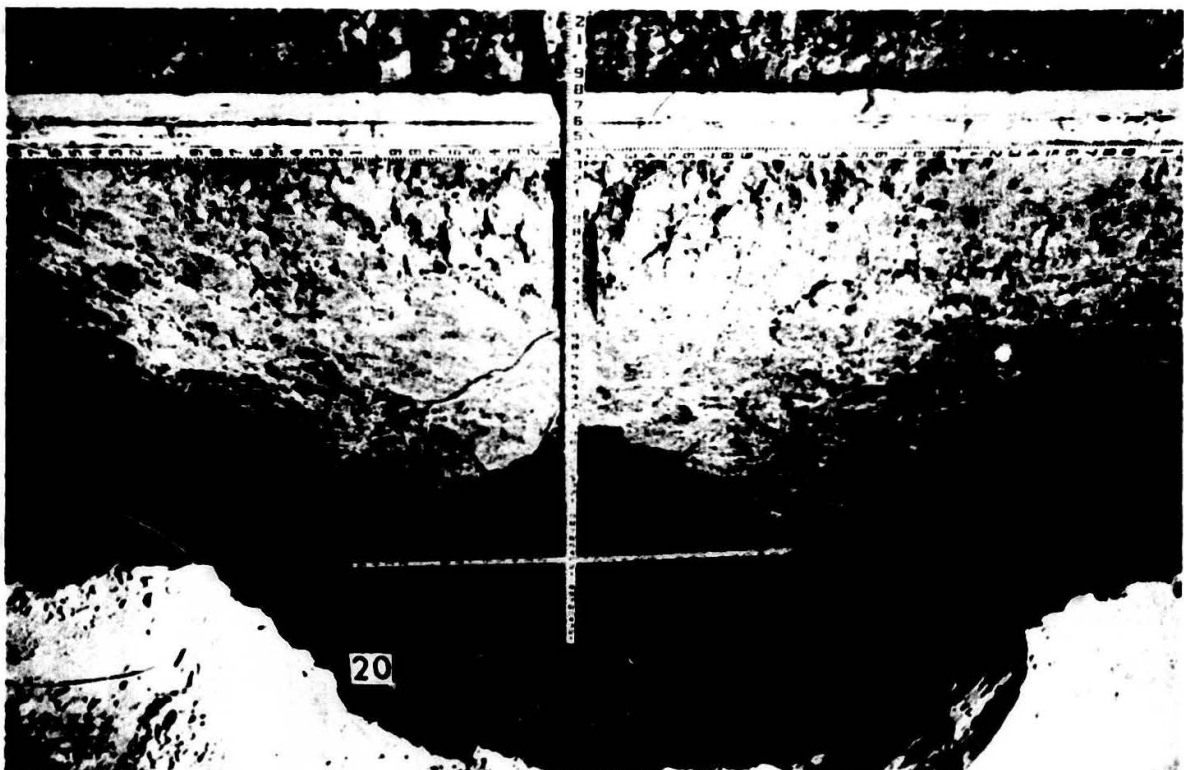


Fig. 10. After trenching, shot 20 ($\lambda_c = -4.0$)

9. Since the number of repeated shots was limited, it is difficult to ascertain the reproducibility of the results. The following values were determined from a cursory study of the scatter associated with the mass of cratering data obtained. The values listed describe the average scatter ranges noted for each dimension.

<u>Crater Dimension</u>	<u>Average Range of Scatter, %</u>
<u>Apparent Craters</u>	
Depth, d_a	$\pm 15-50$
Width, w_a	$\pm 20-50$
<u>True Craters</u>	
Depth, d_t	$\pm 3-5$
Width, w_t	$\pm 10-15$
Volume, V_t	$\pm 10-20$
<u>Camouflets</u>	
Horizontal diameter, D_h	$\pm 3-5$
Vertical diameter, D_v	$\pm 3-5$
Volume, V_c	$\pm 10-20$

It should be noted that the presence of relatively large clods of the loess

or clay material within the crater cavity may seriously affect the consistency of measurements when apparent crater dimensions are being analyzed. Examination of figs. 2, 4, 6, and 8 illustrates this condition.

Discussion of Test Results

Variables that affect cratering

10. The variables normally considered of major importance in cratering are: properties of the explosive used, weight of charge, strength properties of the earth material, and position of charge with respect to the air-ground interface. Since C-4 was used exclusively as the explosive, no variation in explosive properties is considered in this report. Because of the restricted range of charge weights used, the effect of varying the charge weight on the size crater formed could not be experimentally determined with a suitable degree of confidence; therefore, cube-root scaling was assumed to describe the charge weight effect. As previously mentioned, two types of soils were used and the effect of soil type is evaluated by comparing the results obtained in the clay with those obtained in loess. The position of the charge is the most critical variable in this study. It exerts the greater influence on the determination of crater shape and size.

Effect of soil type

11. A comparison of the densities, moisture contents, and cohesive properties of the two materials shows that they are remarkably similar (see table in paragraph 3). When the cratering effects obtained in the two materials (tables 1, 2, and 3) are compared, it is difficult to delineate which material developed the larger crater as a result of similar shots. For example, where direct comparison of the crater dimensions in loess and clay is possible, the linear dimensions of the true craters were found to differ by less than 5% in most cases. Since the pattern of scatter previously discussed in paragraph 9 indicates a spread of roughly 5 to 15%, it is concluded that little or no effect on cratering resulted from material variation when linear dimensions are considered as the basis of comparison. When the true crater volume is used as a basis of comparison, there is an indication that craters produced in clay were larger than those in loess for identical shot geometries.

Effect of charge
position on cratering

12. Cratering range. The range of charge positions that produced the conventionally shaped crater (concave upward) was confined to the range of charge positions where $\lambda_c \geq -2.0$ in the case of the apparent crater and to $\lambda_c \geq -3.0$ in the case of the true crater. The profile of a typical crater is illustrated in plate 1. The following paragraphs describe the manner in which varying the charge position affects the magnitude of the resulting crater.

13. Apparent crater depth. The apparent crater-capability curve* for depth (d'_a vs λ_c) is shown in plate 42 for both the loess and clay materials. The curves indicate similar trends in both media. These data indicate that if they were used to predict results of future tests the apparent crater depth could not be predicted closer than $\pm 50\%$. Other cratering studies involving the use of heavier charges have indicated a range of scatter in the order of $\pm 25\%$. Both curves indicate that the maximum apparent crater depth resulted when the charges were placed at about $\lambda_c = -1$, and that the maximum height of the earth dome (positive values of d_a and d'_a), resulting from a bulging upward of the earth mass, occurred when the charges were positioned such that λ_c was about -3.0 to -3.5. No evidence of surface failure or measurable upward displacement at ground zero was associated with charges placed at $\lambda_c = -10$ or below.

14. Apparent crater width. The crater-capability plot for apparent crater width (plate 43) convincingly shows that the crater width is much less consistent than the crater depth. It was believed inadvisable to attempt to draw a curve through the plotted points. The major reasons for these inconsistencies were pointed out in paragraph 9. In spite of the inconsistencies, the plots indicate that the apparent crater width increases with depth of burial of the charge to the point where λ_c is about -4.0. Below this depth of burial, the apparent crater width describes the diameter of the earth dome created by the bulging upward of the earth mass. When λ_c is about -10, no evidence remains to indicate residual displacement of a magnitude sufficient to warrant measurement.

* A crater-capability curve is any plot of a reduced crater dimension versus reduced charge position, e.g., d'_a vs λ_c , w'_a vs λ_c , d'_t vs λ_c , etc.

15. True crater depth. The true crater-capability curve for depth is presented in plate 44. These plots show that true craters were obtained over the range of charge positions defined by $0 > \lambda_c \geq -3.2$. Over this range, a linear relationship exists between the true crater depth and the depth of burial of the charge. This variation is described by the equations,

$$d_t' = -0.88 + 1.06 \lambda_c \quad (\text{loess}) \quad (1)$$

and

$$d_t' = -0.95 + 1.04 \lambda_c \quad (\text{clay}) \quad (2)$$

for the loess and clay soil materials, respectively. For estimating purposes, it is convenient to assume the regression coefficients equal to 1, as in the following expression,

$$d_t' = -1 + \lambda_c \quad (3)$$

Equation 3 may be altered such that,

$$d_t/W^{1/3} = -1 + Z/W^{1/3} \quad (4)$$

Simplifying,

$$d_t = -W^{1/3} + Z \quad (5)$$

Since λ_c and Z are always negative for charges positioned below the air-ground interface, then d_t will also be negative, indicating that the crater is concave upward and that the bottom of the crater lies below the original ground level. From equation 5, it is obvious that the depth of a true crater in loess or clay may be estimated by adding the cube root of the charge weight to the actual depth of burial. Similar analysis of results obtained from true crater measurements in a sand-gravel mixture¹ (see dashed curve, plate 44) shows that true crater depth is closely approximated by

$$d_t = -0.5 W^{1/3} + z \quad (6)$$

for values of $0 > \lambda_c > -1.0$. When this equation is algebraically modified so as to be similar to equation 3, the following results:

$$d'_t = -0.5 + \lambda_c \quad (7)$$

Comparison of equations 7 and 3 over the range $0 > \lambda_c \geq -3.2$ indicates that cratering in a sand-gravel mixture (Nevada Test Site) is less extensive depthwise than in loess or clay. Fig. 11 shows a comparison of the reduced

crater depth in loess or clay (equation 3) to the same dimension in a sand-gravel mixture as a function of λ_c . The term

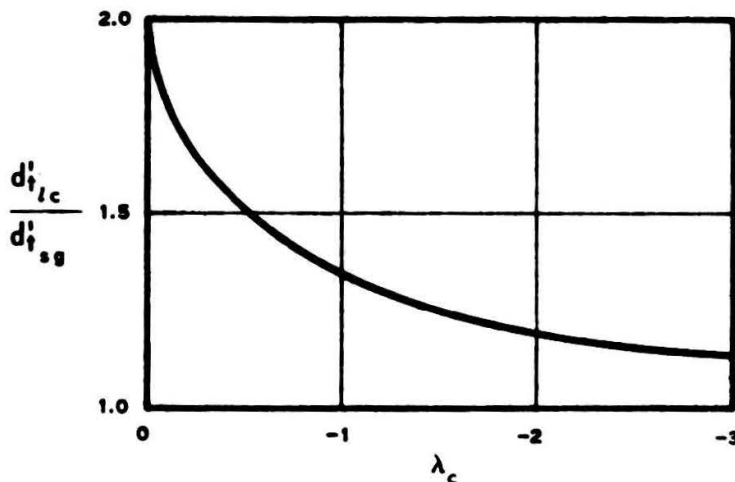


Fig. 11. Soil factor (for true crater depth) as a function of reduced charge position

is actually the so-called "soil factor" for true crater depth. Fig. 11 indicates that the soil

factor varies with depth of burial of the charge and that the maximum effect of the soil type on the crater depth is obtained when the charge is placed at the ground surface.

16. True crater width. The crater-capability curve for true crater width (plate 45) is characterized by considerable scatter and indicates only general trends. The data indicate that the width remains essentially constant for charges placed such that $-1.5 > \lambda_c > -3.5$. Over the range $0 > \lambda_c > -1.0$, the data from AFSWP 290 show similar trends for the sand-gravel mixture. The true crater width in the sand-gravel material is less than the width of the true crater in loess or clay over the range of charge positions where direct comparison is possible. If the sand-gravel curve (plate 45) is extrapolated,

$$\frac{d'_t_{lc}}{d'_t_{sg}}$$

then it is possible to construct a soil factor for true crater width vs λ_c curve as shown in fig. 12. This plot shows that the crater width is much less sensitive to variation in soil type than is the crater depth. Again the soil variation effect was a maximum when the charge was placed at the surface.

17. True crater volume. Examination of the data listed under the columns headed v_t and v'_t in tables 1 and 2 suggests

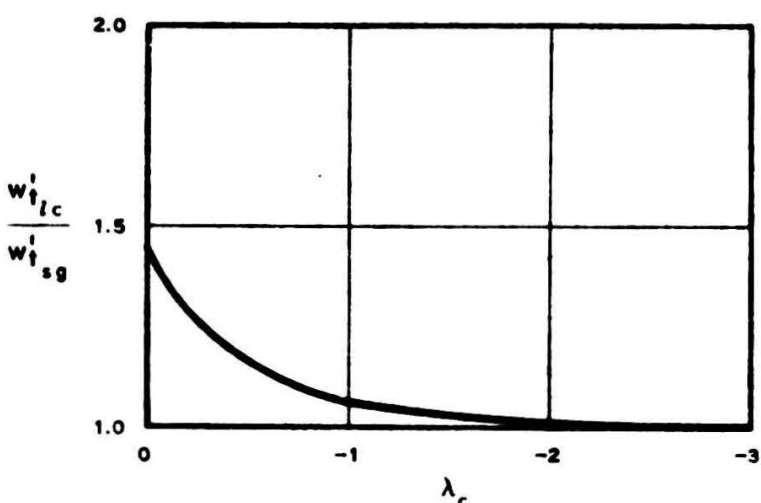


Fig. 12. Soil factor (for true crater width) as a function of reduced charge position

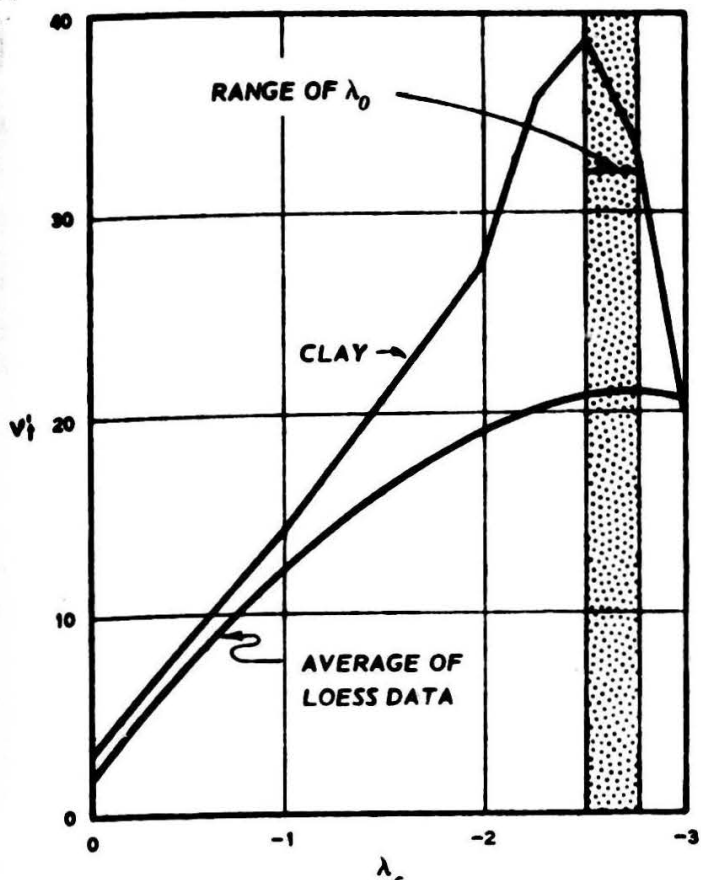


Fig. 13. True crater volume as a function of reduced charge position

that the depth of burial of the charge (λ_0) that produced the maximum true crater volume lies in the range $-2.5 > \lambda_c > -2.75$, as shown graphically in fig. 13.

Effect of charge position on camouflet

18. Camouflet range.

Camouflets were formed in every instance where charges were buried at scaled depths below about a λ_c of -3.0. The minimum scaled depth where a full camouflet was formed was observed for the case where two 1/2-lb charges were positioned at $\lambda_c = -3.15$ in the loess material. The 1-lb-charge tests in loess indicated that the camouflet depth was at a

λ_c of about -3.25. In the clay tests, no intermediate depths of burial were tested between the scaled depths of $\lambda_c = -3.0$ and $\lambda_c = -3.5$. These observations lead to the conclusion that ordinarily camouflets will be formed by charges positioned such that $\lambda_c \leq -3.2$ in materials that are similar to the loess and clay media described herein.

19. Size and shape of the camouflet. The size of the camouflet was determined by measuring the diameter in both the horizontal and vertical direction. These data are listed in table 3. The geometry of the camouflets formed was in most cases almost perfectly symmetrical about the pre-shot center of gravity of the charge. In fig. 14, the vertical diameter

is plotted as a function of the horizontal diameter for all tests that produced a camouflet in both loess and clay soils. The least-squared equation of the data plotted is,

$$D_v = 0.14 + 0.96 D_h \quad (8)$$

For all practical purposes,

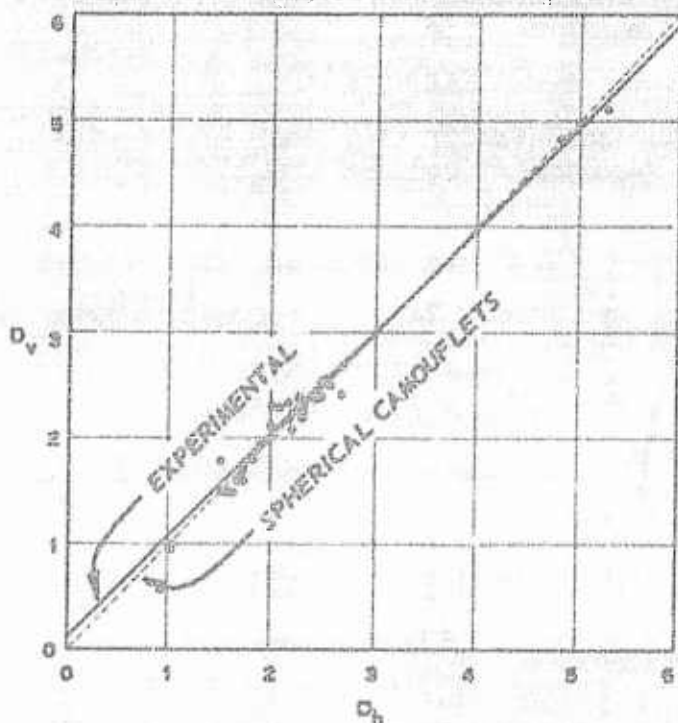
$$D_v = D_h \quad (9)$$

which implies that the shape of the camouflet is spherical. From plate 2, it should be noted that the dimension D_v does not include

Fig. 14. Vertical diameter as a function of the horizontal diameter

the conically shaped irregularity at the apex of the camouflet. This irregularity is attributed to the original disturbance of the soil in the drilling of the access hole for charge placement and subsequent backfilling. The limits of the access hole and the irregularity described can be seen in figs. 9 and 10.

20. Plates 46 and 47 can be used to estimate the size of a camouflet resulting from the detonation of a given HE charge at a specified depth. In plate 46, the reduced horizontal and vertical diameters of the various



camouflets are plotted as a function of the reduced depth of burial of the charge. A variation in the size of camouflet is noted as the charge depth of burial changes. If this variation is neglected and all dimensions of D'_v and D'_h are averaged, then the camouflet size may be estimated by

$$D'_v \text{ or } D'_h = 2.27 \pm 0.4$$

where the spread quoted is for a confidence level of 95%. In the loess soil, the maximum camouflet was noted at a λ_c of about -8.0. A similar conclusion in clay is not possible because of the paucity of the data. In plate 47, where the reduced volumes of the camouflets are plotted as a function of the reduced charge position, it is also established that the maximum size camouflet in loess occurred when λ_c is about -8.0.

Investigation of the Permanent Radial Displacement

21. Permanent displacements at the ground surface were obtained by pre- and postshot surveys of tacks placed radially about ground zero along four radial axes for the 1-lb tests in loess. The tacks were placed at reduced distances (λ) of 3, 5, 7, and 9 from ground zero. Fig. 15 shows the

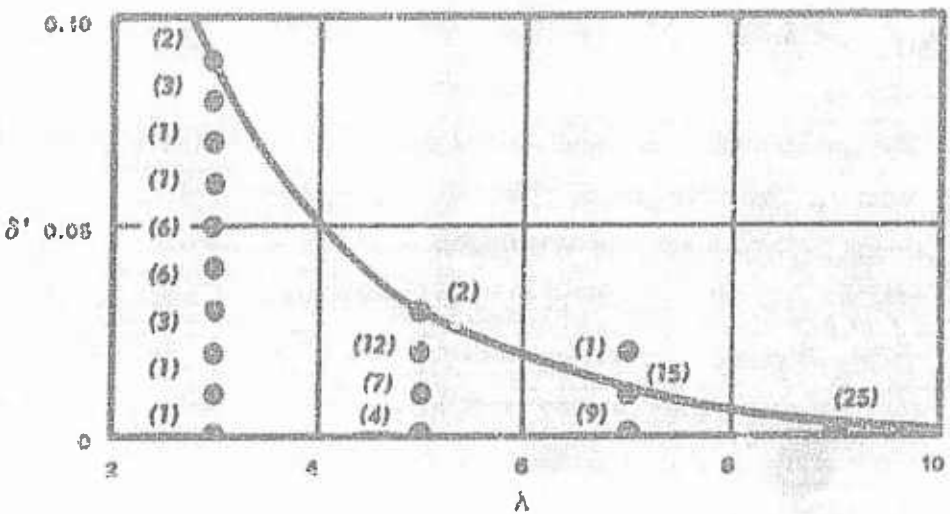


Fig. 15. Reduced displacement as a function of reduced horizontal distance

results of the displacement survey. The values plotted include the data from various charge positions $0 > \lambda_c > -4.0$. The figures in parentheses

denote the number of readings obtained at the particular ordinate value.

22. The curve as drawn represents the maximum reduced displacement associated with the various values of λ . The point at which the curve intersects the λ -axis denotes the outer limit of the plastic zone or failure. Beyond $\lambda \approx 10$, the media acted elastically. Similar measurements reported in other crater studies⁴⁻⁹ indicate that for a variety of soil materials and for charge weights up to 200 lb, the outer limits of the plastic zone extend over a range of $\lambda = 9$ to $\lambda = 17$; however, significant displacements were essentially confined within the range $\lambda \leq 10$.

Conclusions

23. Since these tests were conducted in soils that may be considered homogeneous, it is believed that the scatter in the data noted for repeated shots must be attributed to a source other than soil property variations. Much of the scatter can be attributed to the small weights of explosives used and the large-size clods of materials which have a definite effect on apparent crater measurements. It is believed that the true crater and camouflet data represent the extent to which cratering experiments, involving repeated tests using small charge weights, are reproducible. Contrary to the general opinion that crater width is more consistent than crater depth, the data indicate that crater depth is a more reliable measure, particularly for true crater dimensions.

24. The properties of the loess and clay soils employed in these tests were similar to the point that differences noted in the test results could not be attributed to the distinct soil types.

25. The range of charge positions resulting in formation of conventional crater shapes (concave upward) was confined to values of $\lambda_c \geq -2.0$ for the apparent crater and $\lambda_c \geq -3.0$ for the true crater. Camouflets were formed for all charges positioned below a λ_c of about -3.2. The range of the reduced diameter of the camouflet was 1.75 to 2.60 over the range of charge positions from $\lambda_c = -3.0$ to $\lambda_c = -14.0$. The following equation (10) provides a means of quickly estimating the camouflet diameter in clay or loess soils when $-3 > \lambda_c > -14$.

$$D_c = 2.27 W^{1/3} \quad (10)$$

26. These results are believed adaptable to most cohesive materials, although variations in the natural moisture content of such materials may well affect the camouflet size. Normally, larger craters will be produced in moist to wet materials than in those in the dry state. This increase in size usually amounts to about 10-40%. The data indicate that camouflets formed in homogeneous cohesive materials are (for all practical purposes) spherical in shape with very little assymetry.

27. Results of residual displacement measurements along the air-ground interface indicated that no measurable radial displacement occurred at ranges greater than $\lambda = 9$.

List of References

1. Stanford Research Institute, Small Explosion Tests, Phase II-B of Project Mole (CONFIDENTIAL). AFSWP-290, Stanford, Calif., December 1954.
2. U. S. Army Engineer Waterways Experiment Station, CE, Study of Energy Partitioning for Partially Confined Explosives (CONFIDENTIAL). Technical Memorandum No. 2-422, AFSWP-788, Vicksburg, Miss., November 1955.
3. , Effects of Stemming on Underground Explosions (U). Technical Report No. 2-438, AFSWP-823, Vicksburg, Miss., January 1957.
4. U. S. Special Engineering Division, The Panama Canal, Crater Tests in Cucaracha and Culebra Formations (U). ICS Memo 283-P, Canal Zone, April 1948.
5. , Crater Tests in Basalt (U). ICS Memo 284-P, Canal Zone, April 1948.
6. , Crater Tests in Gatun Sandstone (U). ICS Memo 285-P, Canal Zone, May 1948.
7. , Crater Tests in Marine Muck (U). ICS Memo 286-P, Canal Zone, May 1948.
8. , Crater Tests in Residual Clay (U). ICS Memo 287-P, Canal Zone, May 1948.
9. , Crater and Slope Tests with Explosives (U). ICS Memo 282-P, June 1948.

Table 1
Results of Cratering Tests in Loose Soil

Shot No.	z ft	λ_c $z/w^{2/3}$	Apparent Crater				True Crater					
			v _a ft	d _a ft	v _a /N ^{1/3}	d _a /N ^{1/3}	v _t ft	c _t ft	v _t ft ³	v _t /N ^{1/3}		
Charge Weight: 1 lb, C-b												
19	0	0	2.40	-0.56	2.40	-0.56	2.40	-0.81	1.10	2.40	-0.81	1.10
25	0	0	2.50	-0.53	2.50	-0.53	2.80	-0.79	1.46	2.80	-0.79	1.46
27	-0.5	-0.5	4.00	-0.98	4.00	-0.98	4.00	-1.47	5.41	4.00	-1.47	6.41
23	-0.5	-0.5	4.00	-1.20	4.00	-1.20	4.50	-1.40	6.98	4.50	-1.40	6.98
24	-1.0	-1.0	4.40	-0.72	4.40	-0.72	5.50	-2.03	13.8	5.50	-2.03	13.8
26	-1.0	-1.0	4.50	-0.65	4.50	-0.65	4.50	-2.07	11.4	4.50	-2.07	11.4
22	-1.5	-1.5	6.40	-0.33	6.40	-0.33	6.00	-2.49	19.6	6.00	-2.49	19.6
28	-1.5	-1.5	4.50	-0.58	4.50	-0.58	5.00	-2.52	17.1	5.00	-2.52	17.1
18	-2.0	-2.0	4.50	-0.20	4.50	-0.20	5.00	-2.99	19.8	5.00	-2.99	19.8
21	-2.0	-2.0	5.20	-0.13	5.20	-0.13	5.50	-3.02	20.3	5.50	-3.02	20.3
16	-2.5	-2.5	4.00	-0.19	4.00	-0.19	5.00	-3.52	20.6	5.00	-3.52	20.6
17	-2.5	-2.5	2.70	-0.50	2.70	-0.40	6.00	-3.52	25.7	6.00	-3.52	25.7
29	-2.75	-2.75	10.0	+0.04	10.0	+0.04	6.00	-3.79	28.5	6.00	-3.79	28.5
31	-2.75	-2.75	10.0	+0.31	10.0	+0.31	5.00	-3.85	18.0	5.00	-3.85	18.0
33	-2.75	-2.75	9.00	+0.31	9.00	+0.31	5.00	-3.75	21.0	5.00	-3.75	21.0
15	-3.0	-3.0	10.0	+0.70	10.0	+0.70	5.50	-4.10	25.6	5.50	-4.10	25.6
12	-3.0	-3.0	8.00	+0.55	8.00	+0.55	5.00	-4.06	22.3	5.00	-4.06	22.3
30	-3.25	-3.25	9.00	+0.48	9.00	+0.48						
32	-3.25	-3.25	9.00	+0.55	9.00	+0.55						
9	-3.5	-3.5	8.00	+0.84	8.00	+0.84						
10	-3.75	-3.75	8.00	+0.63	8.00	+0.63						
19	-3.75	-3.75	10.0	+0.45	10.0	+0.45						
11	-4.0	-4.0	8.00	+0.30	8.00	+0.30						
13	-4.0	-4.0	9.00	+0.31	9.00	+0.31						
20	-4.0	-4.0	4.50	+0.31	4.50	+0.31						
1	-6.0	-6.0	6.00	+0.02	6.00	+0.02						
2	-6.0	-6.0	6.00	+0.35	6.00	+0.05						
7	-6.0	-6.0	8.00	+0.04	8.00	+0.04						
3	-8.0	-8.0	9.00	+0.01	9.00	+0.01						
4	-8.0	-8.0	8.00	+0.02	8.00	+0.02						
5	-10.0	-10.0	7.00	+0.01	7.00	+0.01						
6	-10.0	-10.0	-----	-----	-----	-----						
8	-14.0	-14.0	-----	-----	-----	-----						
Charge Weight: 1/2 lb, C-b												
39	0	0	2.20	-0.28	2.77	-0.35	2.24	-0.75	1.18	2.82	-0.94	2.36
34	0	0	1.80	-0.20	2.26	-0.25	1.90	-0.62	0.73	2.39	-0.78	1.46
42	-0.50	-0.63	3.00	-0.60	3.78	-0.76	3.40	-1.21	3.77	4.28	-1.52	7.54
52	-0.50	-0.63	4.00	-0.35	5.04	-0.44	4.00	-1.33	6.40	5.04	-1.68	12.80
47	-1.00	-1.26	3.50	-0.35	4.41	-0.44	3.70	-1.73	6.26	4.56	-2.18	12.52
35	-1.00	-1.25	4.00	-0.31	5.04	-0.31	4.00	-1.73	5.89	5.04	-2.18	11.78
50	-1.50	-1.89	6.00	+0.02	7.56	+0.03	4.00	-2.28	8.63	5.04	-2.67	17.26
54	-1.50	-1.89	3.00	-0.70	3.78	-0.88	3.00	-2.23	6.81	3.78	-2.81	13.62
53	-2.00	-2.52	6.00	+0.12	7.56	+0.15	3.00	-2.74	7.40	3.78	-3.45	14.80
40	-2.00	-2.52	6.50	+0.07	8.18	+0.09	3.50	-2.76	8.36	4.41	-3.48	16.72
36	-2.00	-2.52	5.00	+0.30	6.30	+0.38	3.50	-2.78	11.1	4.41	-3.50	22.2
44	-2.18	-2.74	6.00	+0.67	7.56	+0.84	-----	-----	-----	-----	-----	-----
48	-2.18	-2.74	6.00	+0.07	7.56	+0.09	3.00	-2.96	8.81	3.78	-3.73	17.62
51	-2.18	-2.74	5.50	-0.02	6.93	-0.03	3.00	-2.99	8.03	3.78	-3.77	16.06
49	-2.50	-3.15	6.00	+0.51	7.56	+0.64						
43	-2.50	-3.15	6.50	+0.28	8.18	-0.35						
37	-3.00	-3.78	6.00	+0.36	7.56	+0.45						
55	-3.00	-3.78	6.00	+0.25	7.56	+0.33						
45	-3.10	-3.90	6.50	+0.17	8.18	+0.21						
41	-3.10	-3.90	5.50	+0.26	6.92	+0.33						
38	-3.25	-4.09	6.00	+0.30	7.56	+0.38						
46	-3.25	-4.09	5.00	+0.27	7.56	+0.34						
Camouflet range												

Note: Minus sign refers to below original ground; plus sign above original ground.

Table 2
Results of Cratering Tests in Clay Soil

Shot No.	z ft	$\lambda_c Z/W^{1/3}$	Apparent Crater						True Crater					
			v_a ft	d_a ft	v_a^t	d_a^t	$v_a/W^{1/3}$	$d_a/W^{1/3}$	v_t ft	d_t ft	v_t^t	d_t^t	$v_t/W^{1/3}$	$d_t/W^{1/3}$
<u>Charge Weight: 1 lb, C-4</u>														
57	0	0	3.00	-0.65	3.00	-0.65	3.00	-0.89	2.37	3.00	-0.89	2.37		
56	-1.0	-1.0	4.60	-1.30	4.60	-1.30	4.60	-2.05	14.0	4.60	-2.05	14.0		
58	-2.0	-2.0	5.00	+0.44	5.00	+0.44	5.00	-3.11	27.6	5.00	-3.11	27.6		
68	-2.25	-2.25	9.00	+0.18	9.00	+0.18	6.00	-3.26	35.6	6.00	-3.26	35.6		
69	-2.50	-2.50	8.00	+0.50	8.00	+0.50	6.00	-3.59	38.6	6.00	-3.59	38.6		
70	-2.75	-2.75	7.00	+0.85	7.00	+0.85	5.50	-3.73	33.4	5.50	-3.73	33.4		
59	-3.00	-3.00	7.00	+1.54	7.00	+1.54	5.00	-4.05	19.5	5.00	-4.05	19.5		
60	-3.50	-3.50	7.00	+0.58	7.00	+0.58								
71	-3.90	-3.90	7.50	+0.57	7.50	+0.57								
61	-4.00	-4.00	6.00	+0.39	6.00	+0.39								
72	-4.25	-4.25	8.00	+0.50	8.00	+0.50								
73	-4.50	-4.50	8.00	+0.08	8.00	+0.08								
62	-4.50	-4.50	7.00	+0.12	7.00	+0.12								
63	-5.50	-5.50	10.0	+0.12	10.0	+0.12								
64	-6.50	-6.50	6.00	+0.03	6.00	+0.03								
65	-7.00	-7.00	6.00	+0.03	6.00	+0.03								
66	-7.50	-7.50	5.00	+0.01	5.00	+0.01								
67	-8.00	-8.00	5.00	+0.01	5.00	+0.01								
<u>Charge Weight: 1/2 lb, C-4</u>														
74	-5.56	-7.00	7.00	+0.01	8.81	+0.01								
75	-6.35	-8.00	-----	-----	-----	-----								
76	-7.14	-9.00	0	0	0	0								
78	-7.54	-10.0	5.00	+0.01	6.30	+0.01								
79	-8.33	-11.0	0	0	0	0								
80	-8.73	-11.0	0	0	0	0								
81	-9.53	-11.5	0	0	0	0								
77	-9.52	-12.0	-----	-----	-----	-----								

Note: Minus sign refers to below original ground; plus sign above original ground.

Table 3

Carboult Measurement in Loess and Clay

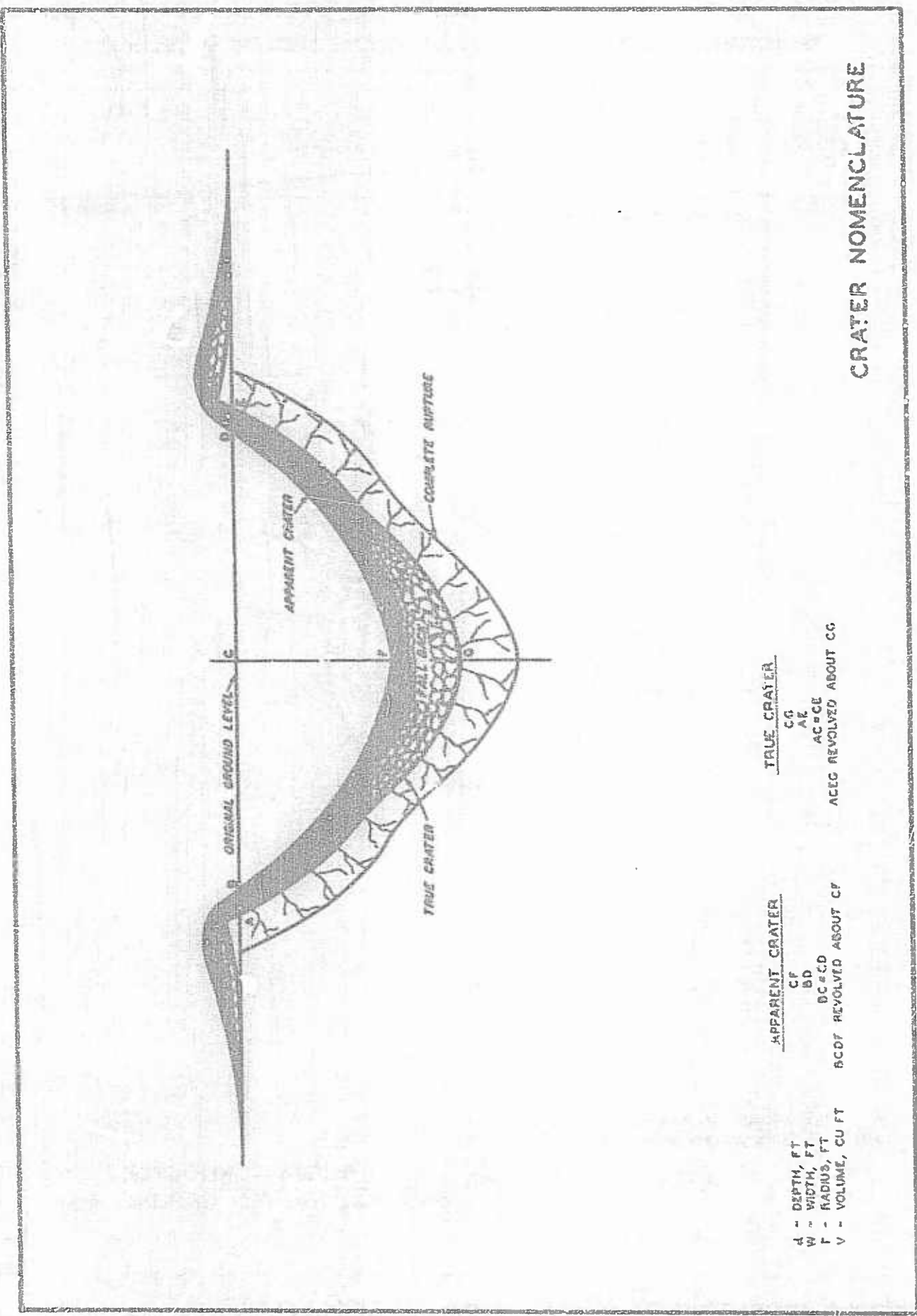
Shot No.	Z ft	λ_c $Z/W^{1/3}$	D_v ft	D_h ft	D_{av} ft	V_c ft ³	D_v^2 $D_v/W^{1/3}$	D_h^2 $D_h/W^{1/3}$	D_{av}^2 $D_{av}/W^{1/3}$	V_c^2 V_c/W
<u>Measurements in Loess Soil, Charge Weight: 9 lb., C-4</u>										
62	-10.0	-5.00	4.84	4.83	4.86	60.28	2.42	2.42	2.42	7.54
63	-10.0	-5.00	5.13	5.30	5.22	78.91	2.56	2.65	2.61	9.86
<u>Measurements in Loess Soil, Charge Weight: 1 lb., C-4</u>										
32	-3.25	-3.25	2.22	2.24	2.23	6.04	2.22	2.24	2.23	6.04
30	-3.25	-3.25	2.19	2.34	2.26	6.11	2.19	2.34	2.26	6.11
9	-3.50	-3.50	2.34	2.36	2.32	6.17	2.34	2.30	2.32	6.17
10	-3.75	-3.75	2.52	2.40	2.46	7.51	2.52	2.40	2.46	7.51
14	-3.75	-3.75	2.30	2.00	2.15	4.46	2.30	2.00	2.15	4.46
20	-4.00	-4.00	2.59	2.50	2.54	7.62	2.59	2.50	2.54	7.62
13	-4.00	-4.00	2.11	2.00	2.06	4.48	2.11	2.00	2.06	4.48
11	-4.00	-4.00	2.34	2.20	2.27	5.74	2.34	2.20	2.27	5.74
7	-6.00	-6.00	2.32	2.28	2.30	6.76	2.32	2.28	2.30	6.76
2	-6.00	-6.00	2.46	2.38	2.42	7.58	2.46	2.38	2.42	7.58
1	-6.00	-6.00	----	----	----	----	----	----	----	----
3	-8.00	-8.00	2.70	2.70	2.70	10.1	2.70	2.70	2.70	10.1
4	-8.00	-8.00	2.62	2.42	2.56	8.18	2.69	2.42	2.56	8.18
5	-10.0	-10.0	2.55	2.56	2.56	8.69	2.55	2.56	2.56	8.69
6	-10.0	-10.0	2.50	2.52	2.51	8.10	2.50	2.52	2.51	8.10
8	-14.0	-14.0	2.43	2.40	2.42	6.98	2.43	2.40	2.42	6.98
<u>Measurements in Loess Soil, Charge Weight: 1/2 lb., C-4</u>										
44	-2.18	-2.75	1.65	1.50	1.58	1.93	2.00	1.89	1.98	3.85
43	-2.50	-3.15	1.65	1.50	1.56	1.98	2.08	1.89	1.98	3.95
49	-2.50	-3.15	1.60	1.50	1.55	1.81	2.02	1.89	1.95	3.62
37	-3.00	-3.78	1.77	1.62	1.70	2.36	2.23	2.04	2.14	4.72
55	-3.00	-3.78	1.74	1.60	1.71	2.74	2.19	2.12	2.16	5.48
45	-3.10	-3.90	1.70	1.60	1.65	2.36	2.14	2.02	2.08	4.72
41	-3.10	-3.90	1.77	1.72	1.74	2.76	2.23	2.17	2.20	5.32
38	-3.25	-4.09	1.56	1.52	1.54	1.89	1.97	1.91	1.94	3.78
46	-3.25	-4.09	1.65	1.60	1.62	2.92	2.33	2.27	2.30	5.84
<u>Measurements in Loess Soil, Charge Weight: 1/8 lb., C-4</u>										
84	-2.50	-5.00	1.00	1.05	1.02	.997	2.00	2.10	2.04	7.98
85	-2.50	-5.00	0.95	1.05	1.00	.952	1.90	2.10	2.00	7.62
<u>Measurements in Clay Soil, Charge Weight: 1 lb., C-4</u>										
60	-3.50	-3.50	2.35	2.26	2.30	7.17	2.35	2.26	2.30	7.17
71	-3.90	-3.90	2.30	2.40	2.35	7.15	2.30	2.40	2.35	7.15
61	-4.00	-4.00	2.30	2.36	2.34	6.54	2.30	2.38	2.34	6.54
72	-4.25	-4.25	2.10	2.30	2.20	5.87	2.10	2.50	2.20	5.87
62	-4.50	-4.50	2.20	2.18	2.19	5.79	2.20	2.18	2.19	5.79
65	-7.00	-7.00	2.09	2.22	2.16	5.28	2.09	2.22	2.16	5.28
<u>Measurements in Clay Soil, Charge Weight: 1/2 lb., C-4</u>										
76	-5.56	-7.00	----	----	----	----	----	----	----	----
77	-9.13	-11.50	1.80	1.54	1.67	2.42	2.27	1.94	2.17	4.84
81	-9.52	-12.0	1.95	1.92	1.94	3.44	2.46	2.42	2.44	6.88

Note: Minus sign refers to below original ground; plus sign above original ground.

Table 4
Measurements of Permanent Horizontal Displacement along the Ground Surface

Shot No.	Z	λ_c	8"				5"			
			$\lambda = 3$	$\lambda = 5$	$\lambda = 7$	<u>$\lambda = 9$</u>	$\lambda = 3$	$\lambda = 5$	$\lambda = 7$	$\lambda = 9$
<u>Measurements in Loess Soil, Charge Weight: 1 lb, C-4</u>										
9	-3.50	-3.50	0.05	0.03	0.01	0	0.05	0.03	0.01	0
10	-3.75	-3.75	0.05	0.02	0.01	0	0.05	0.02	0.01	0
11	-4.00	-4.00	0.03	0.01	0.01	0	0.03	0.01	0.01	0
12	-3.00	-3.00	0.05	0.02	0.01	0	0.05	0.02	0.01	0
13	-4.00	-4.00	0.03	0.01	0.01	0	0.03	0.01	0.01	0
14	-3.75	-3.75	0.04	0.02	0.02	0	0.04	0.02	0.02	0
15	-3.00	-3.00	0.06	0.02	0.01	0	0.06	0.02	0.01	0
16	-2.50	-2.50	0.08	0.02	0.01	0	0.08	0.02	0.01	0
17	-2.50	-2.50	0.04	0.02	0.01	0	0.04	0.02	0.01	0
18	-2.00	-2.00	0.05	0.01	0	0	0.05	0.01	0	0
19	0	0	0.01	0	0	0	0.01	0	0	0
20	-4.00	-4.00	0.04	0.02	0.01	0	0.04	0.02	0.01	0
21	-2.00	-2.00	0.05	0.02	0.01	0	0.05	0.02	0.01	0
22	-1.50	-1.50	0.05	0.01	0	0	0.05	0.01	0	0
23	-0.50	-0.50	0.02	0	0	0	0.02	0	0	0
24	-1.00	-1.00	0.04	0.01	0	0	0.04	0.01	0	0
25	0	0	0	0	0	0	0	0	0	0
26	-1.00	-1.00	0.04	0.01	0	0	0.04	0.01	0	0
27	-0.50	-0.50	0.03	0	0	0	0.03	0	0	0
28	-1.50	-1.50	0.04	0.01	0	0	0.04	0.01	0	0
29	-2.75	-2.75	0.09	0.02	0.01	0	0.09	0.02	0.01	0
30	-3.25	-3.25	0.09	0.03	0.01	0	0.09	0.03	0.01	0
31	-2.75	-2.75	0.08	0.02	0.01	0	0.08	0.02	0.01	0
32	-3.25	-3.25	0.08	0.02	0.01	0	0.08	0.02	0.01	0
33	-2.75	-2.75	0.07	0.02	0.01	0	0.07	0.02	0.01	0
<u>Measurements in Loess Soil, Charge Weight: 1/2 lb, C-4</u>										
34	0	0	0	0	0	0	0	0	0	0
35	-1.00	-1.26	0.03	0	0	0	0.04	0	0	0
36	-2.00	-2.52	0.03	0.01	0	0	0.04	0.01	0	0
37	-3.00	-3.78	0.03	0.01	0	0	0.04	0.01	0	0
38	-3.25	-4.09	0.02	0.01	0	0	0.02	0.01	0	0
39	0	0	0.01	0	0	0	0.01	0	0	0
40	-2.00	-2.52	0.04	0.01	0	0	0.05	0.01	0	0
41	-3.10	-3.90	0.03	0.01	0	0	0.04	0.01	0	0
42	-0.50	-0.63	0.02	0	0	0	0.02	0	0	0
43	-2.50	-3.15	0.03	0.01	0	0	0.04	0.01	0	0
44	-2.18	-2.75	0.06	0.01	0	0	0.08	0.01	0	0
45	-3.10	-3.90	0.03	0.01	0	0	0.04	0.01	0	0
46	-3.25	-4.09	0.03	0.01	0	0	0.04	0.01	0	0
47	-1.00	-1.26	0.04	0.01	0	0	0.05	0.01	0	0
48	-2.18	-2.75	0.04	0.01	0	0	0.05	0.01	0	0
49	-2.50	-3.15	0.04	0.01	0	0	0.05	0.01	0	0
50	-1.50	-1.89	0.05	0.01	0	0	0.06	0.01	0	0
51	-2.18	-2.75	0.05	0.01	0	0	0.06	0.01	0	0
52	-0.50	-0.63	0.06	0.01	0	0	0.08	0.01	0	0
53	-2.00	-2.52	0.04	0.01	0	0	0.05	0.01	0	0
54	-1.50	-1.89	0.04	0.01	0	0	0.05	0.01	0	0
55	-3.00	-3.78	0.03	0.01	0	0	0.04	0.01	0	0
<u>Measurements in Clay Soil, Charge Weight: 1 lb, C-4</u>										
71	-3.90	-3.90	0.05	0.03	0.01	0	0.05	0.03	0.01	0
72	-4.25	-4.25	0.04	0.01	0.01	0	0.04	0.01	0.01	0

* Values recorded are an average of six to nine independent observations.



CRATER NOMENCLATURE

TRUE CRATER

CC

AA

AC

ACG REVOLVED ABOUT CC'

APPARENT CRATER

CC'

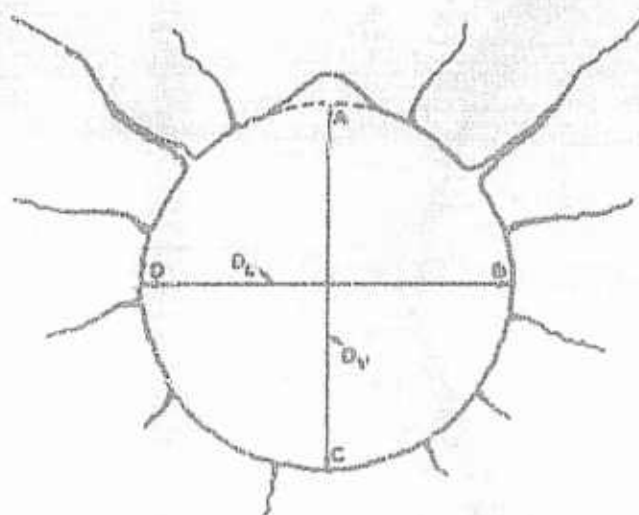
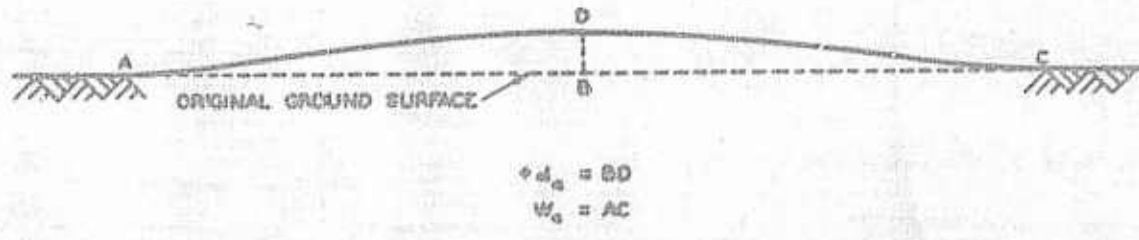
BD

DC

BCDF REVOLVED ABOUT CC'

A = DEPTH, FT
W = WIDTH, FT
R = RADIUS, FT
V = VOLUME, CU FT

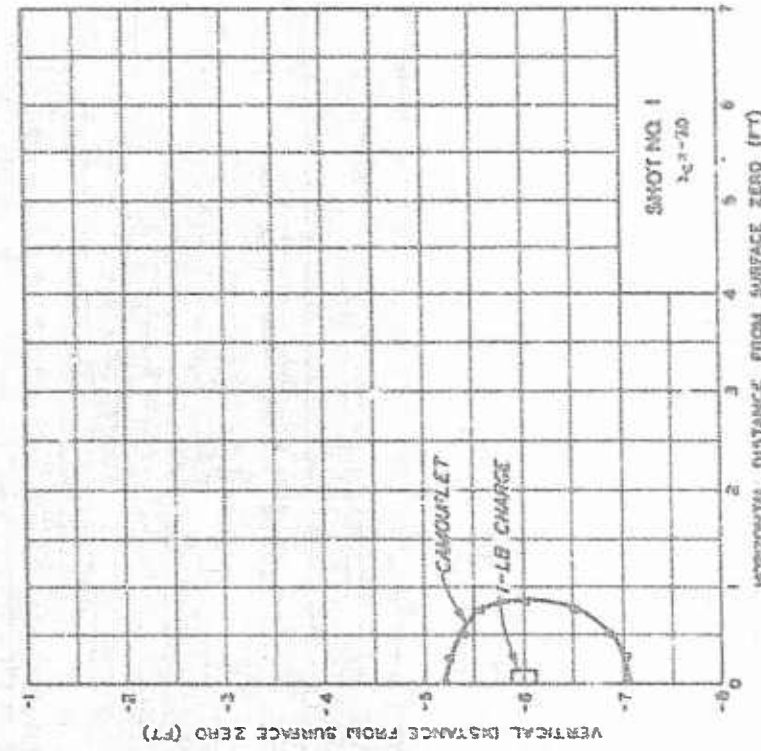
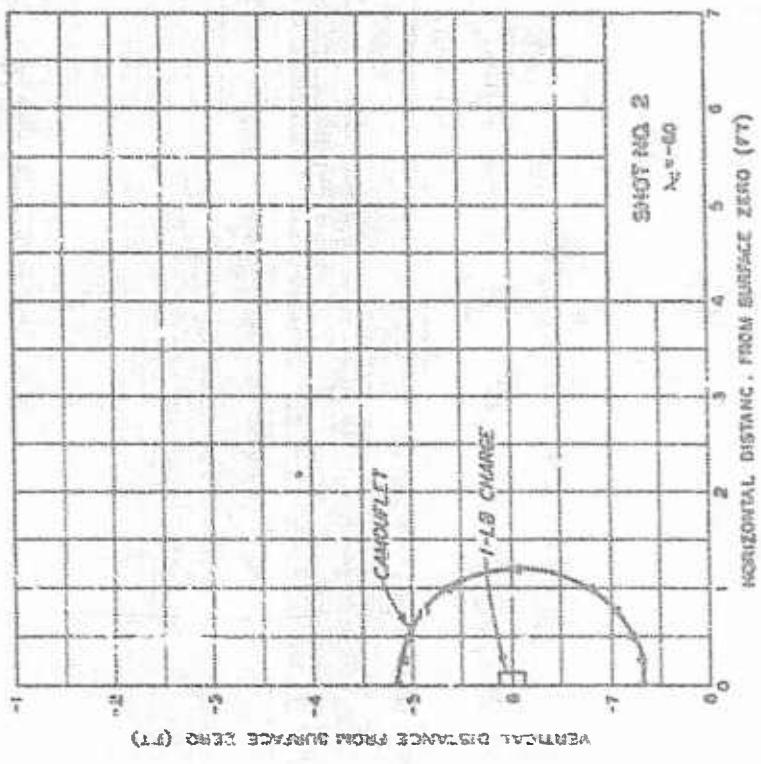
PLATE I



VOLUME OF CAMOUFLET =
 AREA ABCD REVOLVED ABOUT AC

TYPICAL CAMOUFLET
 AND ASSOCIATED GROUND RISE

PLATE 2



MAP F-CRATER PROFILES
SOIL MATERIAL - LOESS
SHOTS NOS. 1 AND 2

SHC	t_c^P	CRATER DIMENSIONS												
		CRATER		TRUE CRATER		CAMOUFLLET								
HO	d	u	v	A	V	θ	s	h	A	V	D	B	A	V
1	1002.600										1.63	1.72	2.46	2.61
2	1005.800										2.40	2.20	4.70	7.59

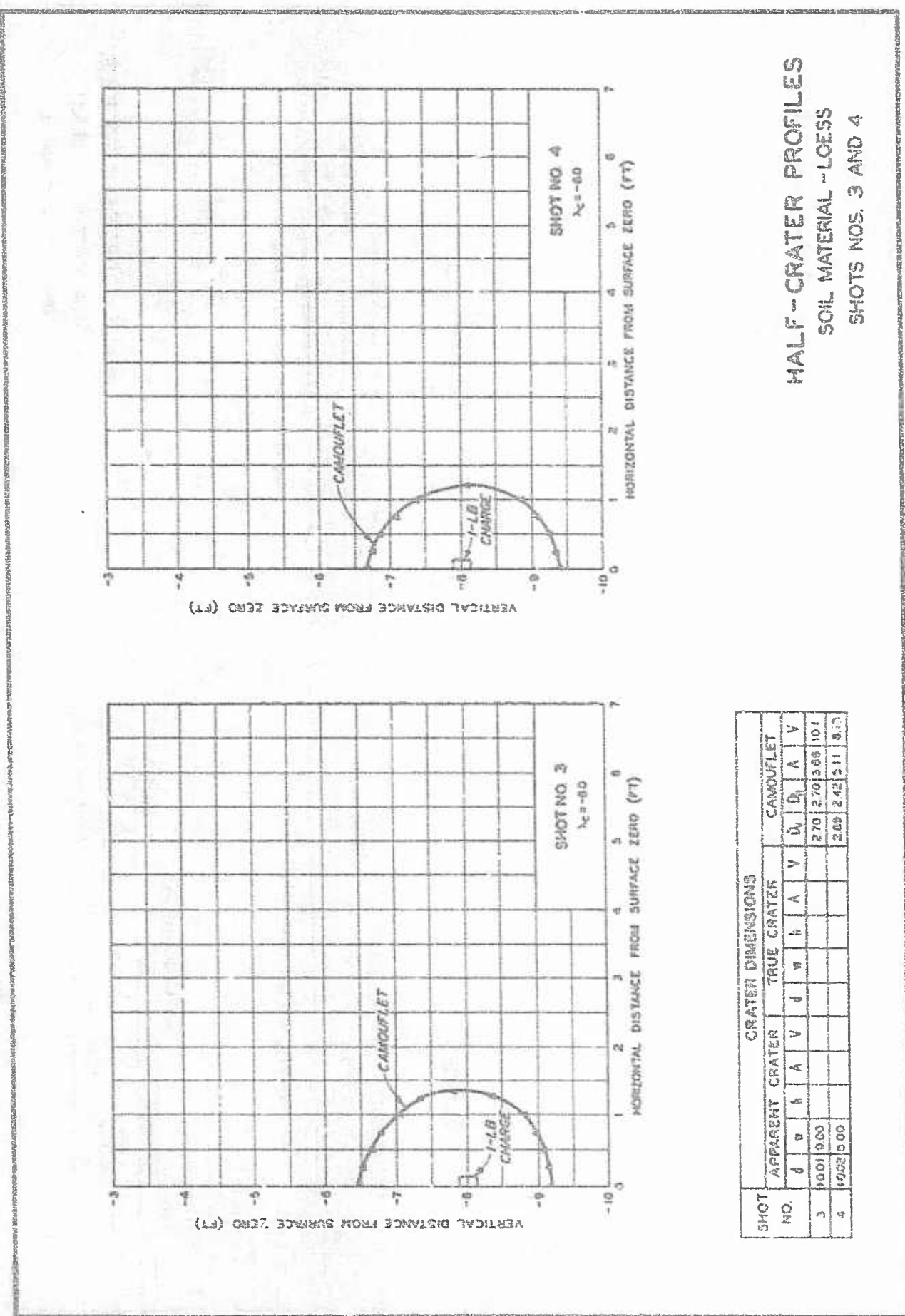
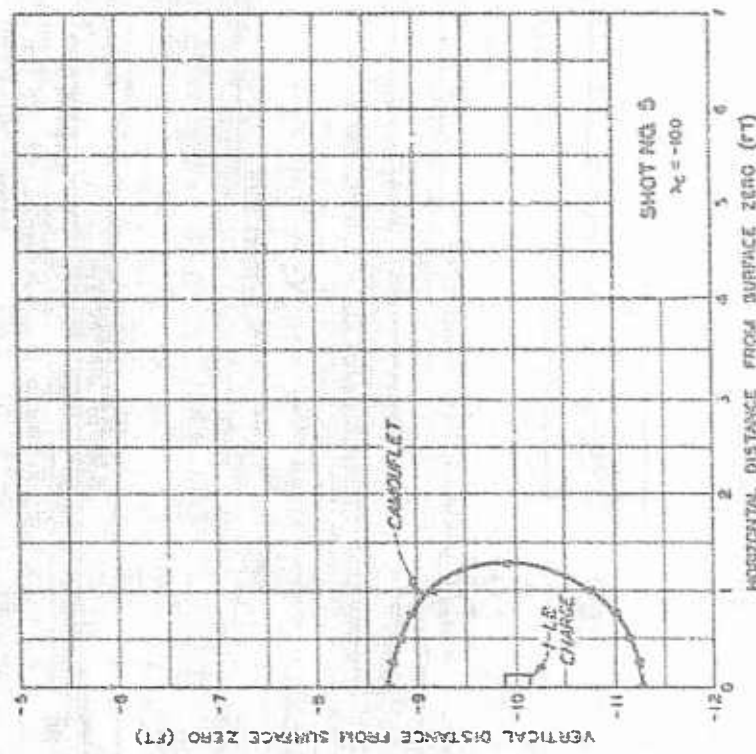
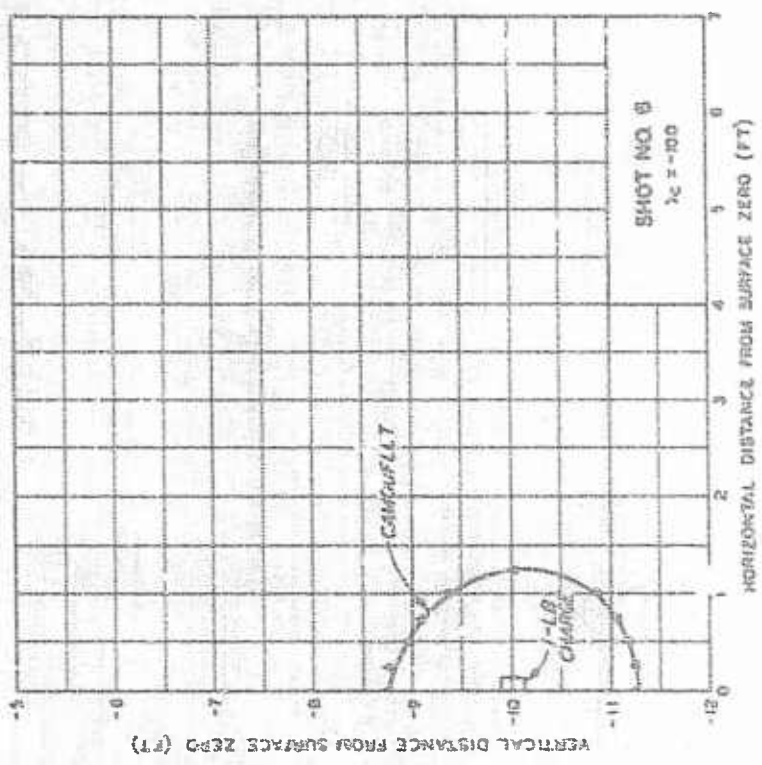
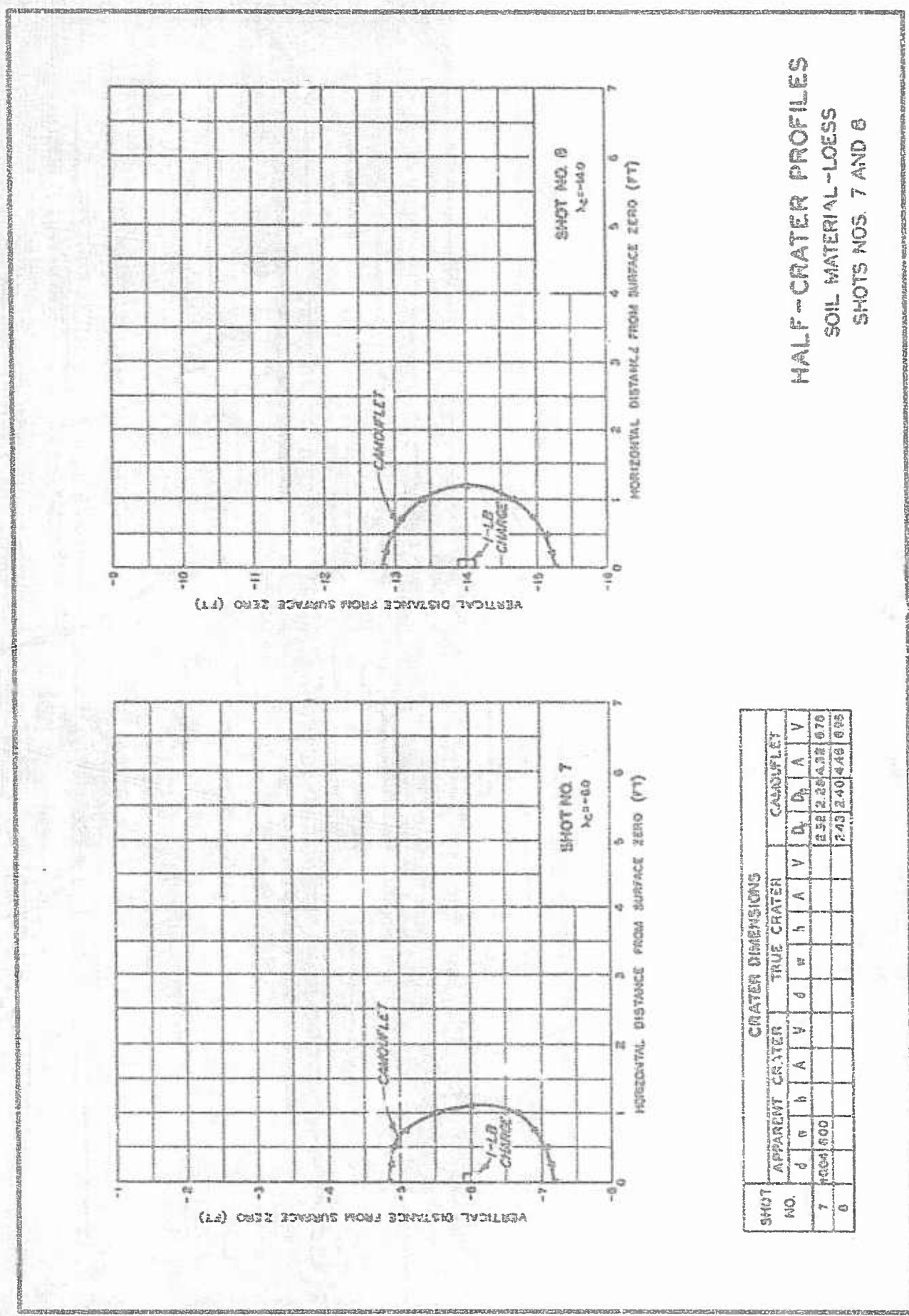


PLATE 4



SHOT NO.	CRATER DIMENSIONS						CRATER PROFILE
	APPARENT CRATER	TRUE CRATER	J	W	H	A	
5	4001	760					2.50 2.50 5.00 3.50
6	-	-					2.50 2.50 4.50 6.10

HALF-CRATER PROFILES
 $z_c = -100$
SOIL MATERIAL-LOESS
SHOTS NOS. 5 AND 6



SHOT NO.	CRATER DIMENSIONS								
	APPARENT CRATER			TRUE CRATER			CRATERLET		
	d	w	b	A	g	d	w	h	A
7	4.00	—	—	—	—	2.32	2.28	4.32	0.70
8	—	—	—	—	—	2.43	2.40	4.46	0.95

HALF-CRATER PROFILES
SOIL MATERIAL-LOESS
SHOTS NOS. 7 AND 8

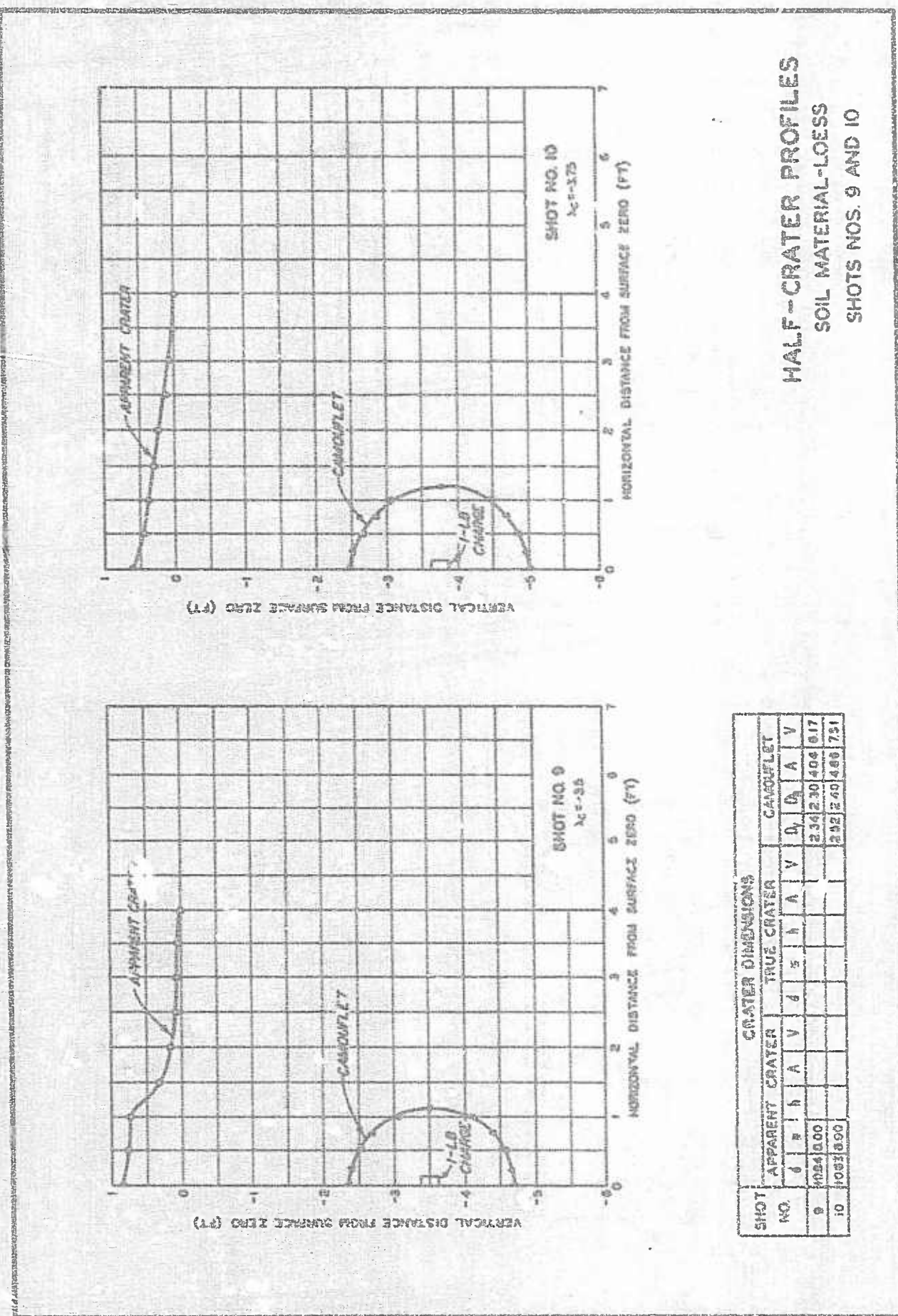
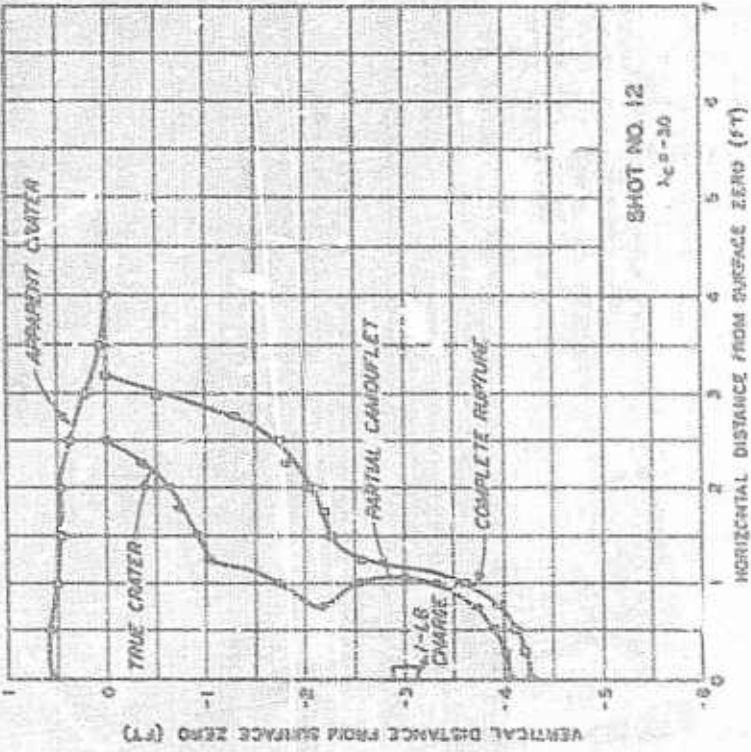
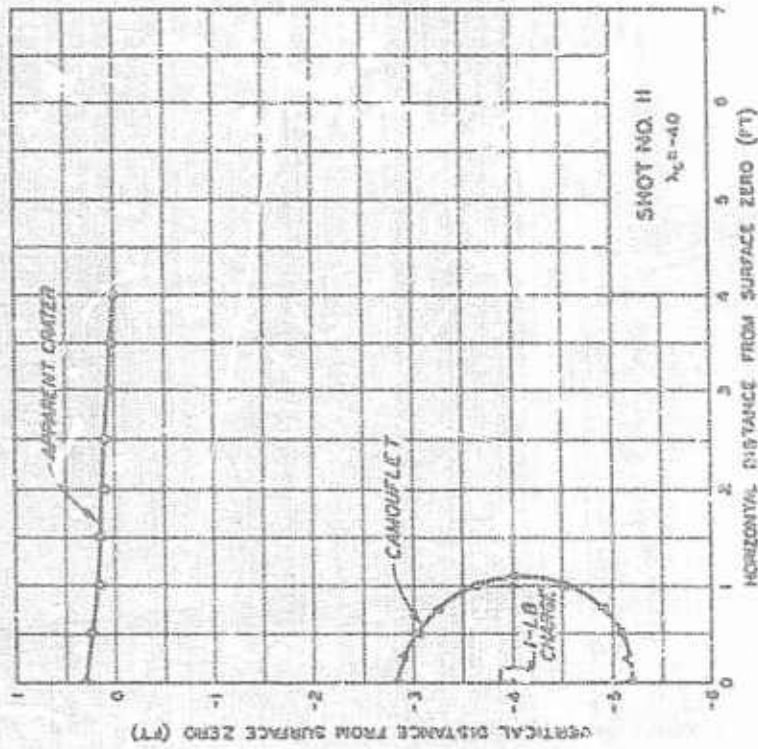
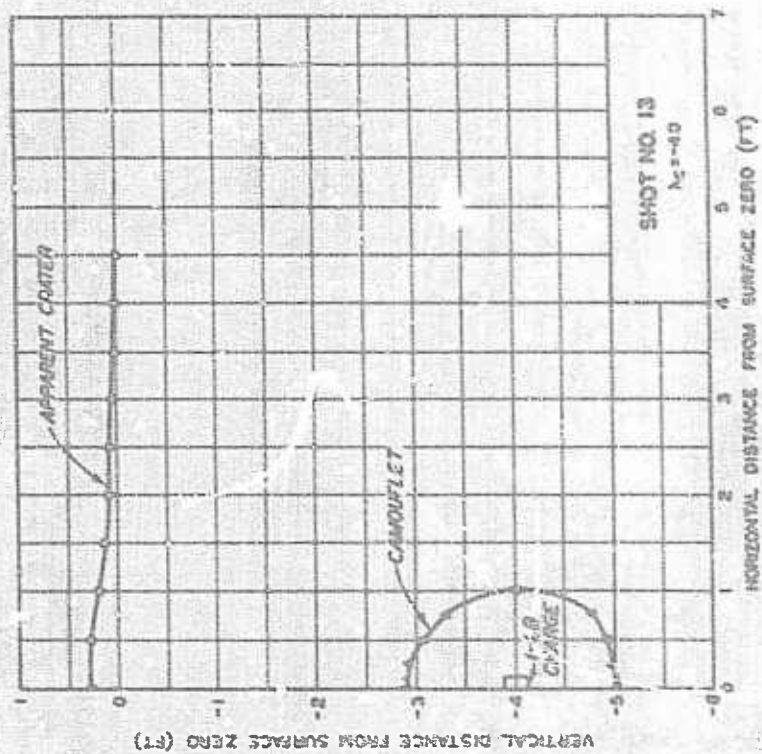
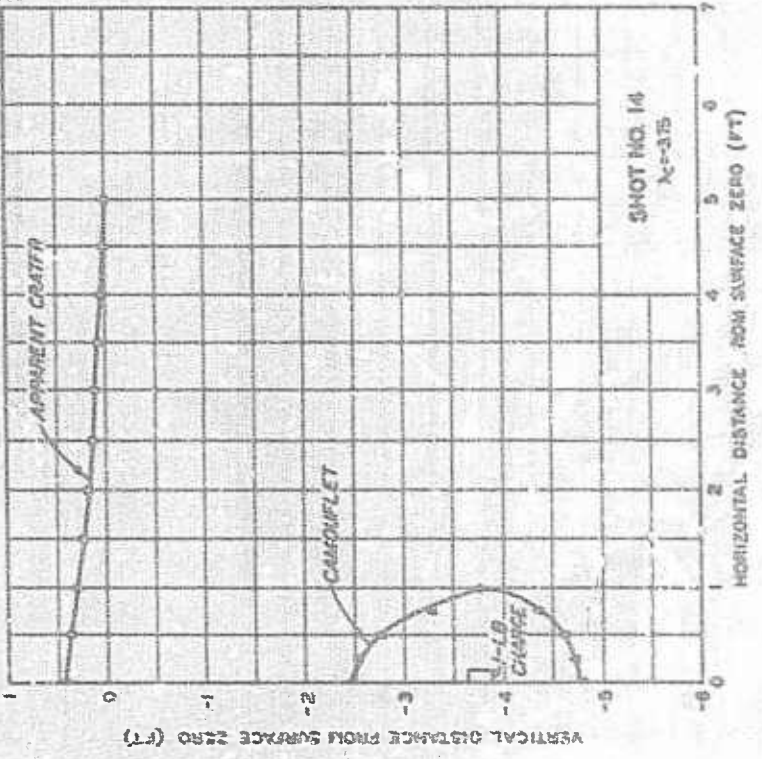


PLATE 7



SHOT NO.	CRATER DIMENSIONS							
	APPARENT CRATER	TRUE CRATER	CAMOUFLAGE	d	s	h	A	V
11	+0.0	0.00						
12	-0.5	0.00						

HALF-CRATER PROFILES
SOIL MATERIAL-LOESS
SHOTS NOS. 11 AND 12



SHOT NO.	CRATER DIMENSIONS						CAMOUFLAGE			
	APPARENT CRATER			TRUE CRATER						
N	S	A	V	d	a	V	D ₁	D ₂	t	v
13	0.31	0.60	-	-	-	-	2.11	2.00	1.34	4.43
14	0.45	1.20	-	-	-	-	2.30	2.00	1.44	4.45

HALF-CRATER PROFILES
SOIL MATERIAL-LOESS
SHOTS NOS. 13 AND 14

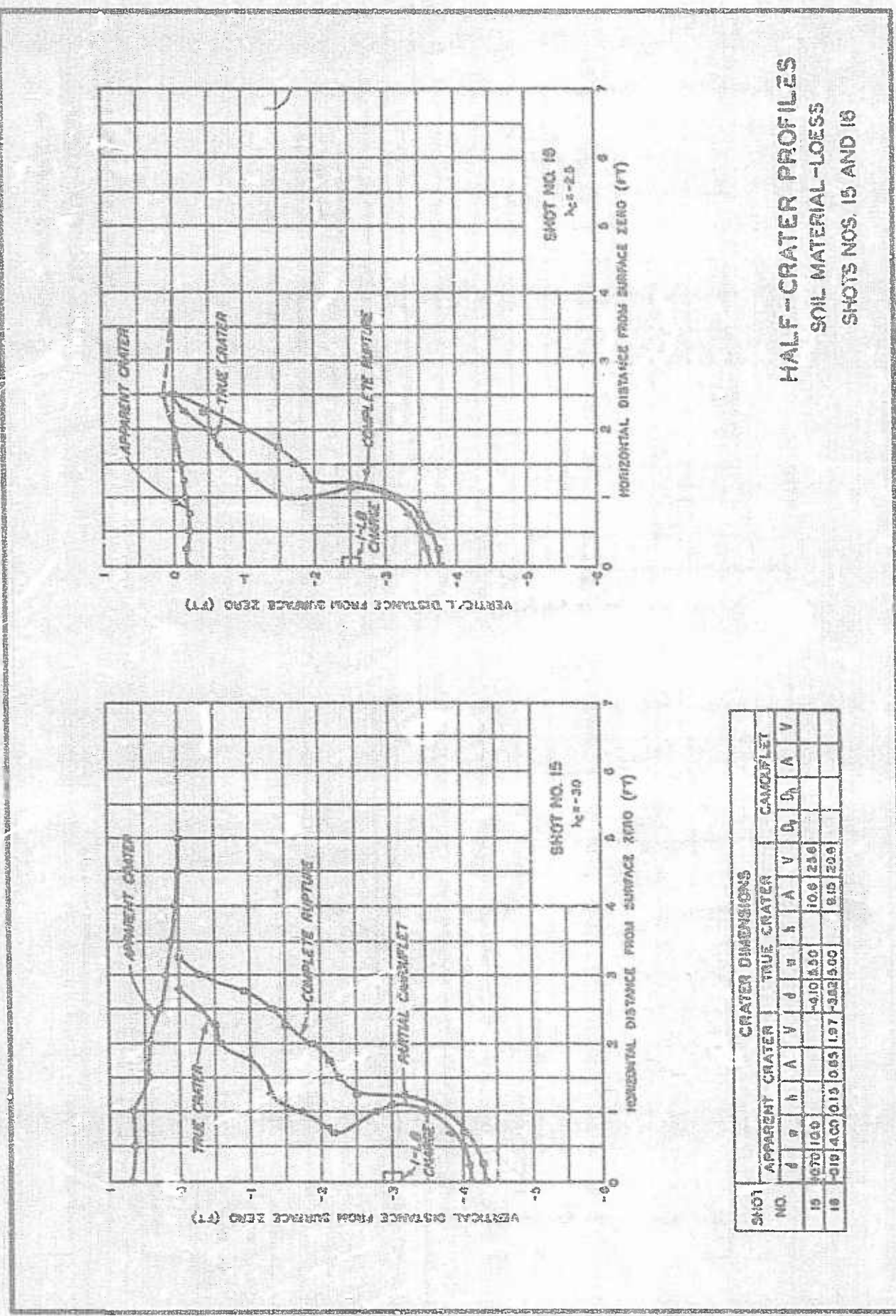
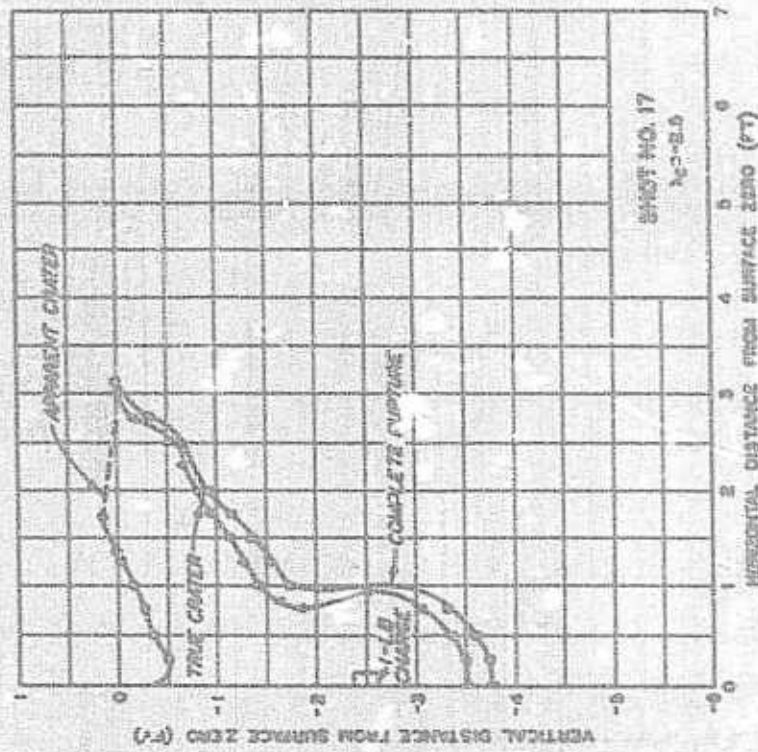
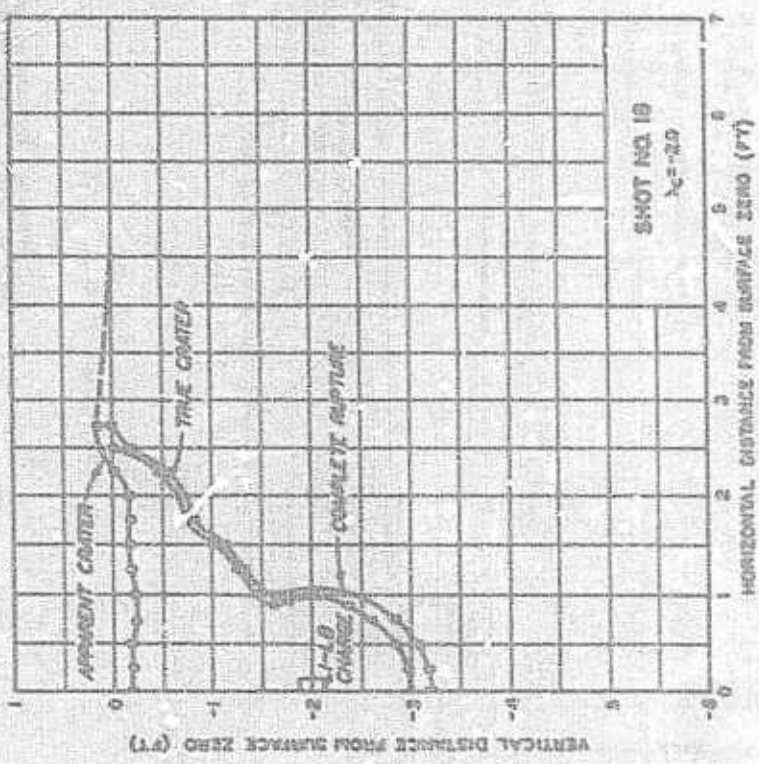


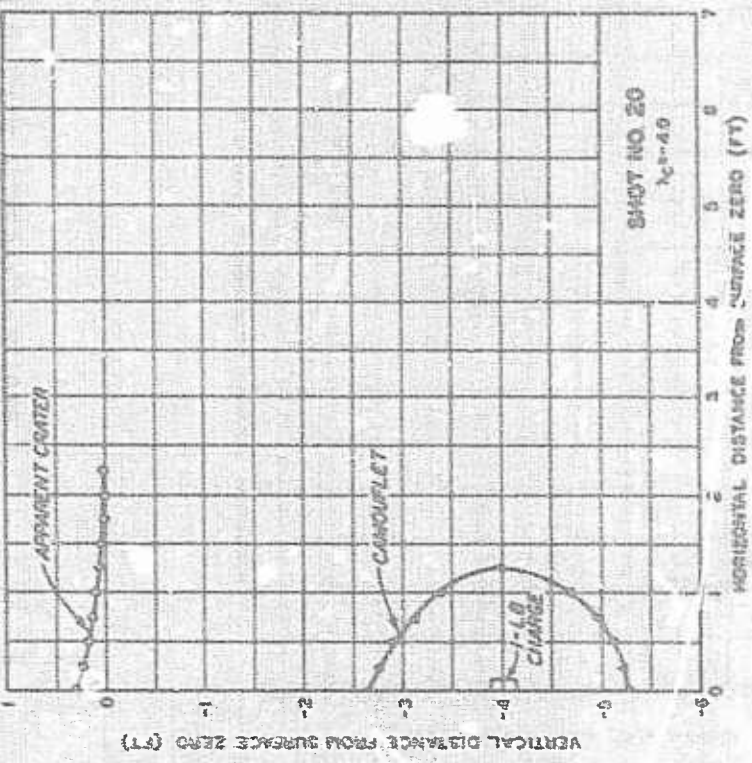
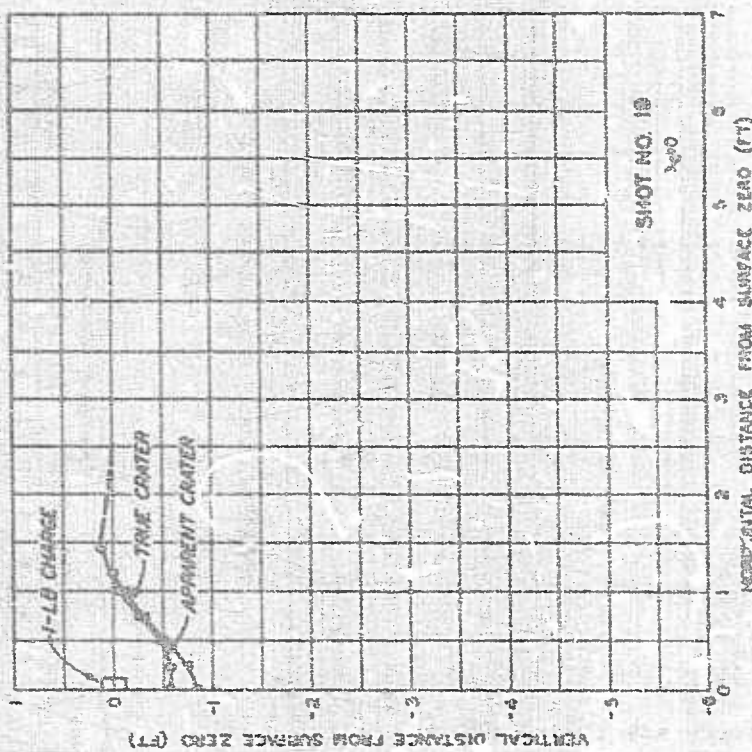
PLATE 10



SHOT NO.	CRATER DIMENSIONS								
	APPARENT CRATER	TRUE CRATER	CAPACITY						
d	s	h	A	V	d	s	h	A	V
16	2.70	0.05	0.74	1.15	-1.08	0.00	0.37	2.57	
17	2.70	0.15	0.74	1.15	-1.08	0.00	0.37	2.57	
18	4.10	0.15	0.65	2.05	-2.25	0.00	0.70	7.90	1.0

HALF-CRATER PROFILES
SOIL MATERIAL-LGESS
SHOTS NOS. 17 AND 18

PLATE II



SHOT NO.	CRATER DIMENSIONS						CANONLET			
	d	s	b	A	V	I	a	b	A	V
19	0.056	2.40	0.15	0.64	101	0.041	2.40	—	0.49	110
20	0.051	4.30	0.14	—	—	—	—	2.50	2.50	474 182

HALF-CRATER PROFILES
SOIL MATERIAL - LOESS
SHOTS NOS. 19 AND 20

HALF-CRATER PROFILES
SOIL MATERIAL - LOESS
SHOTS NOS. 21 AND 22

SHOT NO.	APPROXIMATE CRATER DIAMETER (ft)	TRUE CRATER DIAMETER (ft)	CRATER DEPTH (ft)					
			A	B	C	D	E	F
21	420	100	0.0	2.3	3.5	4.5	5.5	6.5
22	440	102	0.0	3.4	4.6	5.6	6.6	7.6

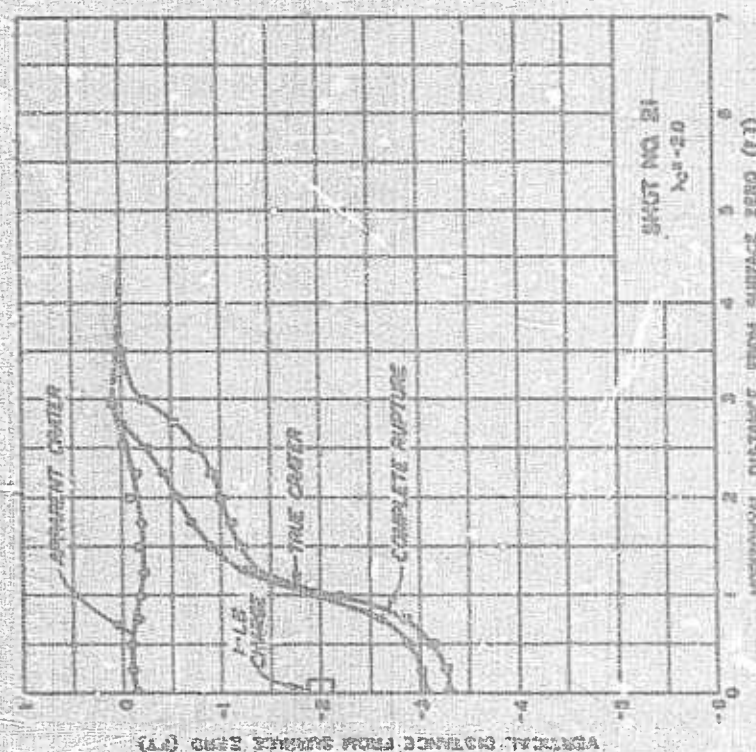
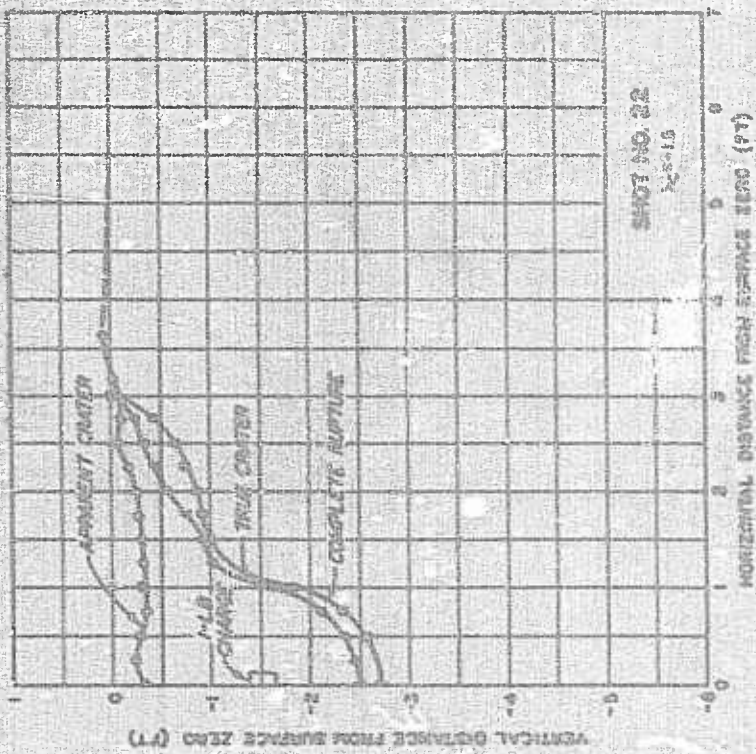
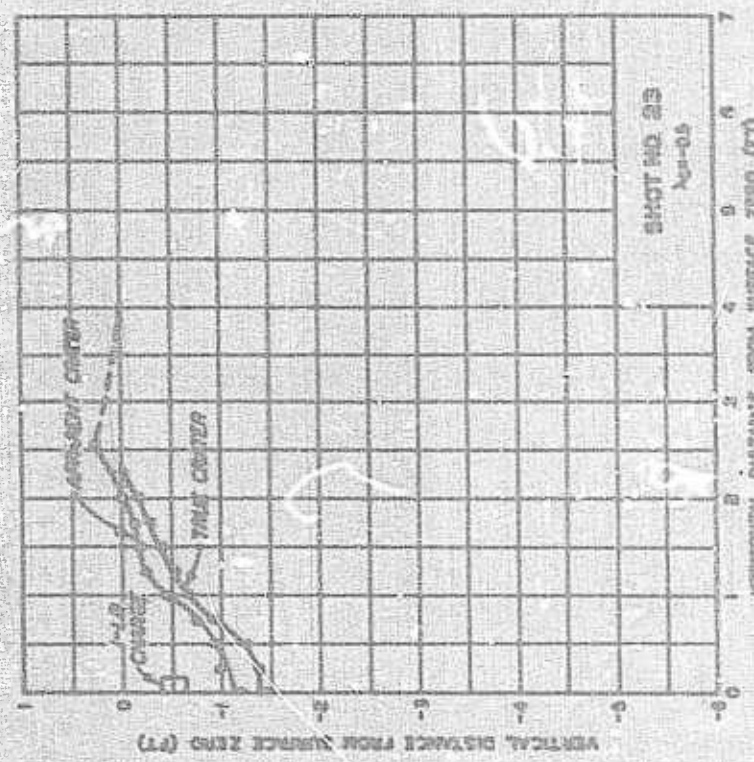
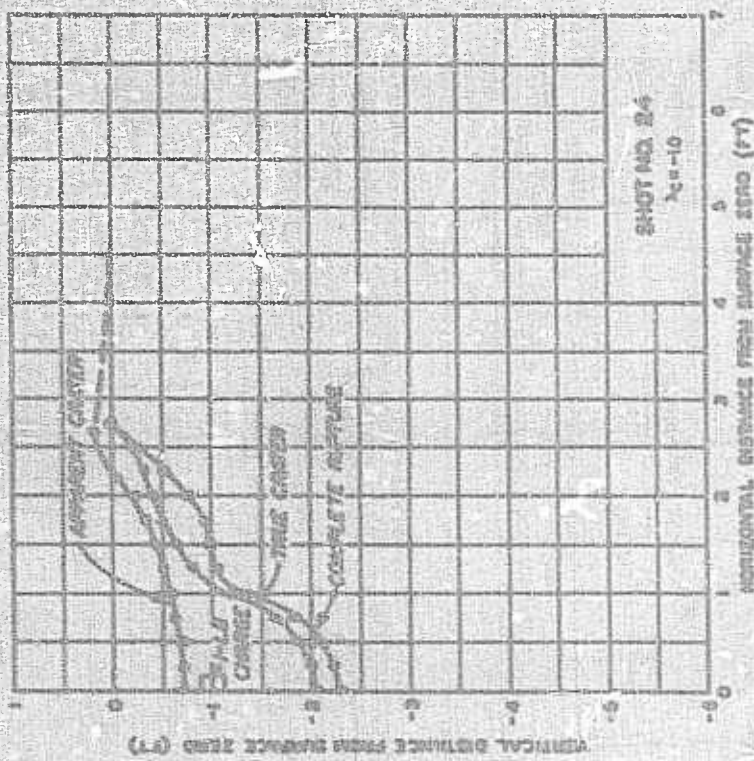


PLATE 13

HALF-CRATER PROFILES
SOIL MATERIAL - LOESS
SHOTS NOS 23 AND 24

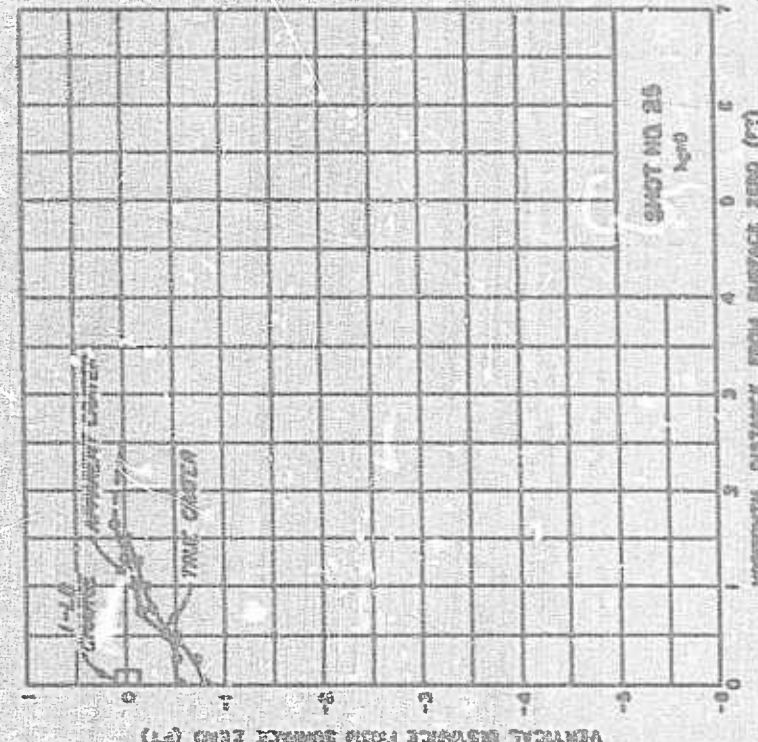
SHOT NO.	CRATER DIMENSIONS							
	A	B	C	D	E	F	G	H
23	4.00	1.00	2.00	4.00	1.00	4.00	4.00	2.00
24	4.00	0.75	5.00	6.00	2.00	5.00	5.00	3.00



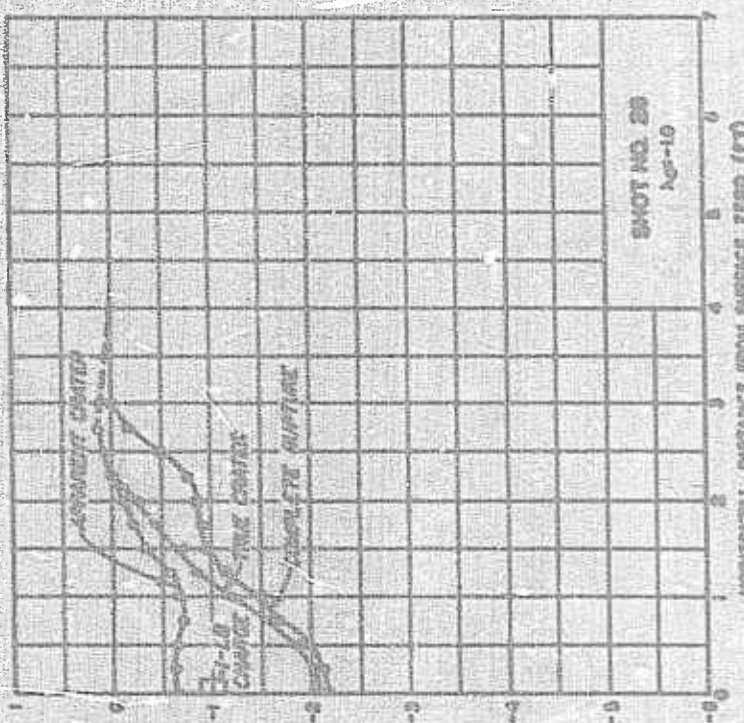
HALF-CRATER PROFILES
SOIL MATERIAL - LOESS
SHOTS NOS. 25 AND 26

SHOT NO.	CRATER DIMENSIONS					CALCULATED
	APPARENT CRATER	TRUE CRATER	V	A	V	
25	0.69290019	0.770600179	2.56	1.03	1.46	
26	-0.69449019	2.155344207	4.90	1.14		

(a) ONE STANDARD DEVIATION PROFILE

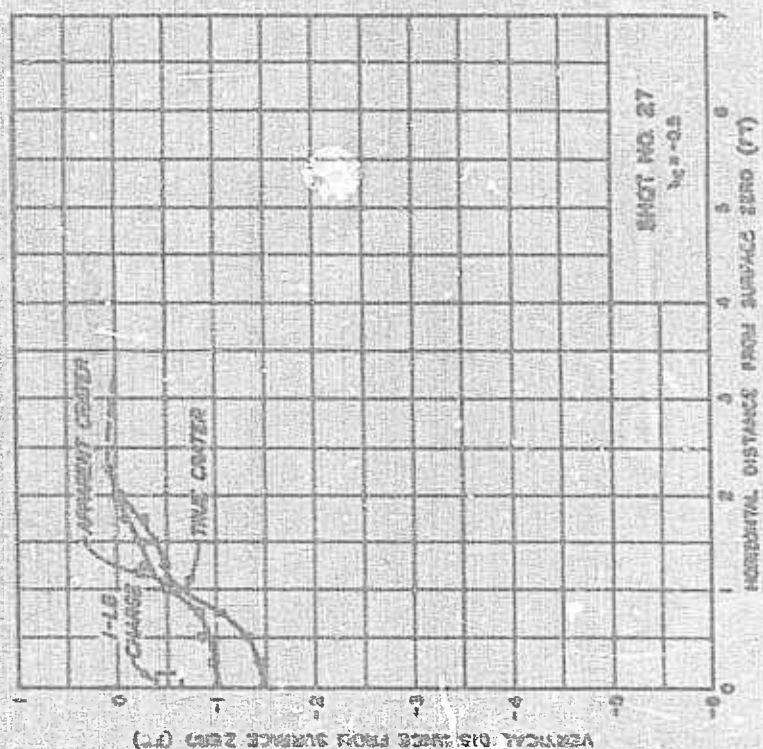


(b) TWO STANDARD DEVIATION PROFILE



(c) THREE STANDARD DEVIATION PROFILE

**HALF-CRATER PROFILES
SOIL MATERIAL-LOESS
SHOTS NOS. 27 AND 28**

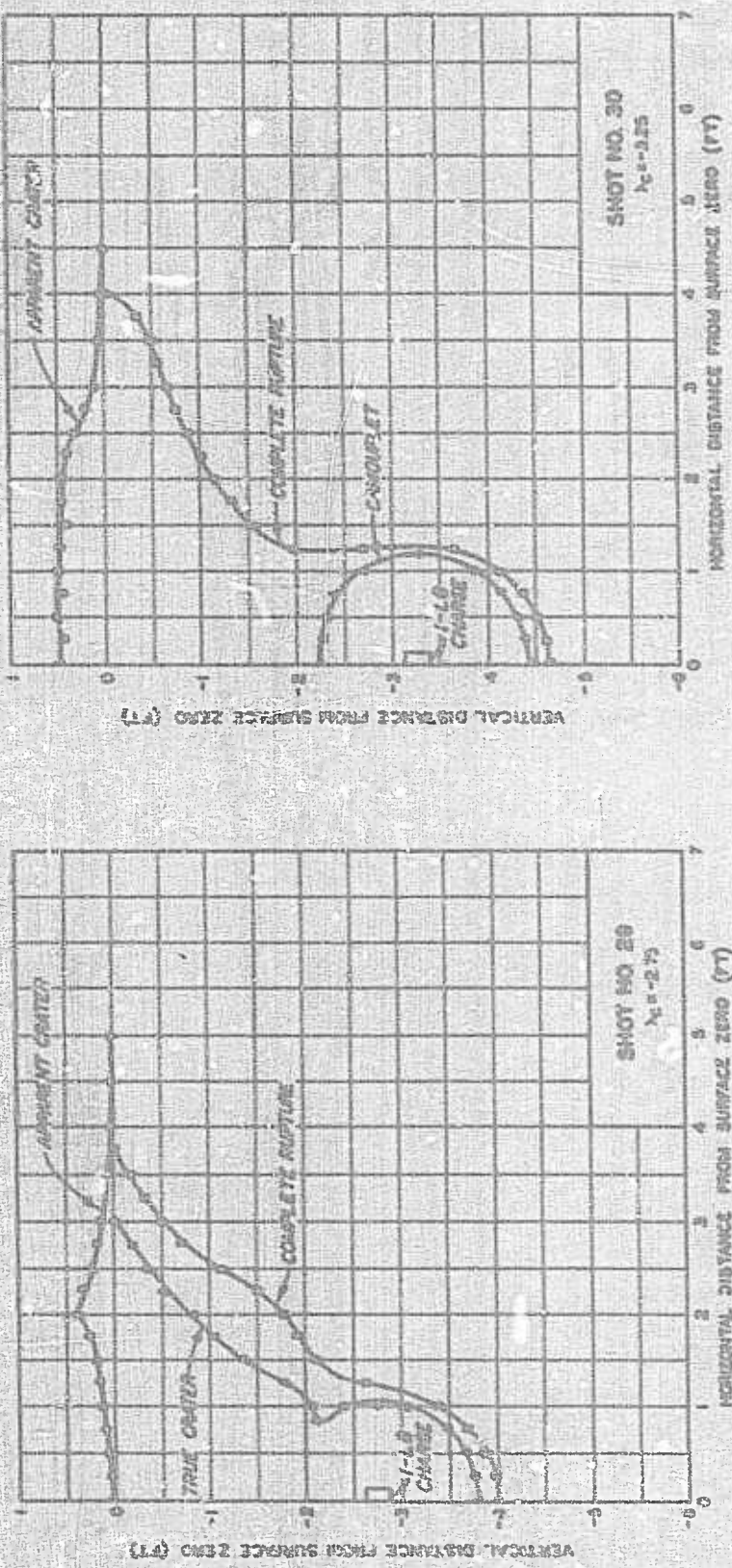


SHOT NO.	CRATER DIMENSIONS						CAMOUFLAGE			
	APPARENT CRATER	TRUE CRATER	CAMOUFLAGE				A	V		
d	b	h	A	V	L	A	V			
27	4.80	4.20	0.10	207.00	-147.400	315.641				
28	0.58	4.60	0.15	1.90	3.66	2.65	5.00	0.74	1.21	

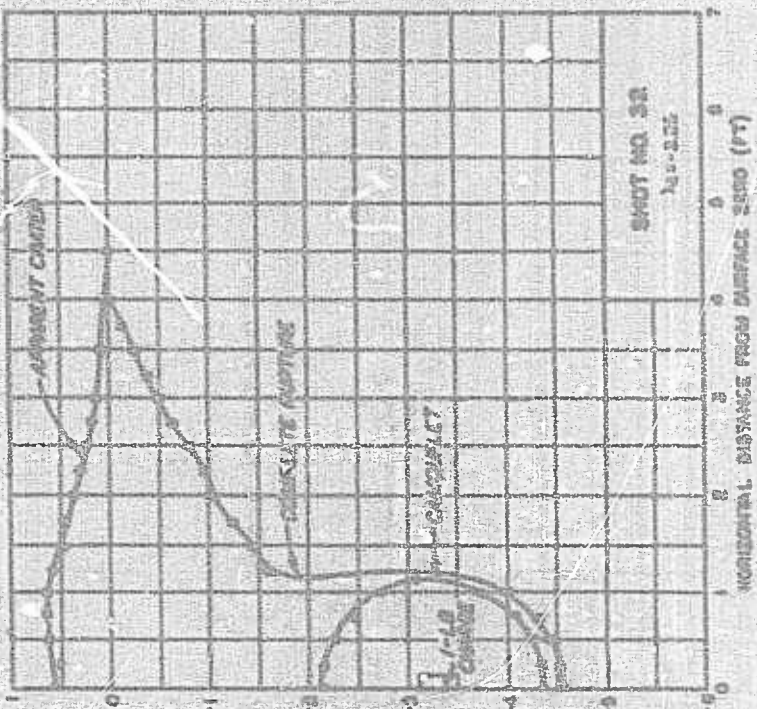
PLATE 16

**HALF-CRATER PROFILES
SOIL MATERIAL-LOESS
SHOTS NOS. 29 AND 30**

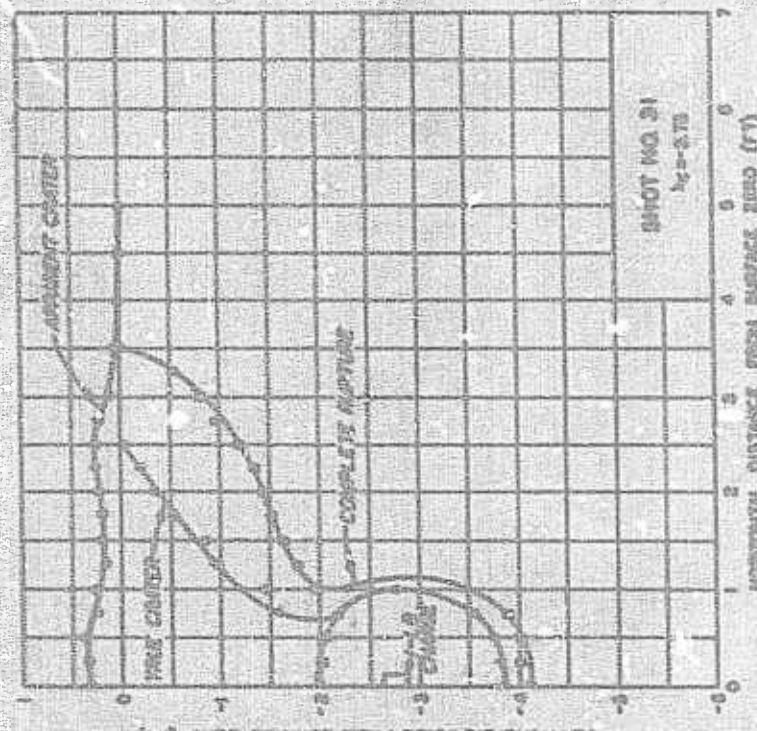
SHOT NO.	CRATER DIMENSIONS						CALCULATED V
	APPARENT CRATER	TRUE CRATER	W	V	U	A	
29	10.410	10.0	1.379	0.00	1.062	0.0	2.192
30	10.450	9.00	1.379	0.00	1.062	0.0	2.192



HALF-CRATER PROFILES
SOIL MATERIAL - LOESS
SHOTS NO. 31 AND 32



(a) HALF-CRATER PROFILE SHOT NO. 32



(b) HALF-CRATER PROFILE SHOT NO. 31

SHOT NO.	CRATER PROFILE								
	APPARENT CRATER	TRUE CRATER	CALIBRAT	V	A	V	A	V	A
31	100	100	100	100	100	100	100	100	100
32	100	100	100	100	100	100	100	100	100
	228	229	230	231	232	233	234	235	236

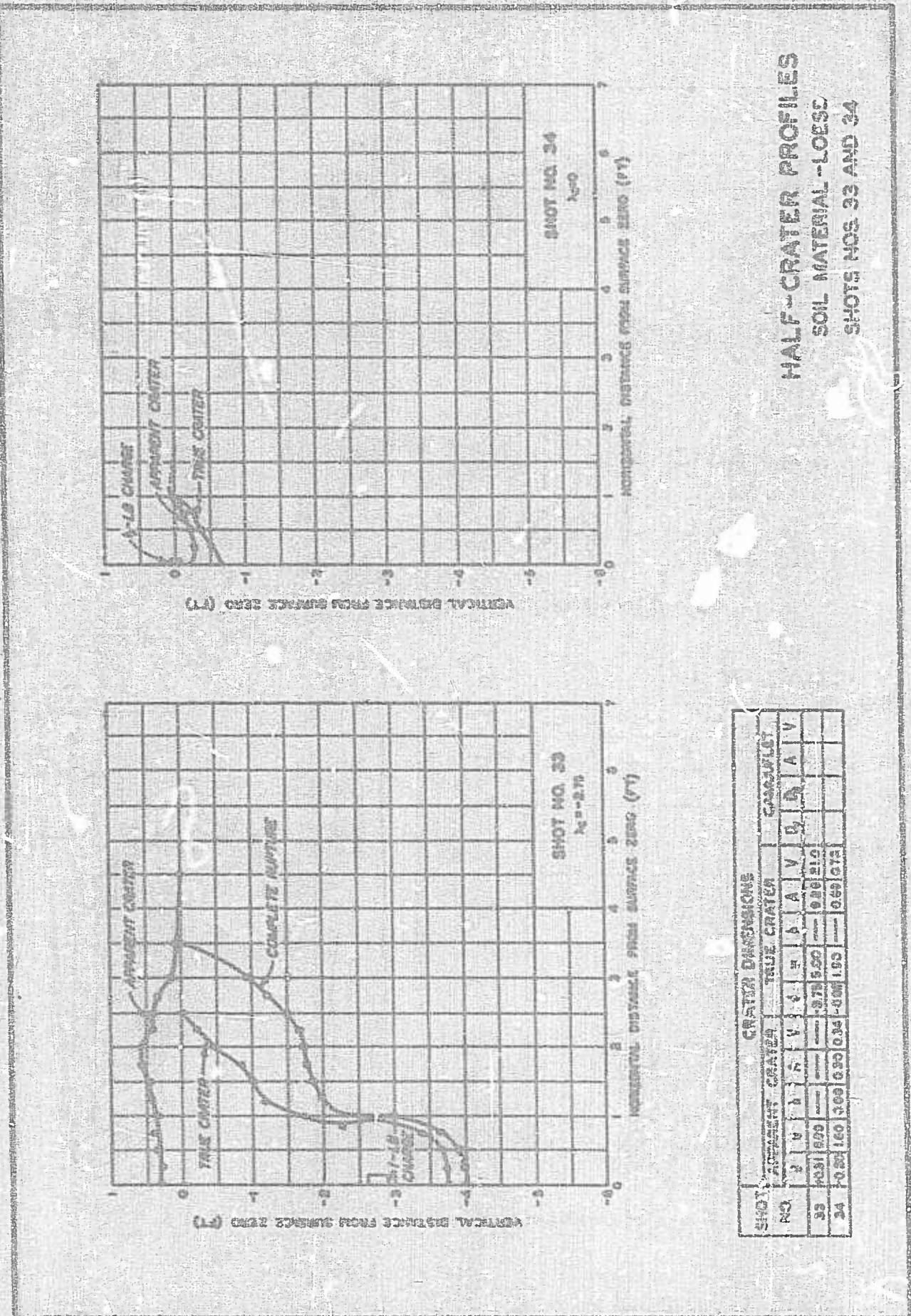
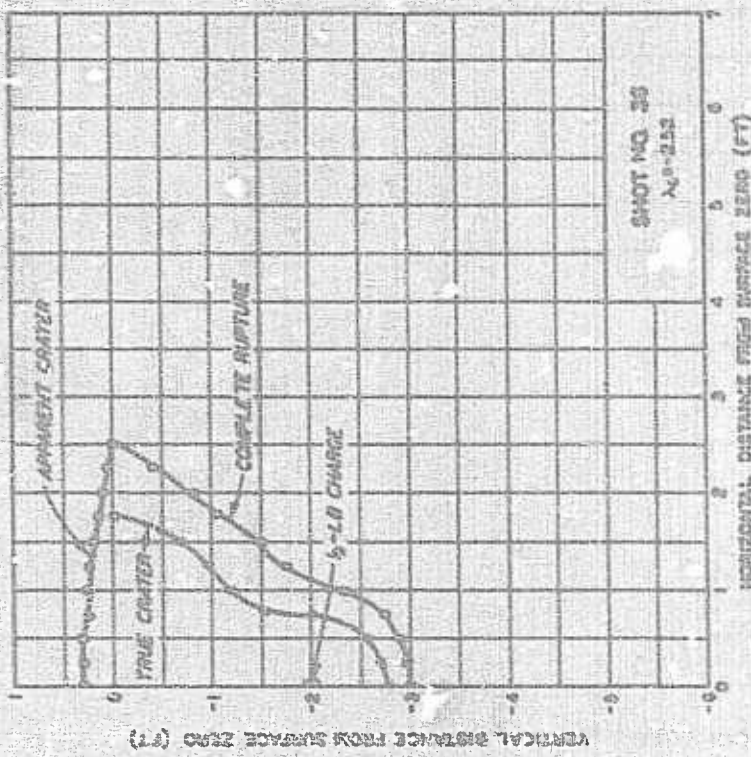
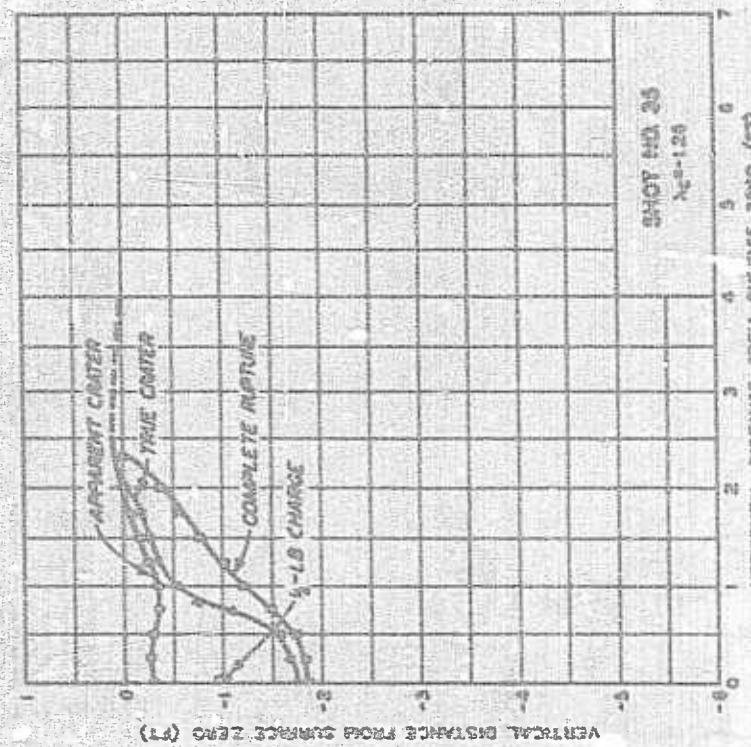
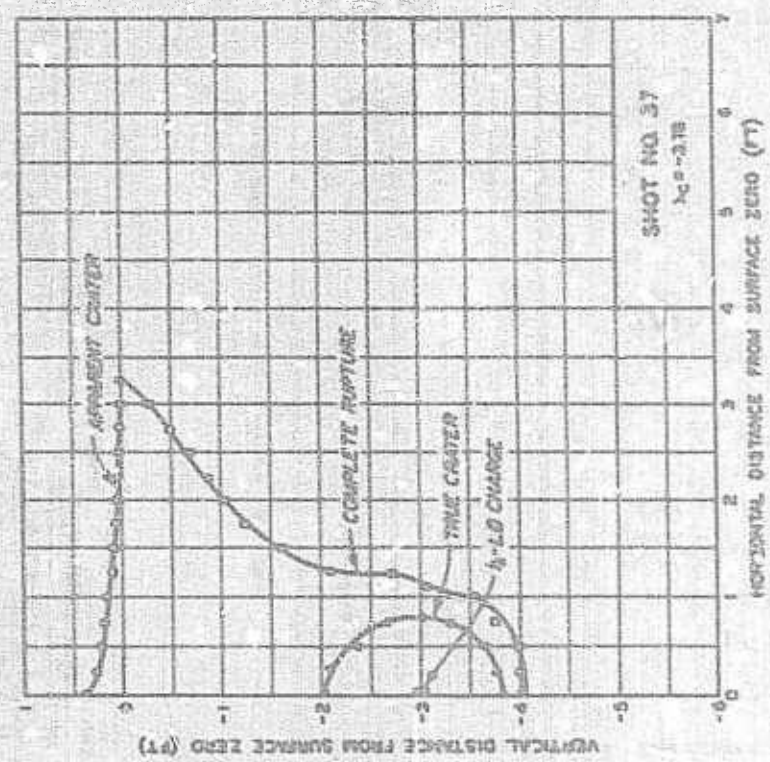
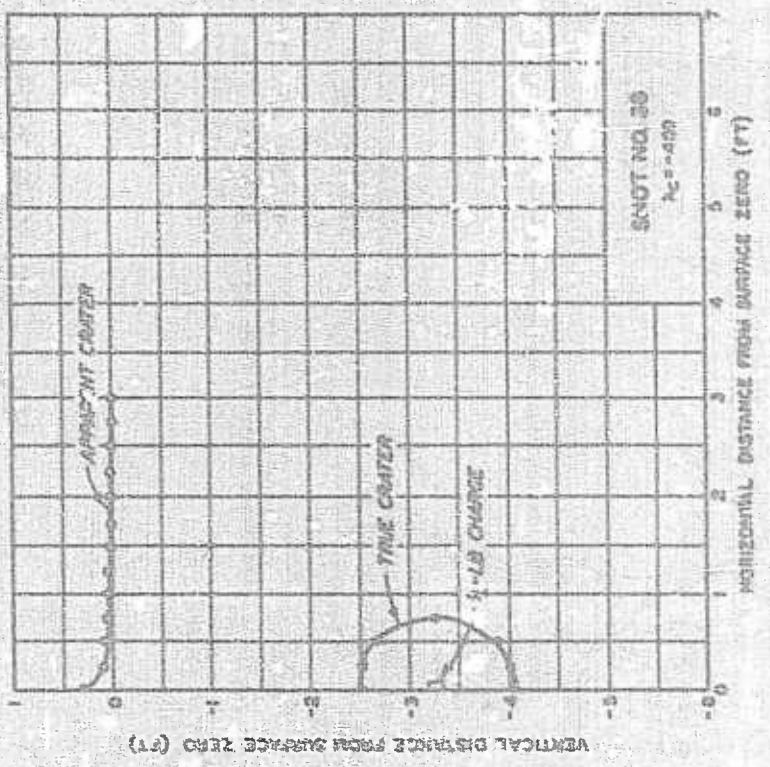


PLATE 10



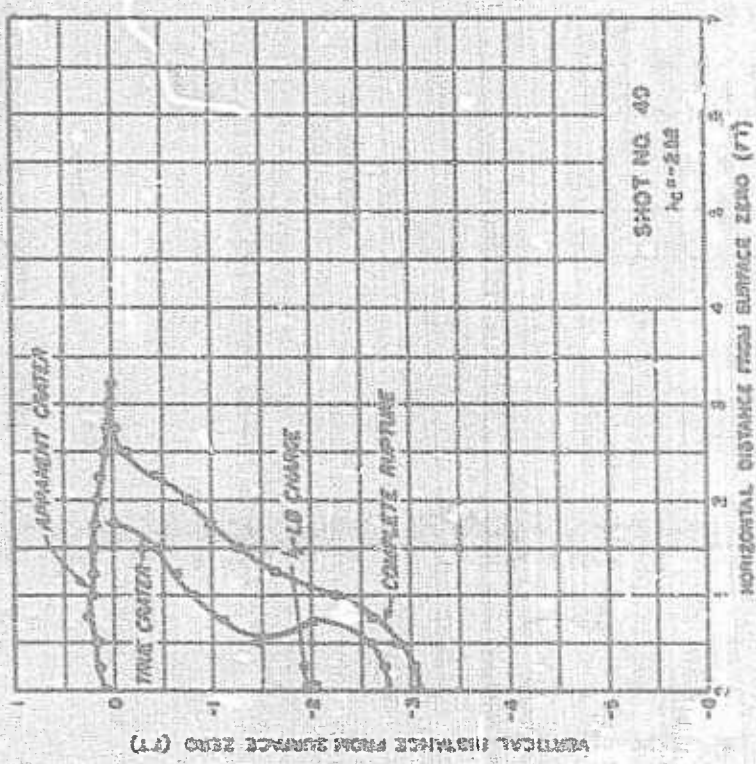
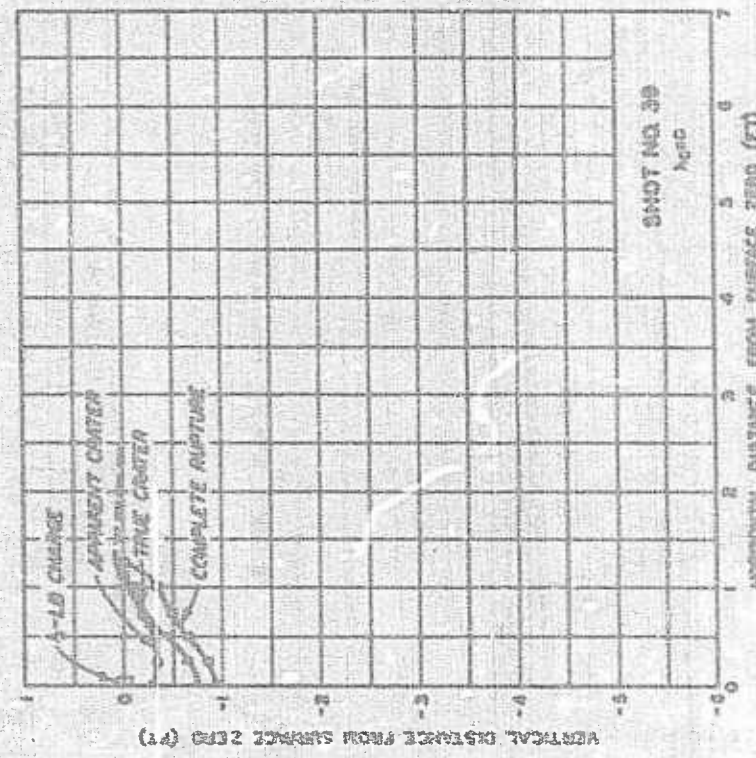
SHOT NO.	CRATER DIMENSIONS						CANTILEVER
	A	B	C	D	E	F	
35	0.31460	0.10110	1.70-1.73	4.00	3.25	5.05	
35	0.283500	1.01111	2.70	3.50	3.70	1.11	

HALF-CRATER PROFILES
SOIL MATERIAL - LOESS
SHOTS NOS. 35 AND 36



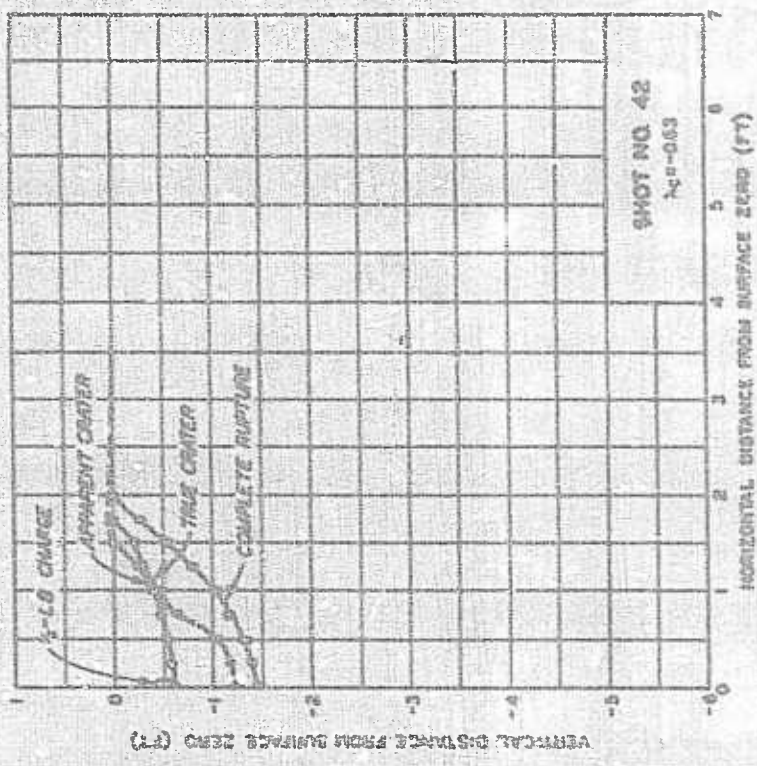
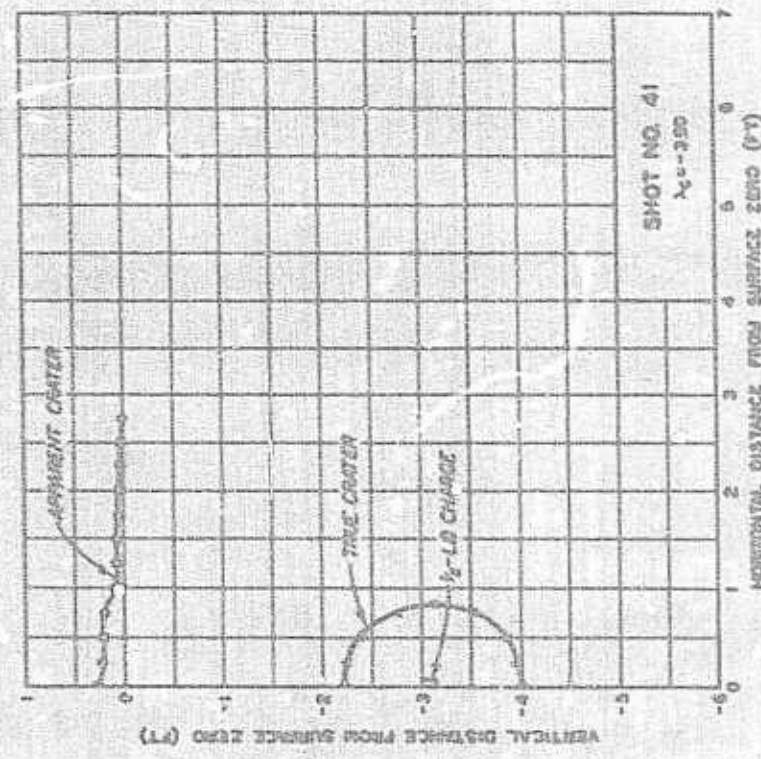
SHOT NO.	CRATER DIMENSIONS						CANNONLET V
	APPARENT CRATER D	A	V	4"	1"	A	
37	0.30	6.00					1.77 (1.63)
38	0.30	6.00					1.60 (1.52)
							1.25
							1.30

HALF-CRATER PROFILES
SOIL MATERIAL - LOESS
SHOTS NOS. 37 AND 38



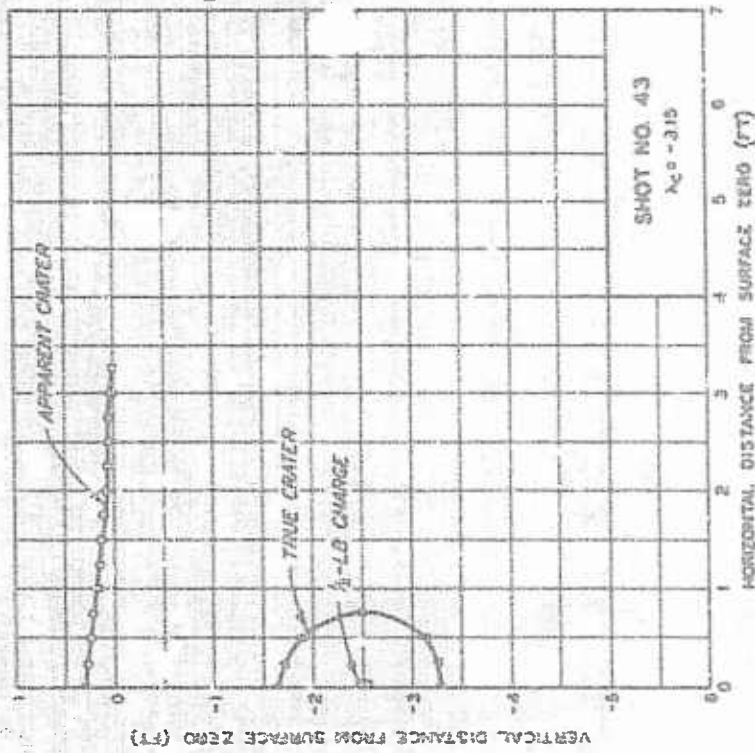
SHOT NO.	CRATER DIMENSIONS						
	APPARENT CRATER	TRUE CRATER	CALIBER FT	A	B	C	D
39	0.270	0.075	0.75	0.75	0.75	0.571	1.10
40	0.277	0.050	0.75	0.75	0.75	0.458	0.85

HALF-CRATER PROFILES
SOIL MATERIAL - LOESS
SHOTS NOS. 39 AND 40

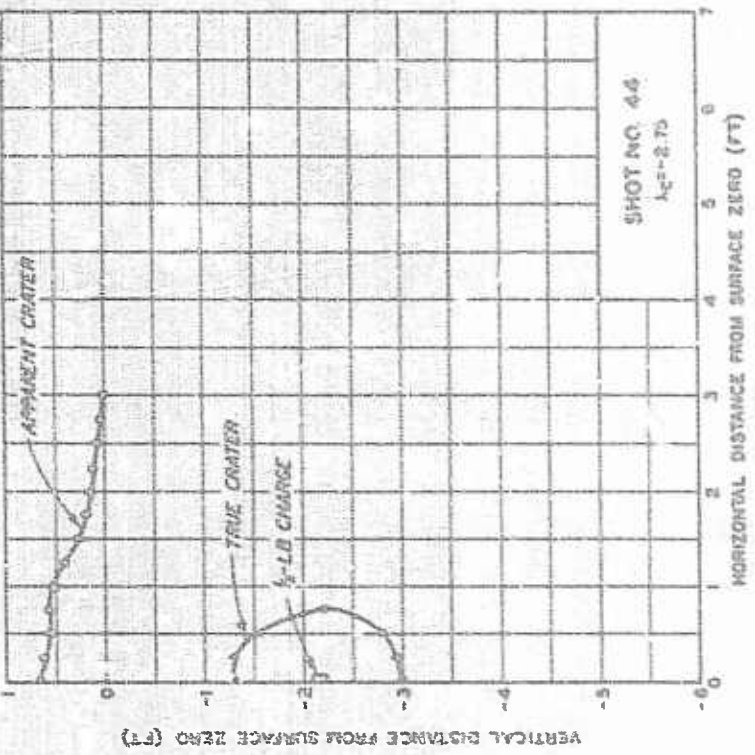


SHOT NO.	CRATER DIMENSIONS						CARTESIAN
	APPARENT CRATER	TRUE CRATER	COMPLETE	V	A	U	
41	0.38	0.41	0.22	2.31	-1.21	3.45	0.92 3.77
42	0.30	0.34	0.22	2.31	-1.21	3.45	0.77 1.72 2.42 2.76

HALF-CRATER PROFILES
SOIL MATERIAL "LOESS
SHOTS NOS. 41 AND 42



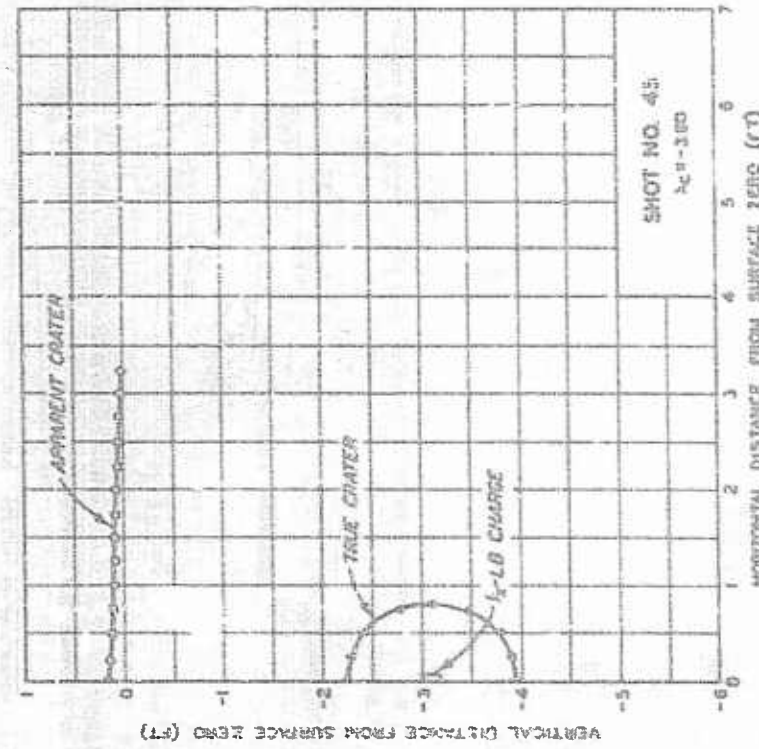
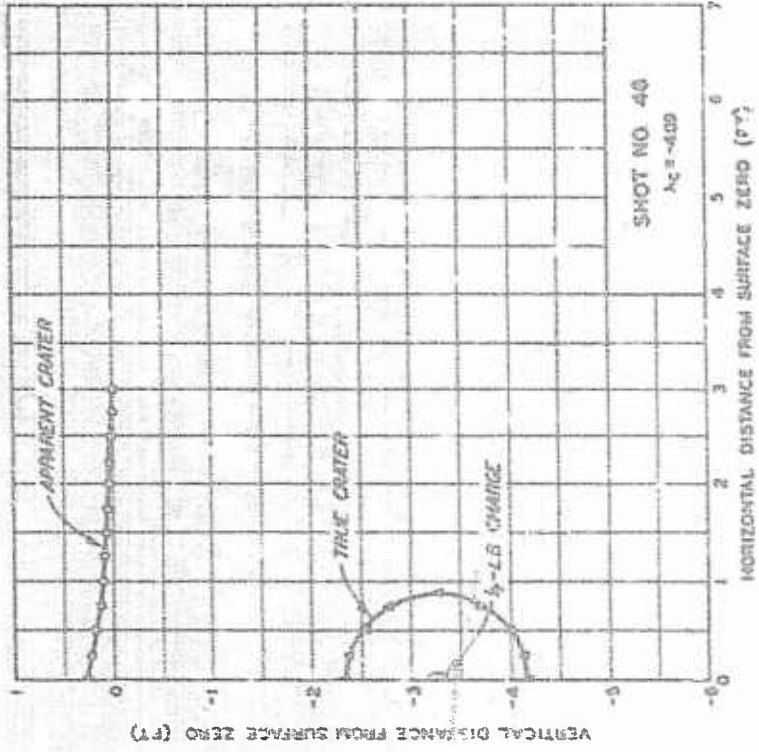
SHOT NO. 43
 $A_c = 3.15$



SHOT NO. 44
 $A_c = 2.75$

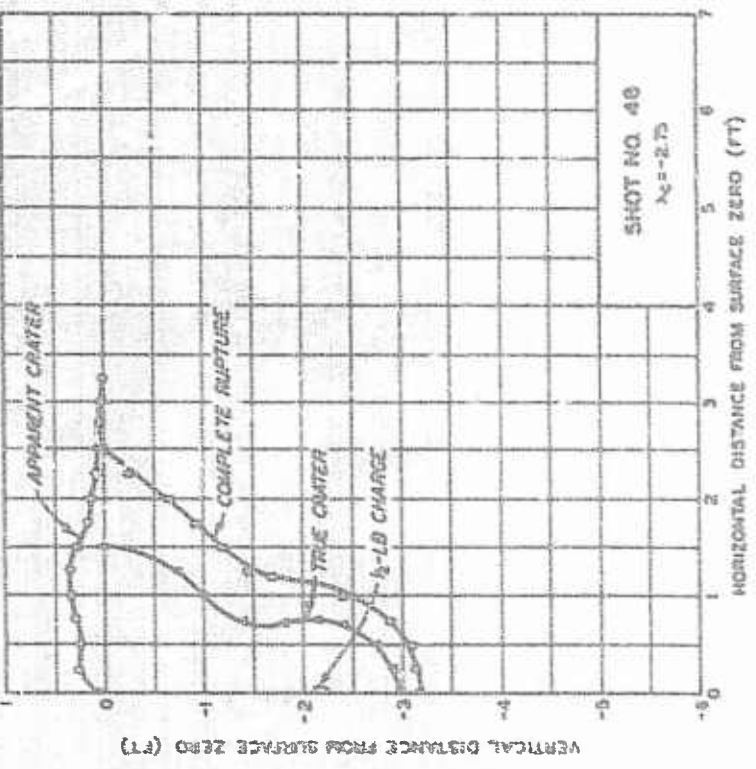
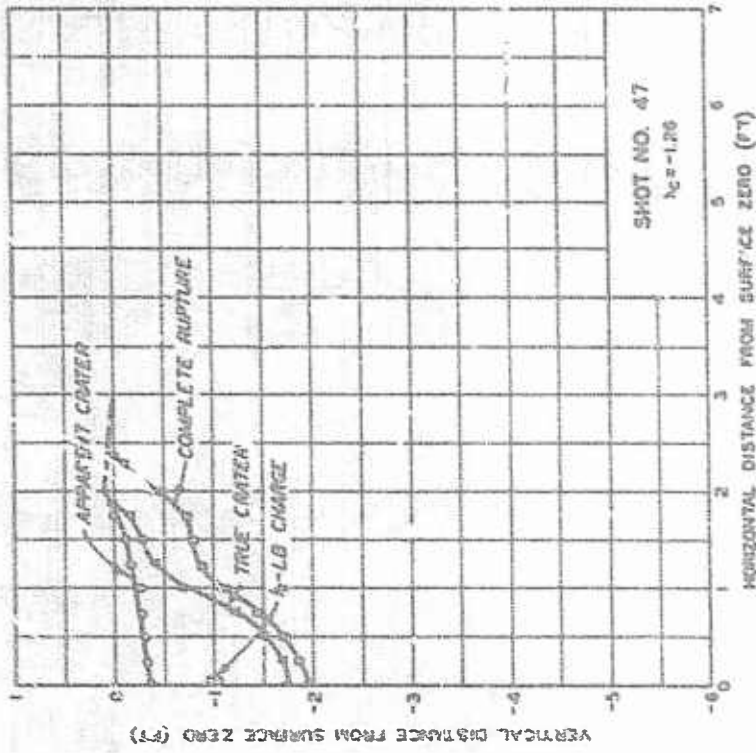
SHOT NO.	CRATER DIMENSIONS							
	APPARENT CRATER	TRUE CRATER	CAMOUFLER	CAMOUFLER	CAMOUFLER	CAMOUFLER	CAMOUFLER	CAMOUFLER
43	0.26	0.50	—	—	—	1.69	1.50	1.05
44	0.07	0.00	—	—	—	1.05	1.50	1.94

HALF-CRATER PROFILES
SOIL MATERIAL-LOESS
SHOT NOS. 43 AND 44



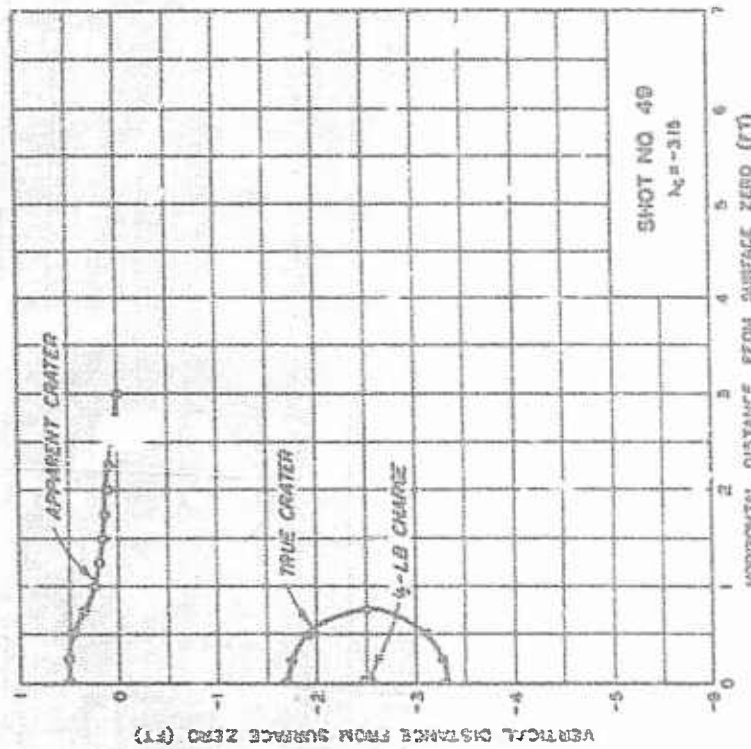
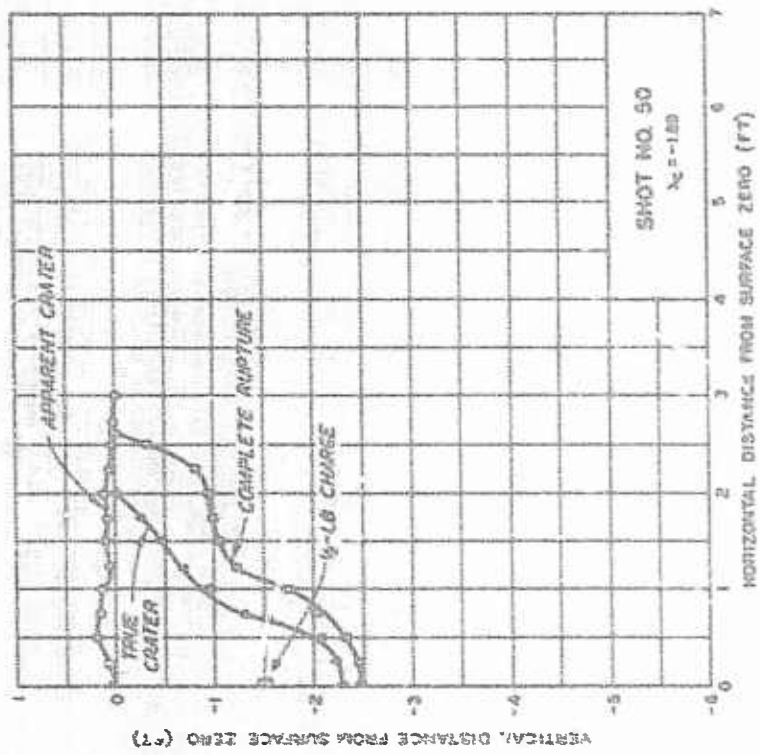
HALF-CRATER PROFILES
SOIL MATERIAL-LOESS
SHOTS NOS. 45 AND 46

SHOT NO.	CRATER DIMENSIONS												
	APPARENT CRATER		TRUE CRATER		CAMSULET								
d	a	b	A	V	d	a	b	A	V	D	A	V	
45	0.017	0.50									70	1.00	2.50
46	0.027	0.00									05	1.00	2.52



SHOT NO.	CRATER GRADIENTS							
	APPARENT CRATER	TRUE CRATER	CANIOUTLET	V	A	B	C	D
47	-0.25	0.01	0.01	0.75	1.54	1.73	3.76	3.42
48	0.07	0.00			2.93	3.00		5.42
								0.81

HALF-CRATER PROFILES
SOIL MATERIAL - LOESS
SHOTS NOS. 47 AND 48



**HALF-CRATER PROFILES
SOIL MATERIAL - LOESS
SHOTS NOS. 49 AND 50**

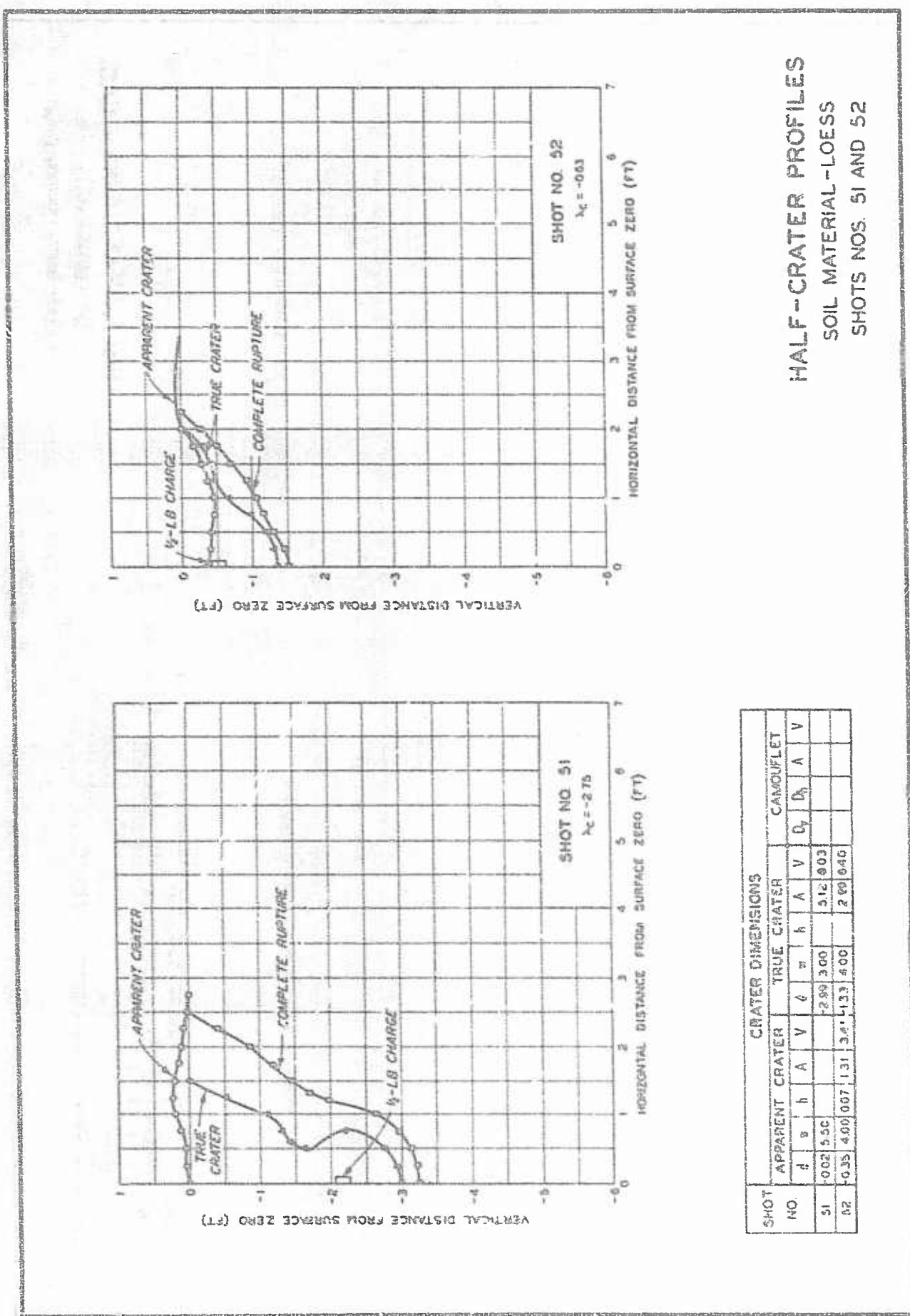
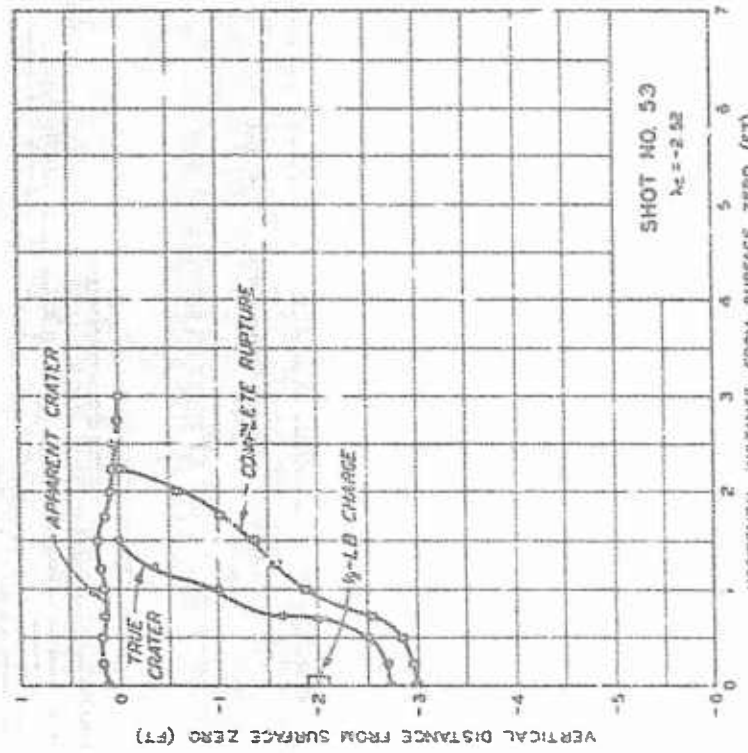
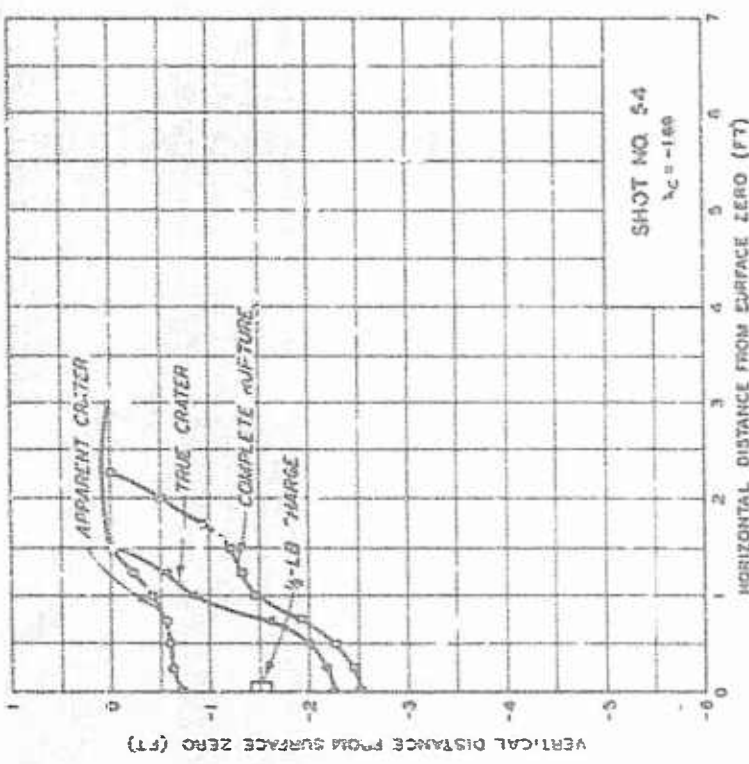


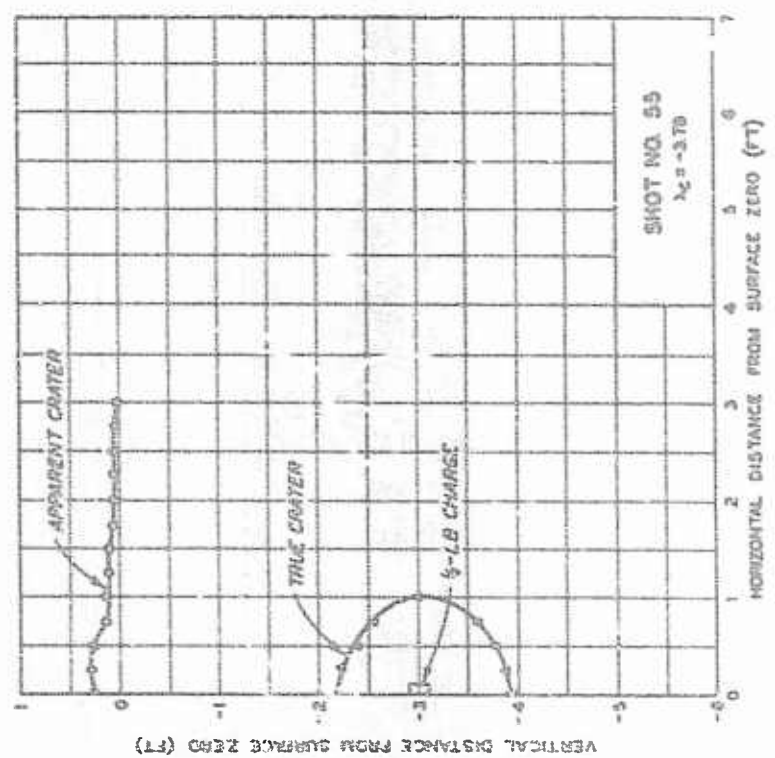
PLATE 28



SHOT NO.	CRATER DIMENSIONS								
	APPARENT CRATER	TRUE CRATER	CAMOUFLAGE	d	y	h	A	V	D
53	102.000	102.000	102.000	-2.74	3.00	4.84	7.40		
54	0.70.300.000	1.34	2.36	2.22	3.00	4.13	6.61		

HALF-CRATER PROFILES
SOIL MATERIAL - LOESS
SHOTS NOS. 53 AND 54

PLATE 30

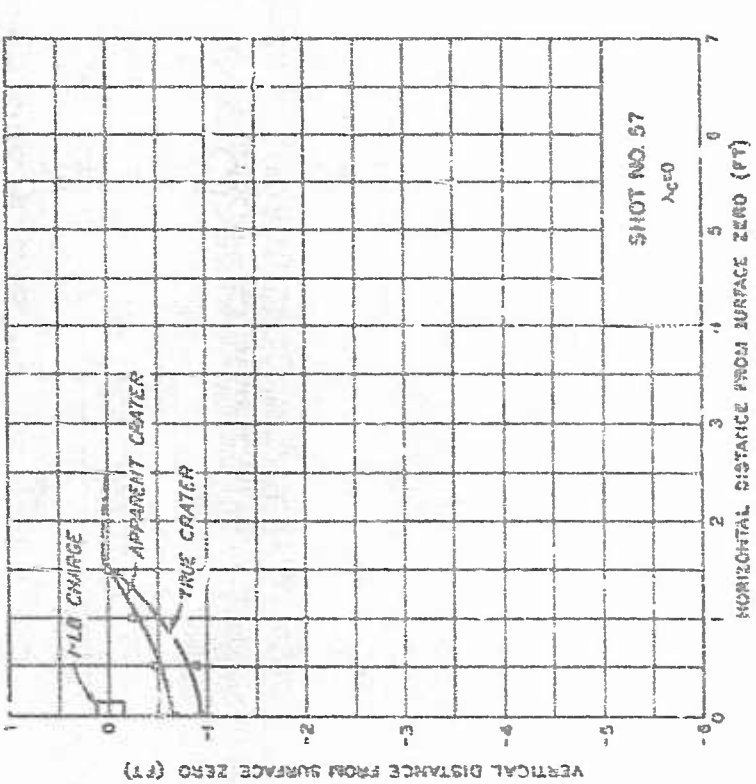
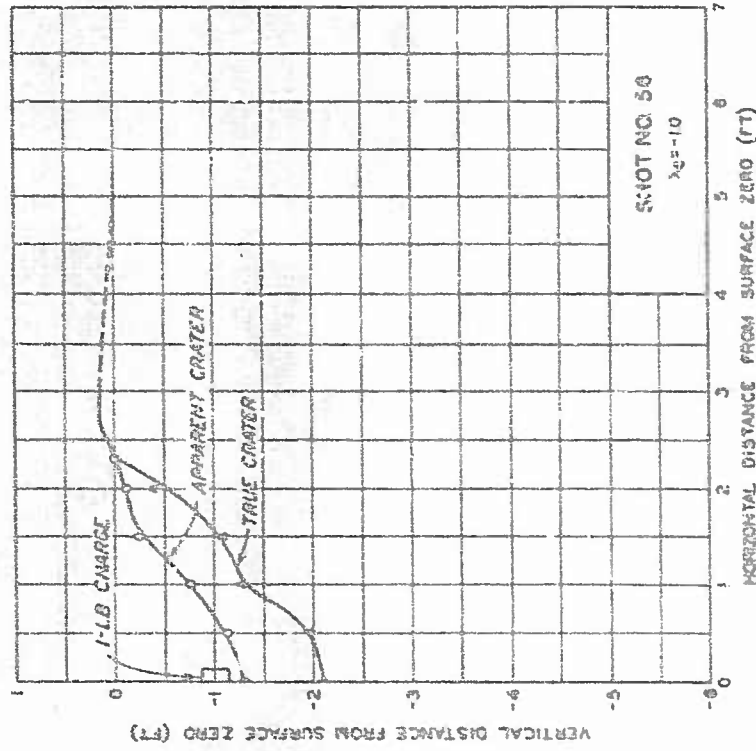


SHOT NO. 55
 $\lambda_2 = -3.75$

HORIZONTAL DISTANCE FROM SURFACE ZERO (FT)

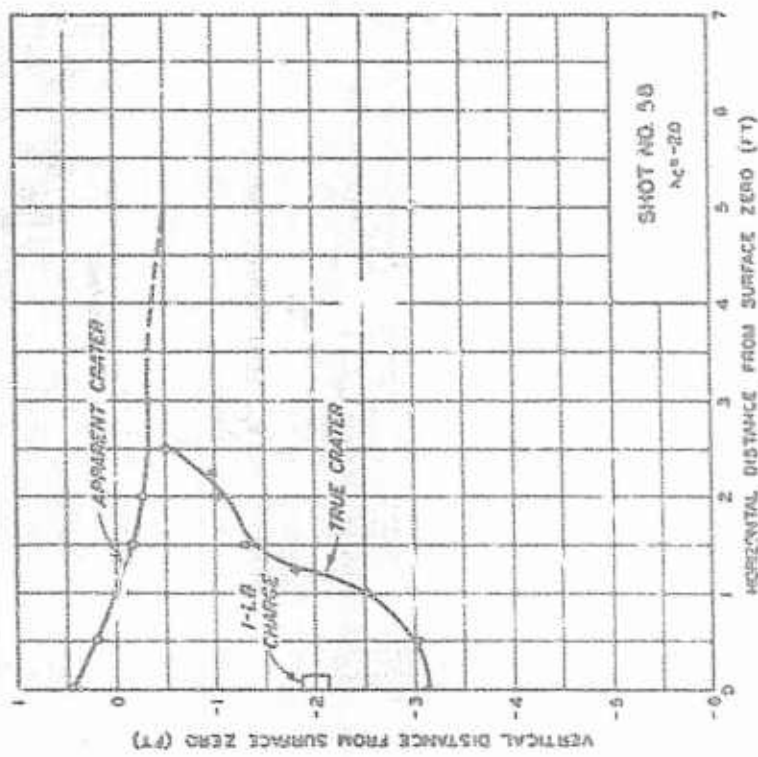
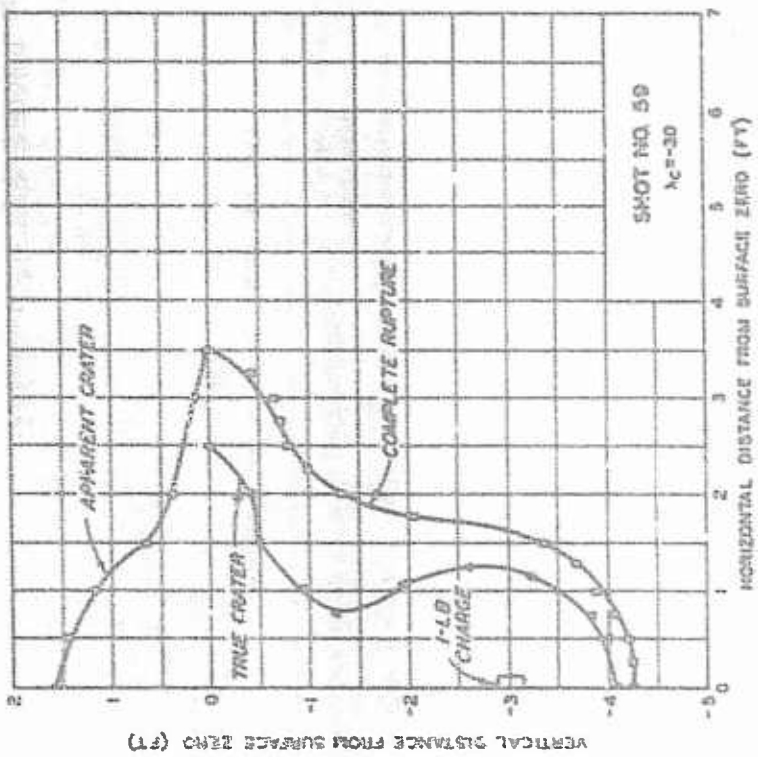
SHOT NO.	CRATER DIMENSIONS										CAMOUFLAGE				
	d	w	h	A	V	d	w	h	A	V	d	w	h	A	V
55	5.26	0.00	—	—	—	—	—	—	—	—	1.74	1.58	2.46	2.74	—

HALF-CRATER PROFILES
SOIL MATERIAL - LOESS
SHOT NO. 55



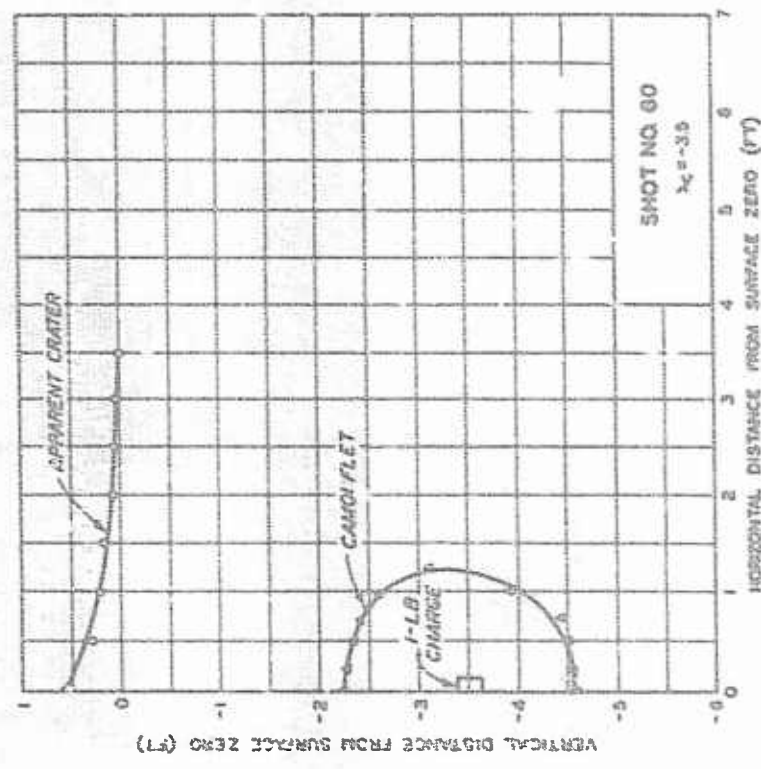
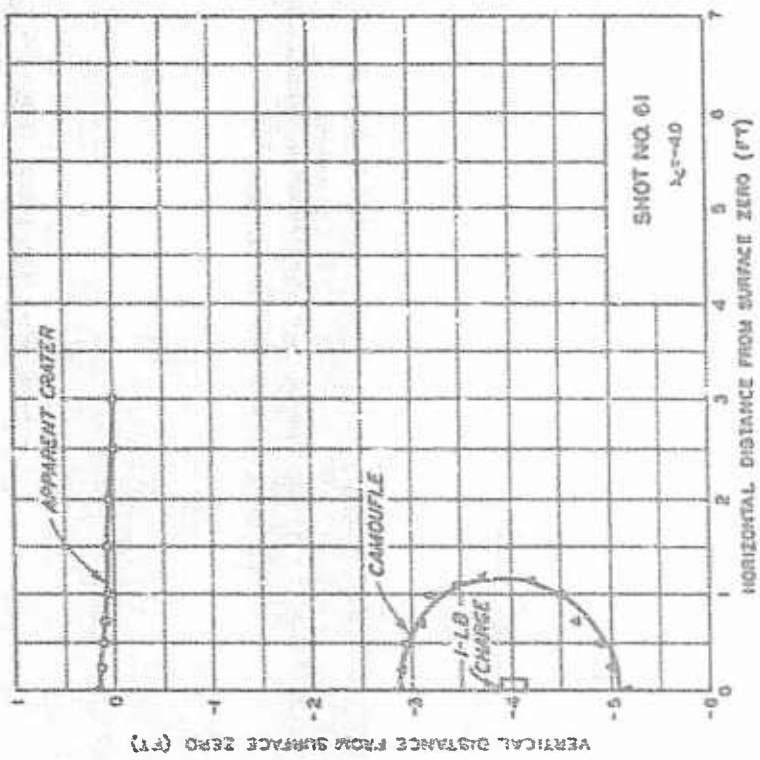
SHOT NO.	CRATER DIMENSIONS											
	APPARENT CRATER		TRUE CRATER		CAROUFLÉ							
d	y	h	A	V	θ	w	A'	V	D ₁	D ₂	A	V
56	-1.36	4.00	0.16	1.12	3.39	-2.04	4.00	3.56	14.0			
57	-0.61	3.60	0.03	1.01	1.03	-0.69	3.60	1.57	2.37			

HALF-CRATER PROFILES
SOIL MATERIAL "CLAY"
SHOTS NOS. 56 AND 57



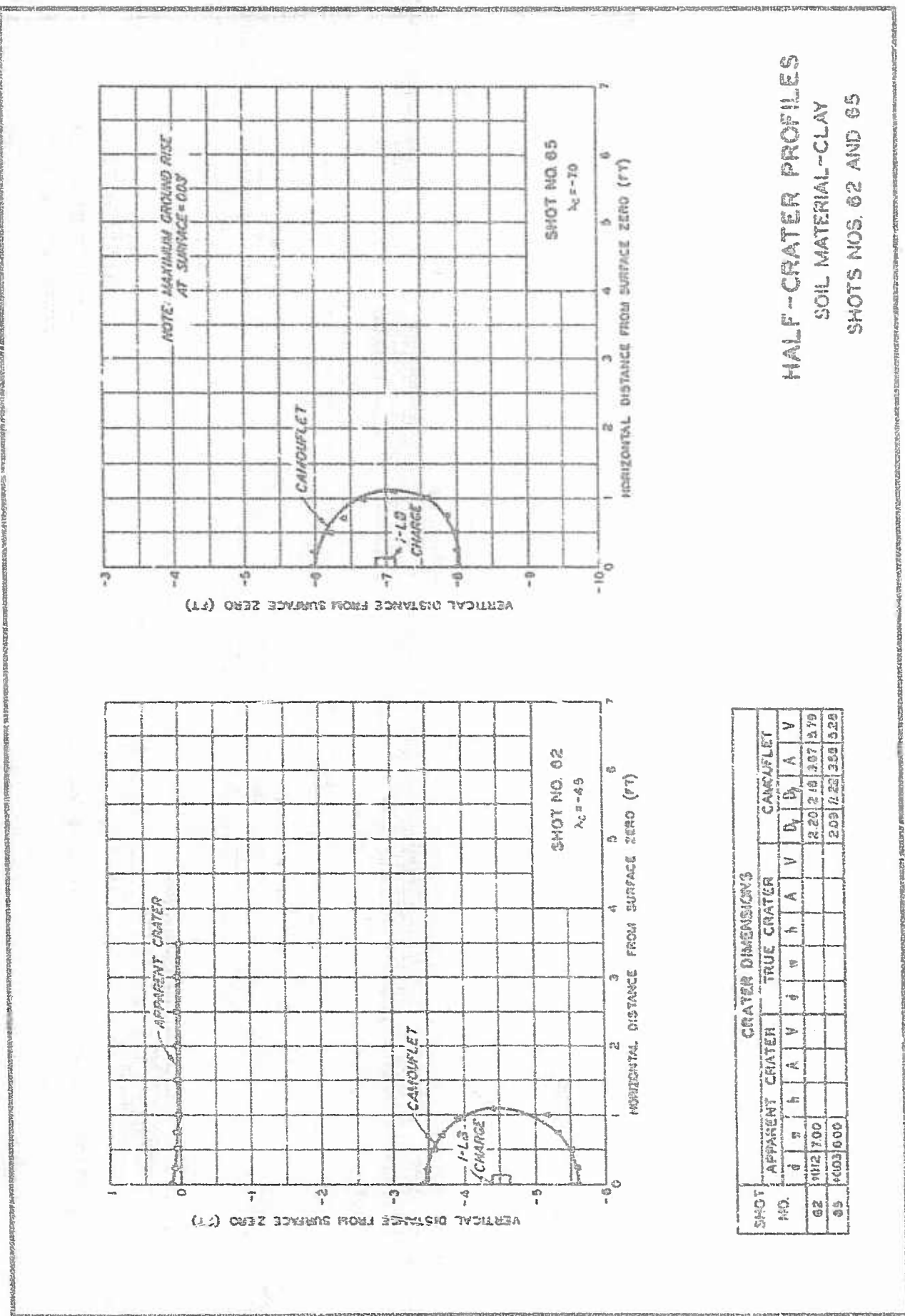
SHOT NO.	CRATER DIMENSIONS													
	APPARENT CRATER			TRUE CRATER			COMPLETE							
	<i>d</i>	<i>a</i>	<i>b</i>	<i>A</i>	<i>V</i>	<i>c</i>	<i>w</i>	<i>b</i>	<i>A</i>	<i>V</i>	<i>D₁</i>	<i>D₂</i>	<i>A</i>	<i>V</i>
59	1044.500	0.200		-311.500		9.60	210							
59	-1.547.00	0.00		-4.025.500		0.35	195							

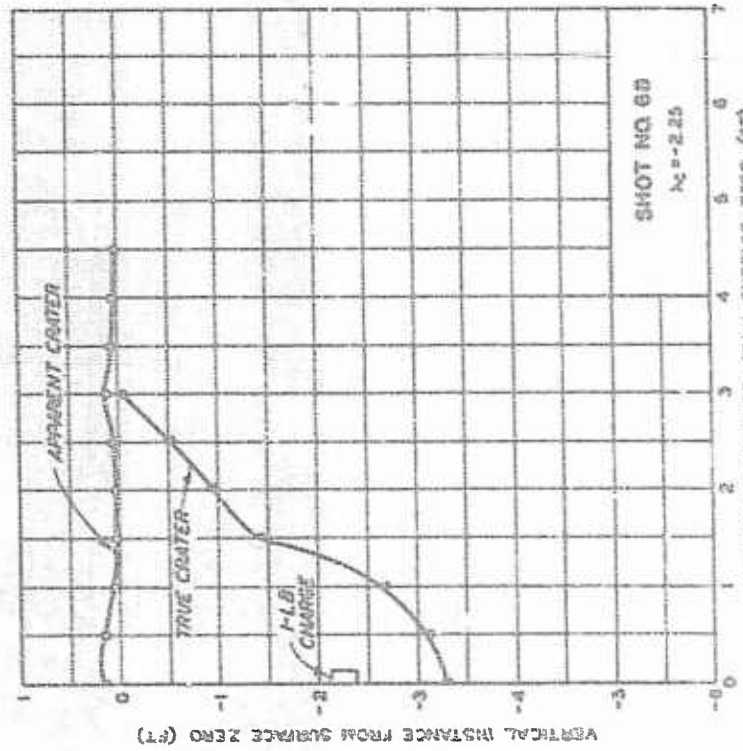
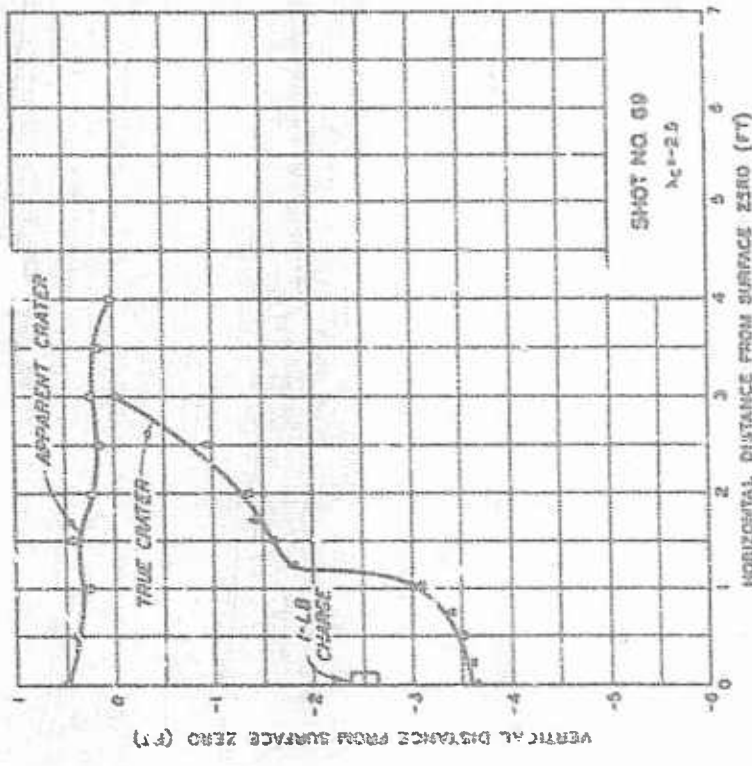
HALF-CRATER PROFILES
SOIL MATERIAL—CLAY
SHOTS NOS. 58 AND 59



SHOT NO.	CRATERS DIMENSIONS													
	APPARENT CRATER			TRUE CRATER			CANNULLE							
	δ	θ	b	A	V	d	w	h	A	V	D_1	D_2	A	V
60	1.15	6.00	7.00								2.35	2.40	6.52	7.17
61	1.15	6.00									2.35	2.40	4.16	6.54

HALF-CRATER PROFILES
SOIL MATERIAL - CLAY
SHOTS NOS. 60 AND 61

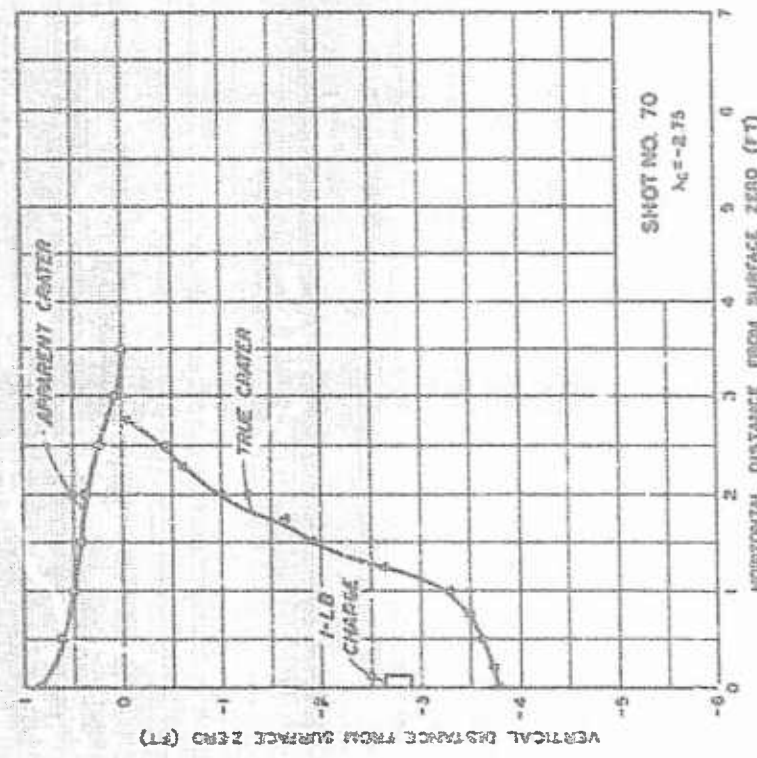
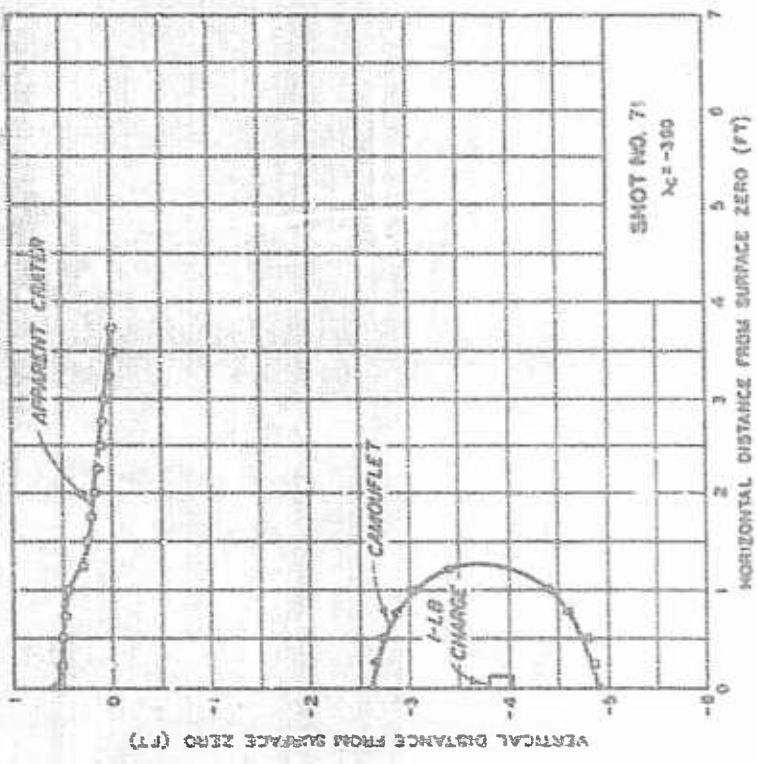




SHOT NO.	CRATER DIMENSIONS						CAMOUFLAGE
	APPARENT CRATER	TRUE CRATER	V	A	Y	B	
68	10.4 160	9.32		1.25 600		1.13 35.4	
69	10.50 600	9.00		1.35 400		1.21 30.6	

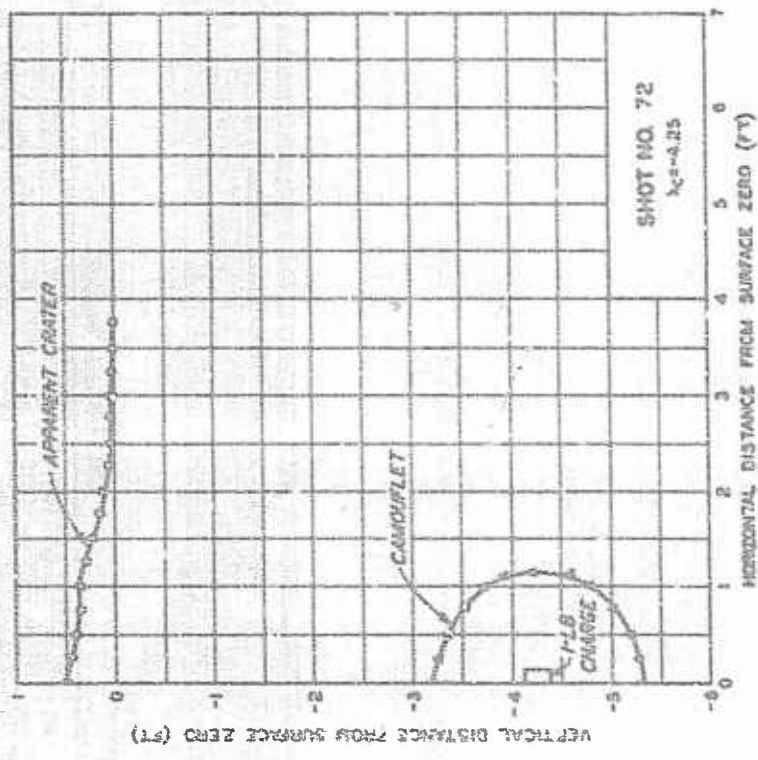
HALF-CRATER PROFILES
SOIL MATERIAL-CLAY
SHOTS NOS. 68 AND 69

PLATE 69



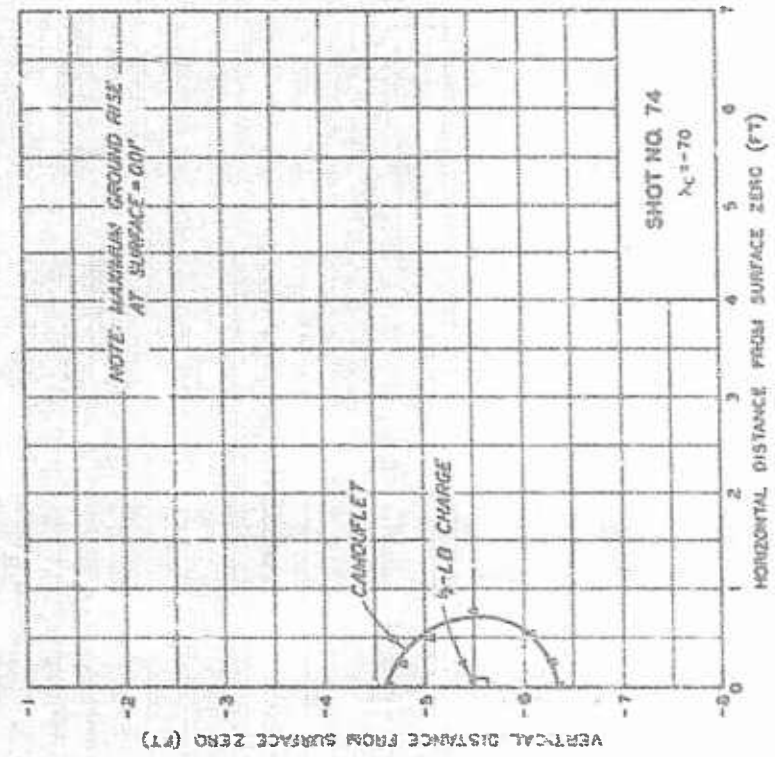
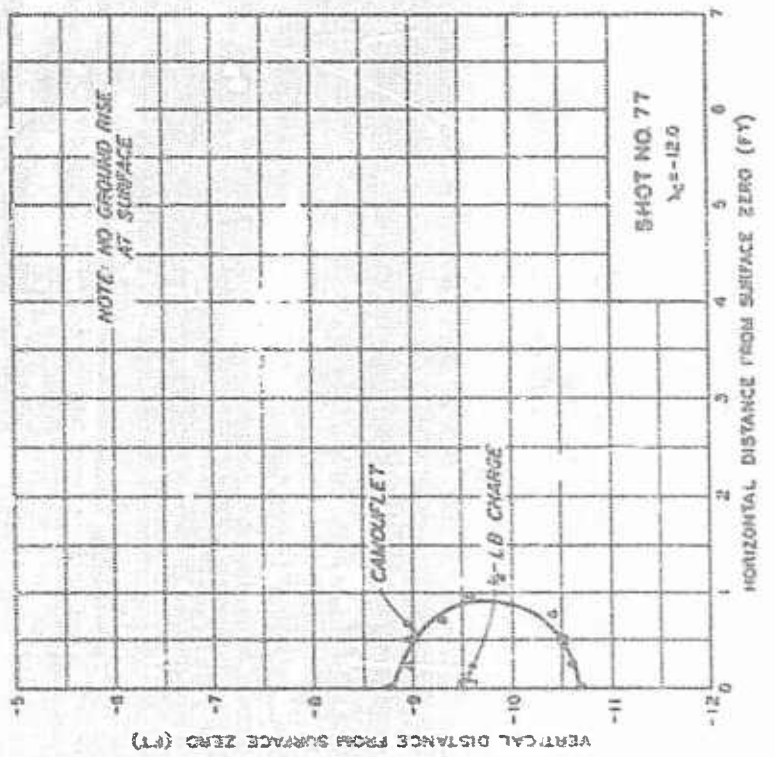
SHOT NO.	CRATER DIMENSIONS						CARTOONLET
	A	B	C	D	E	V	
70	+020.761			-373.550		11.9	33.4
71	+037.761					2.39	40.442

HALF-CRATER PROFILES
SOIL MATERIAL-CLAY
SHOTS NOS. 70 AND 71



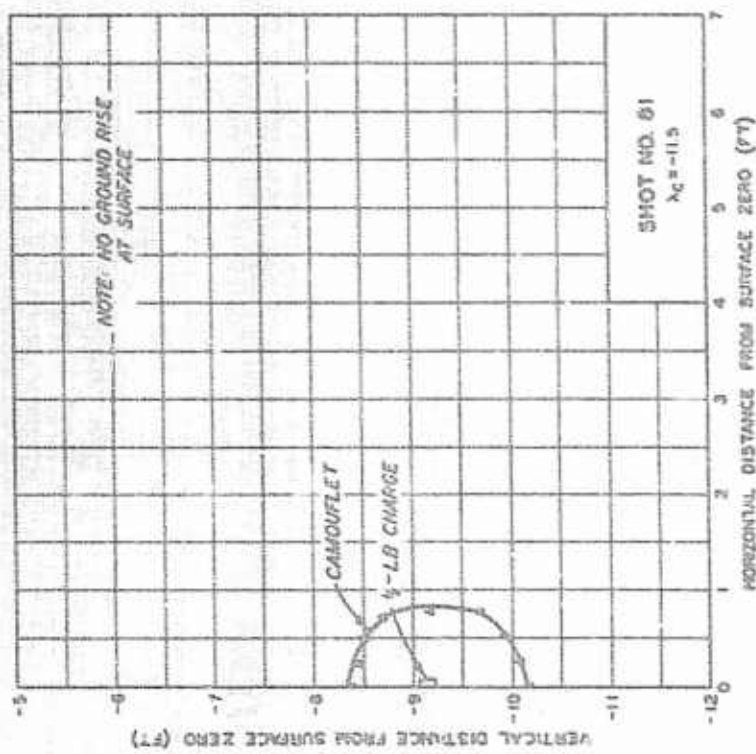
**HALF-CRATER PROFILES
SOIL MATERIAL-CLAY
SHOT NO. 72**

SHOT NO.	APPARENT CRATER				TRUE CRATER				CAMOUFLAGE			
	D	G	A	V	D	G	A	V	D	G	A	V
72	(0.5750)	(0.50)							210.230	303.587		



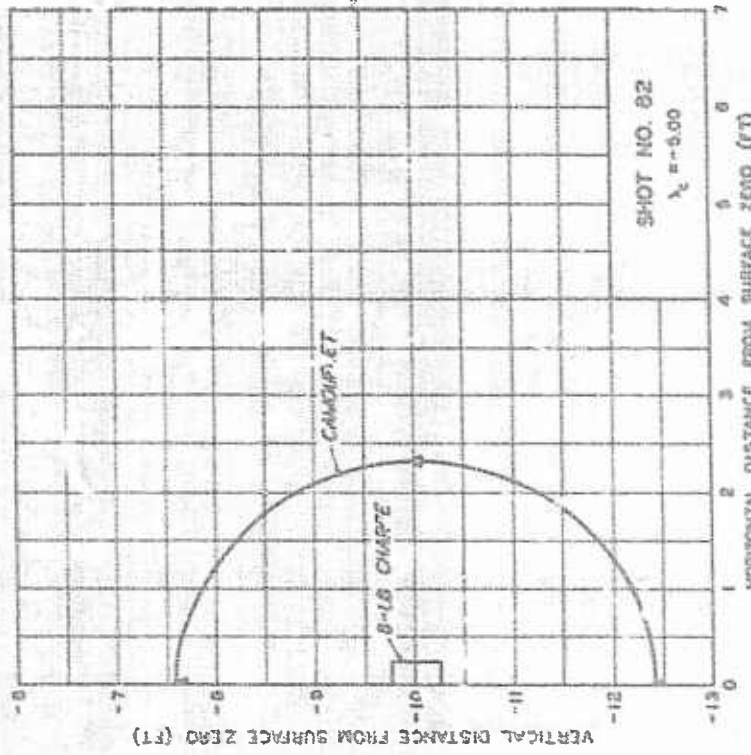
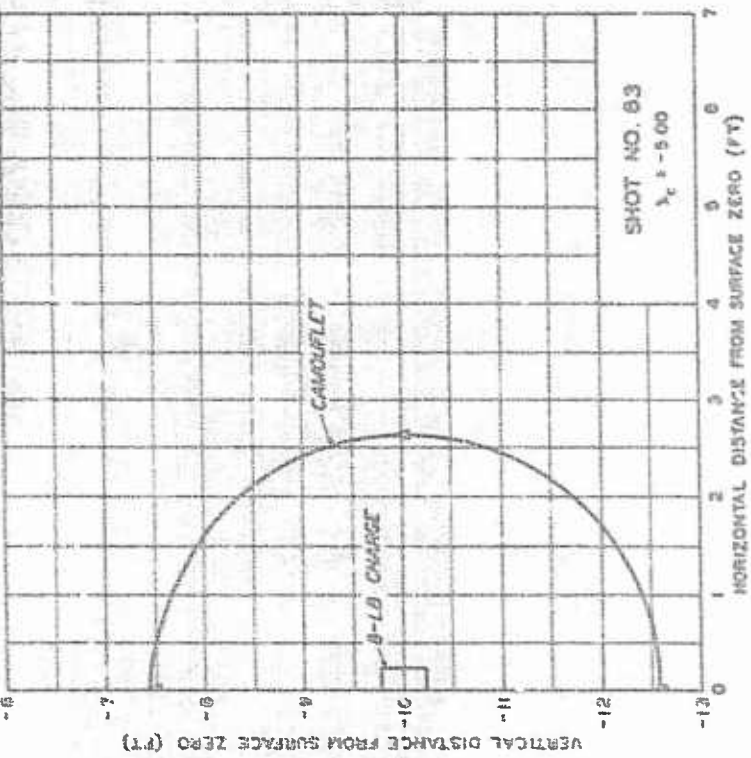
SHOT NO.	CRATER DIMENSIONS						CAMOUFLET			
	APPARENT CRATER	TRUE CRATER	J	V	A	W	D	A	V	
74	+0.01	-	-	-	-	-	1.61	1.59	1.78	1.55
77	-	-	-	-	-	-	1.51	1.50	2.05	1.54

HALF-CRATER PROFILES
SOIL MATERIAL-CLAY
SHOTS NOS. 74 AND 77



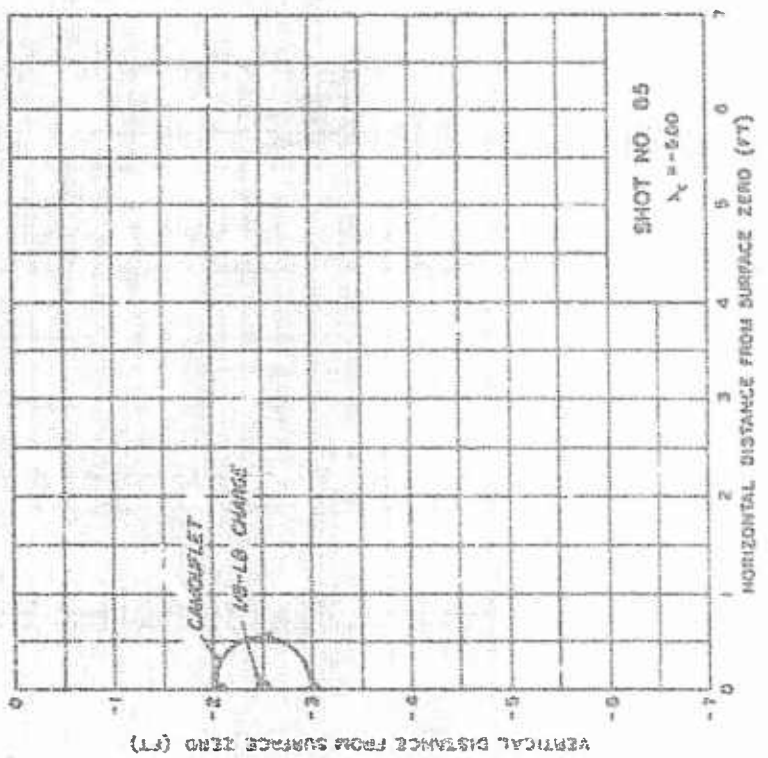
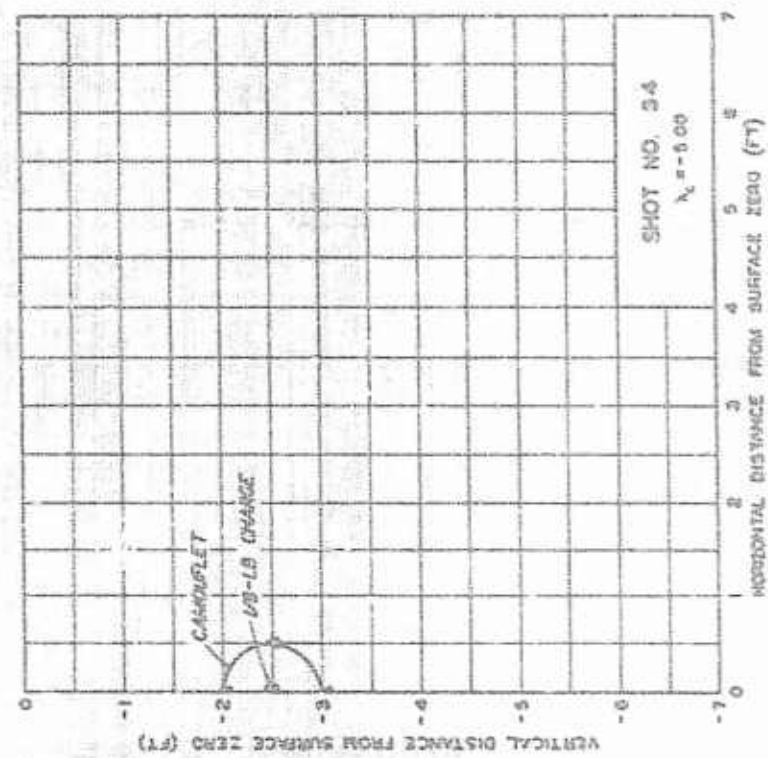
SHOT	CRATER DIMENSIONS						CAMOUFLAGE
	APPARENT CRATER	TRUE CRATER	V	d	w	h	
10	0	0	0	0	0	0	1.80
61	0	0	0	0	0	0	1.74

HALF-CRATER PROFILES
SOL MATERIAL - CLAY
SHOT NO. 61



SHOT NO.	CRATER DIMENSIONS						CRATER VOLUME	
	A APPARENT CRATER d	a h	A V	δ	=	h	A	V
82							4.04	6.01
83							5.13	9.30

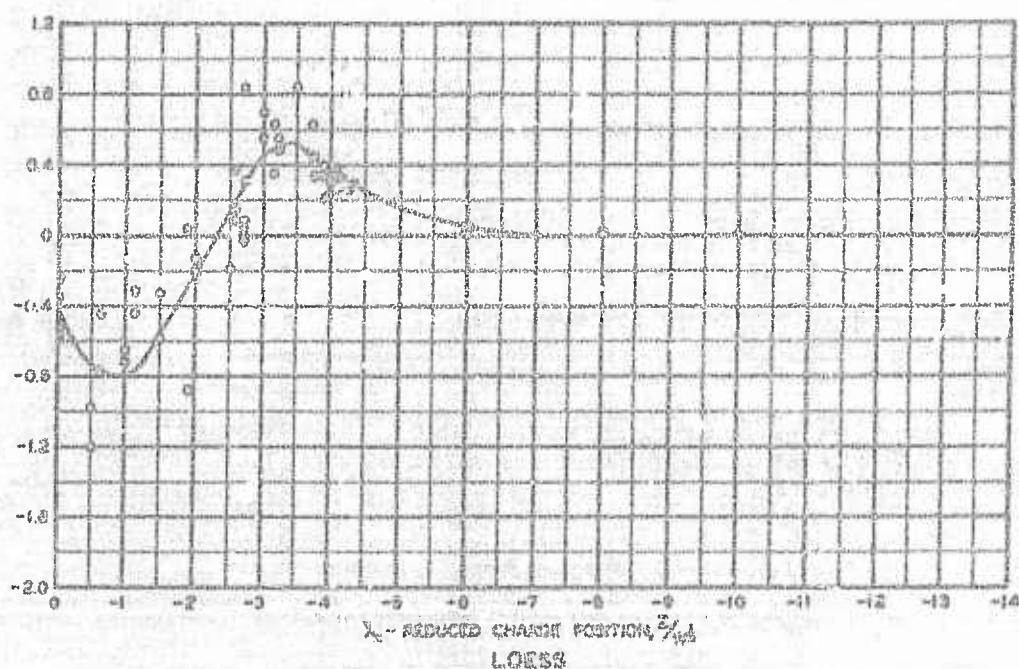
HALF-CRATER PROFILES
SOIL MATERIAL—LOESS
SHOTS NOS. 82 AND 83



SHOT NO.	CRATER DIMENSIONS						
	APPARENT CRATER	TRUE CRATER	CRATERLET				
64	4	2	1	A	V	I	W
65	4	2	1	A	V	I	W

HALF-CRATER PROFILES
SOIL MATERIAL-LOESS
SHOTS NOS. 64 AND 65

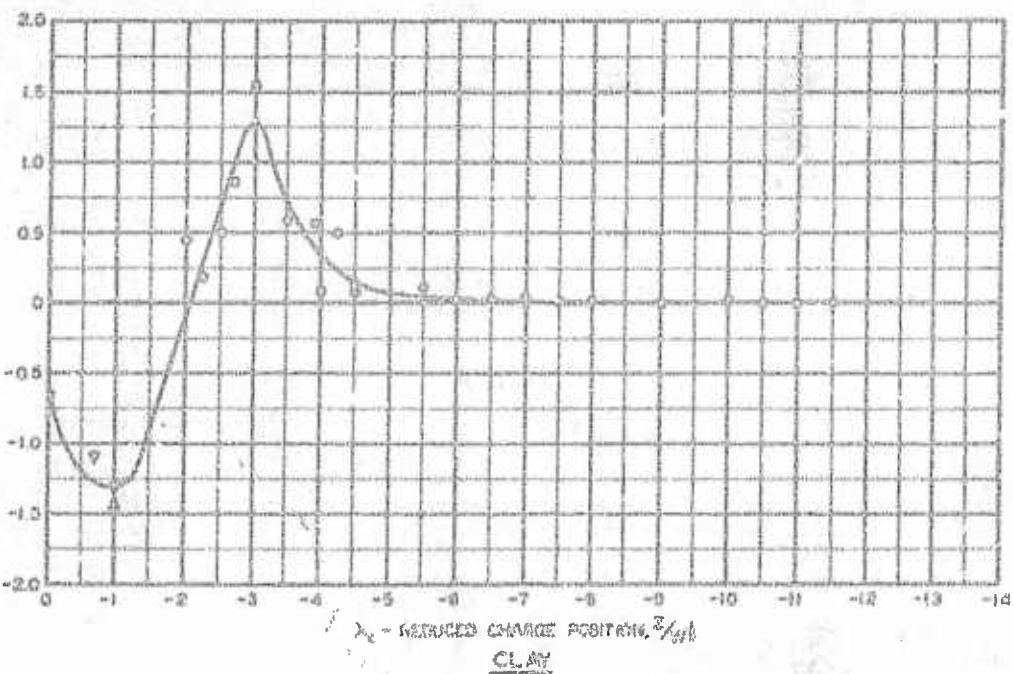
α'_e = REDUCED ADYMER CONCENTRATION, kg/m^3



λ_e = REDUCED CHARGE POSITION, kg/m^3

LOESS

α'_e = REDUCED ADYMER CONCENTRATION, kg/m^3



λ_e = REDUCED CHARGE POSITION, kg/m^3

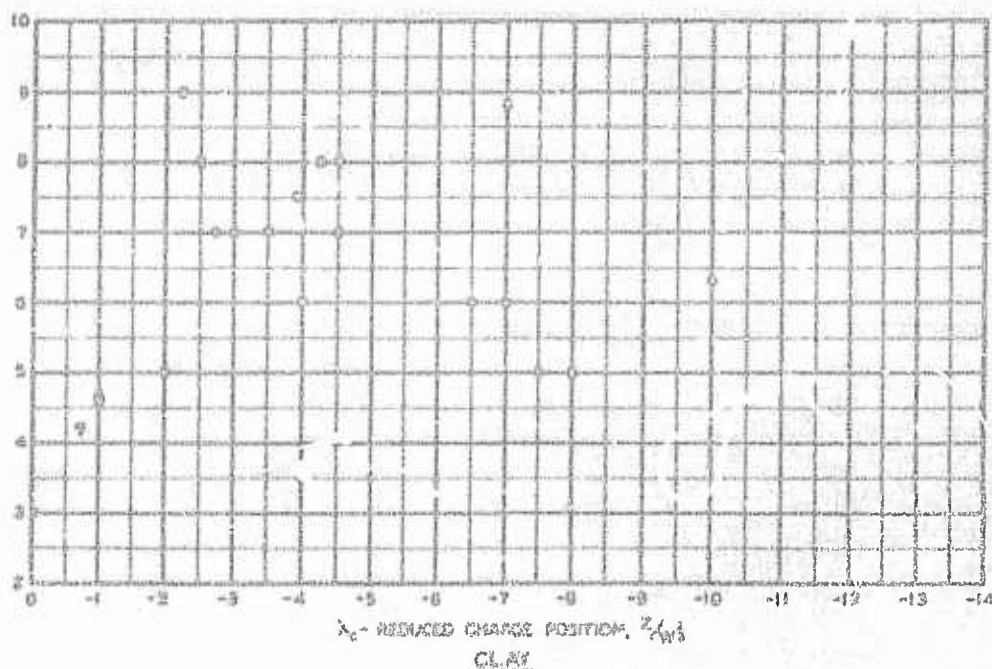
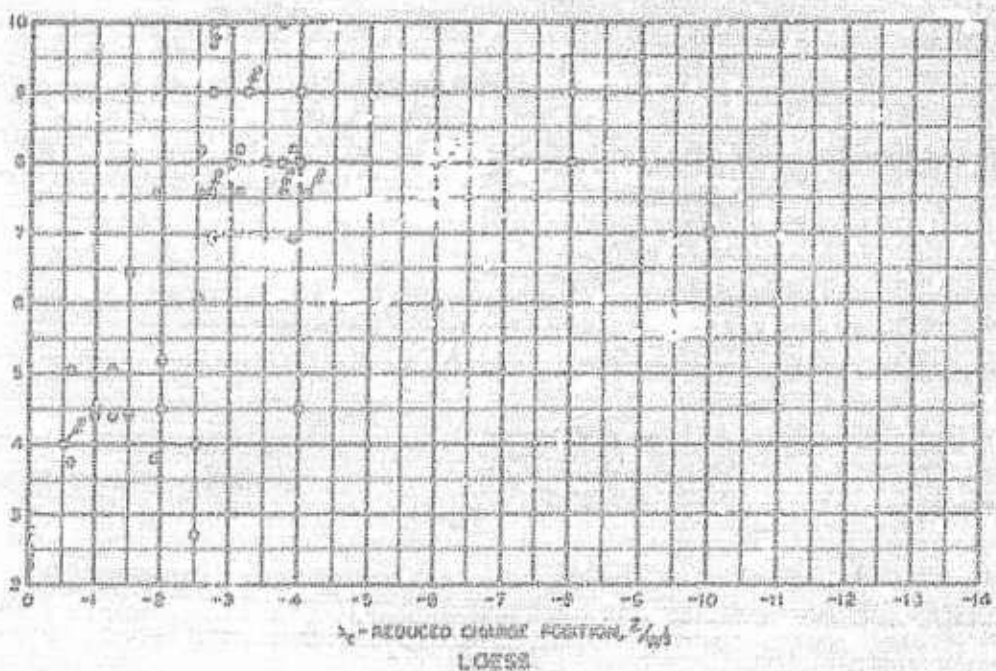
CLAY

▲ = AFBDP-828
▼ = AFBDP-1000

VARIATION OF α'_e WITH λ_e
IN LOESS AND CLAY

PLATE 42

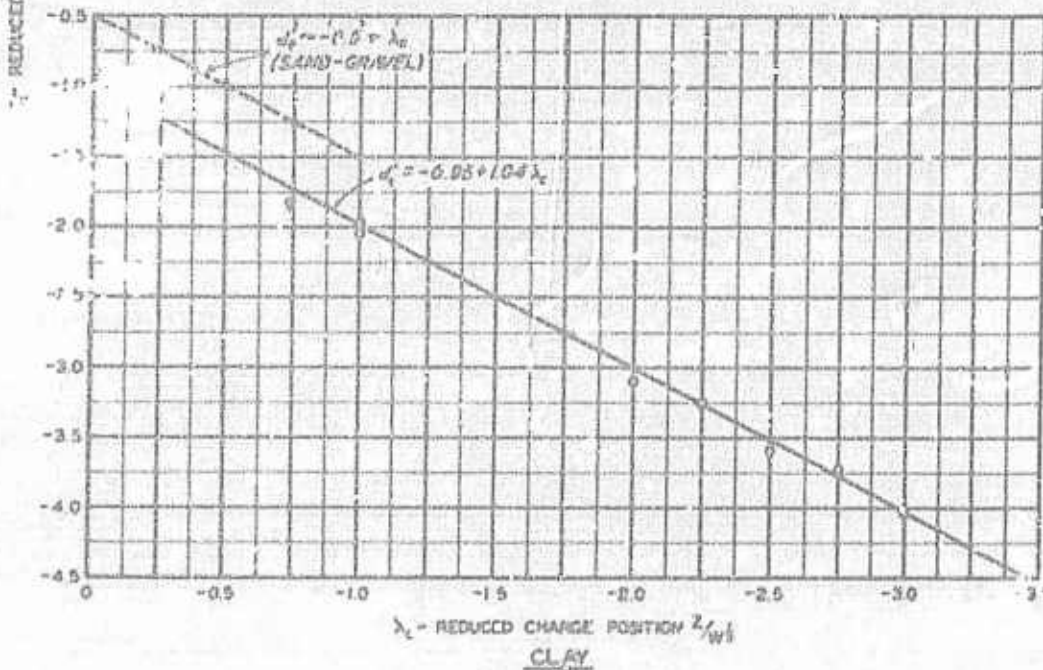
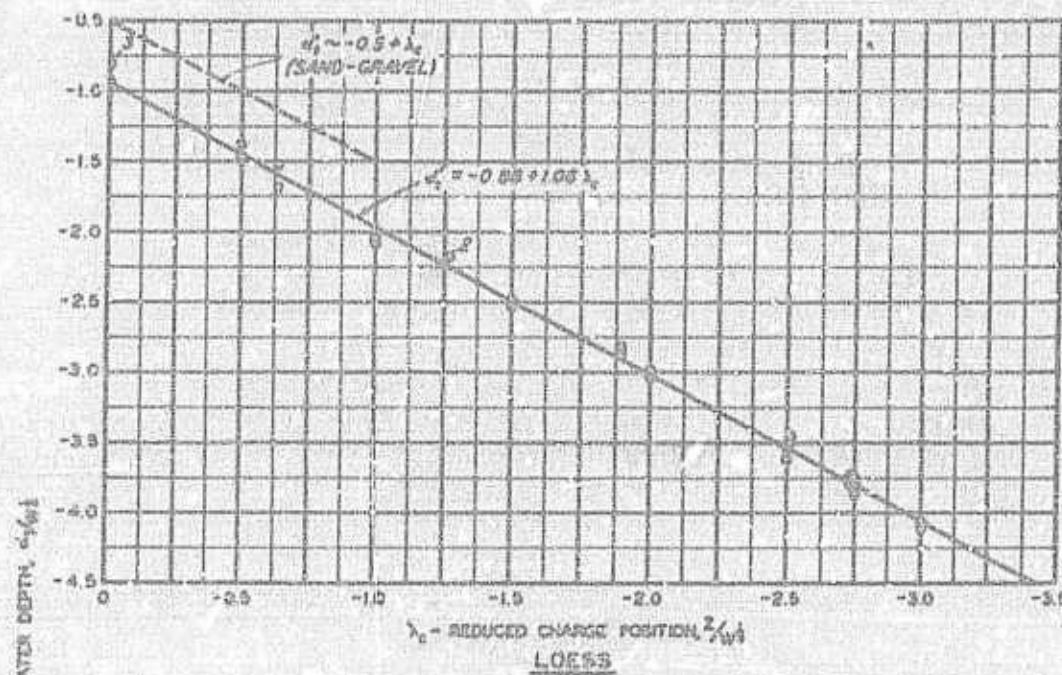
W - WINDWARD SIDE OF CREST EROSION



S - AF3WP-928
T - AF3WP-1003

VARIATION OF w_c WITH λ_c IN LOESS AND CLAY

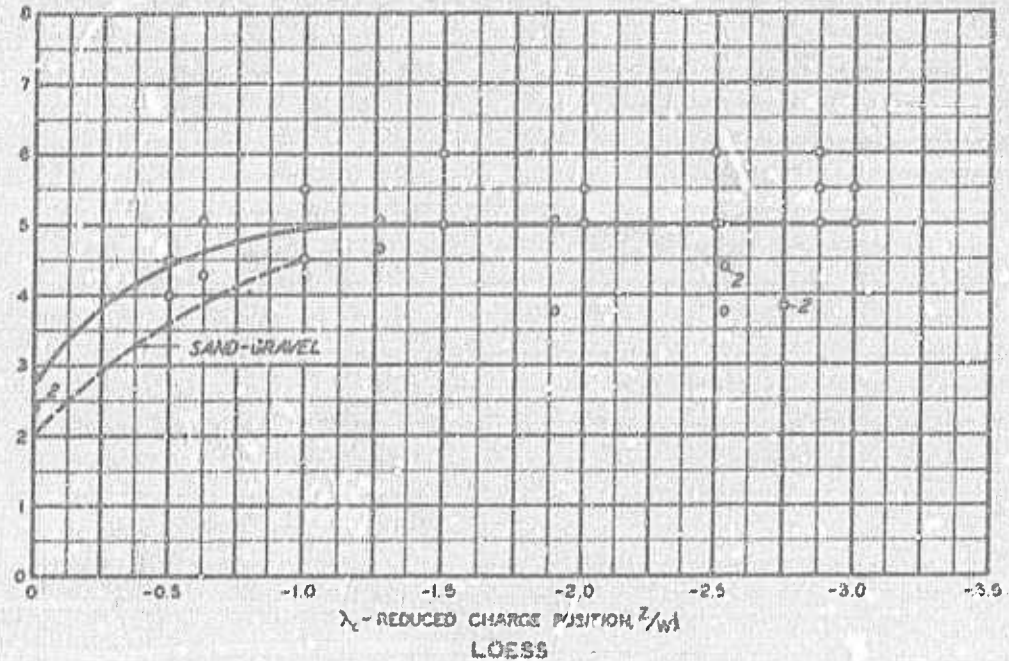
PLATE 43



Δ - A1SWP-623
 \square - A1SWP-1003
 $--$ - WT-1105

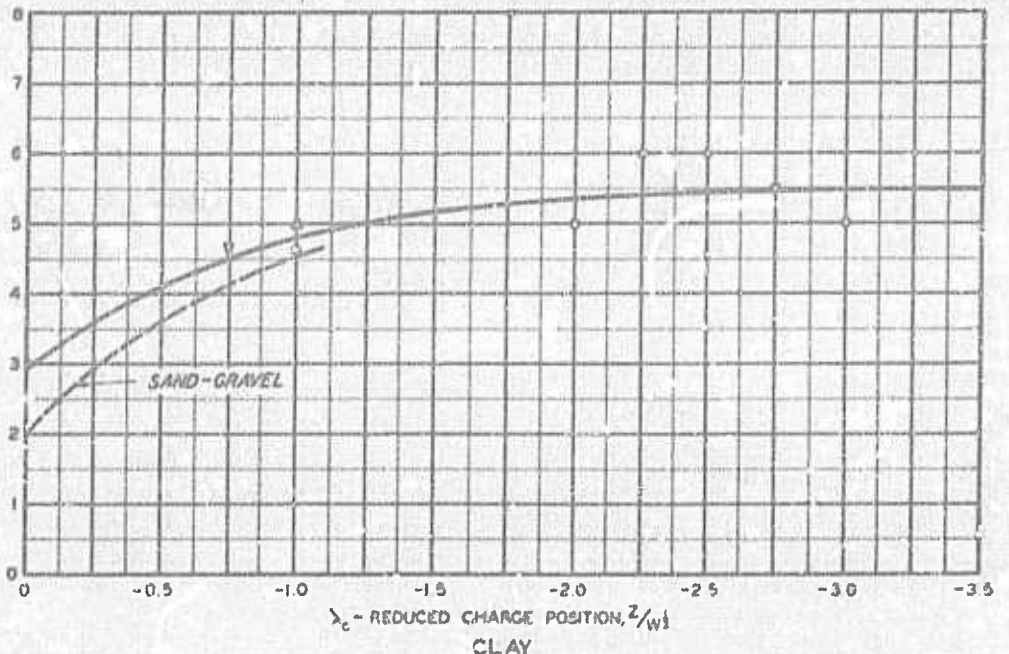
VARIATION OF d_t' WITH λ_c
IN LOESS AND CLAY

$w_t - N$ REDUCED TRUE CRATER WIDTH, $\frac{w_t}{W_t}$



λ_c - REDUCED CHARGE POSITION, Z/W_t

LOESS

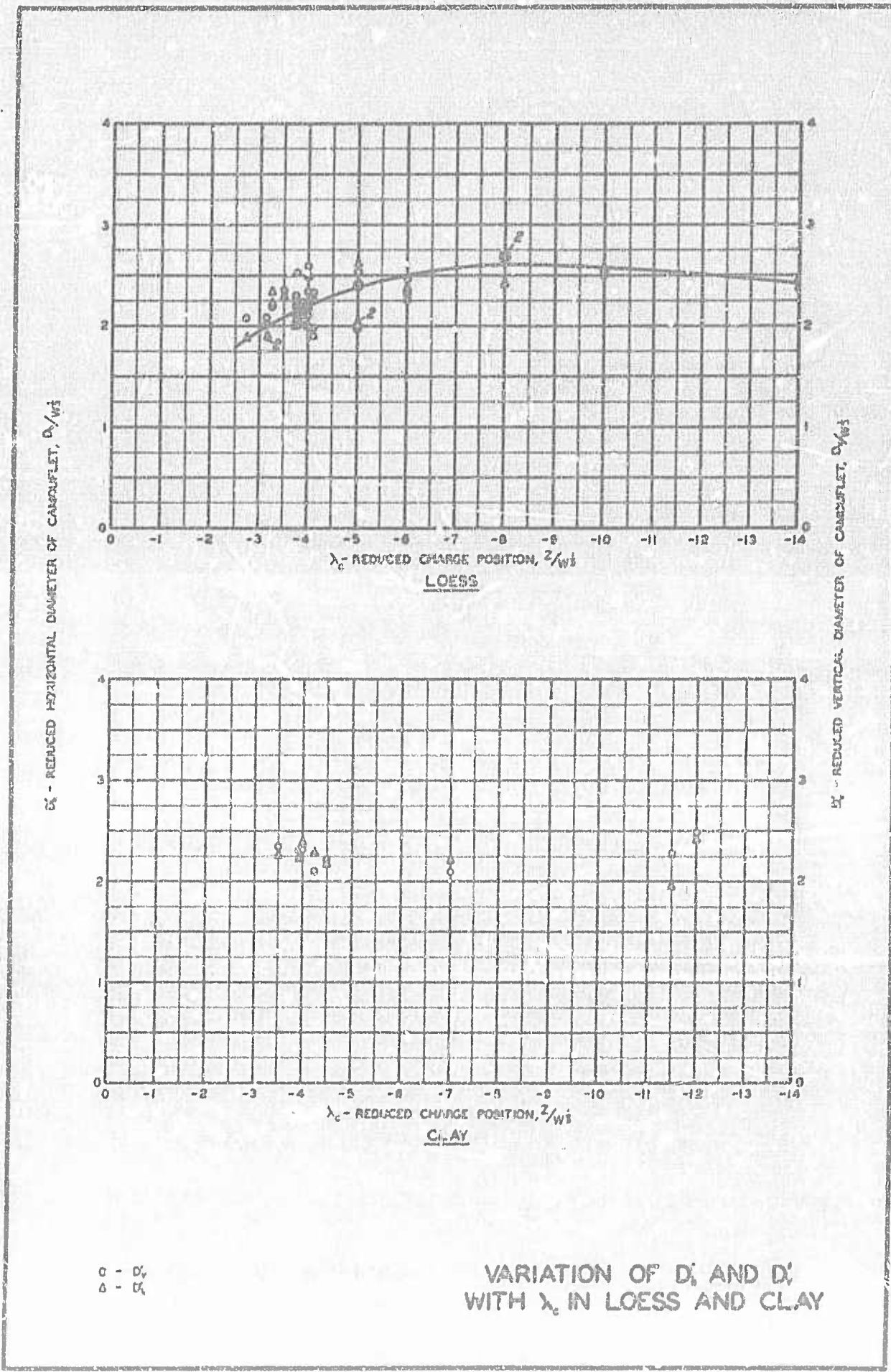


λ_c - REDUCED CHARGE POSITION, Z/W_t

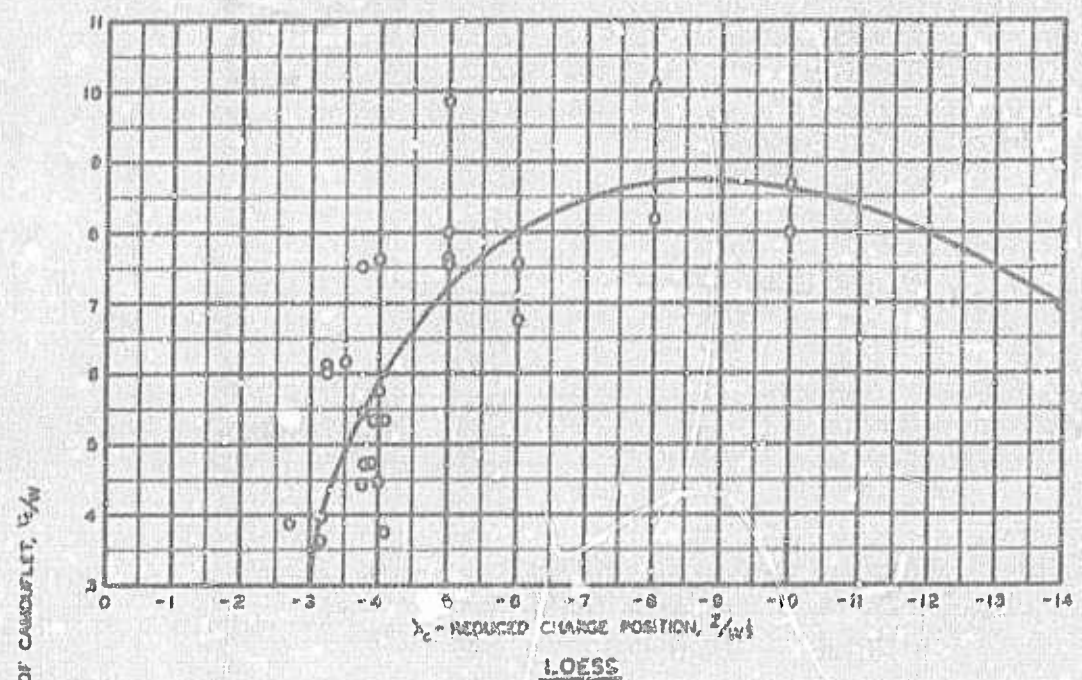
CLAY

- Δ - AFSWP-B23
- ▽ - AFSWP-1003
- - WT-1105

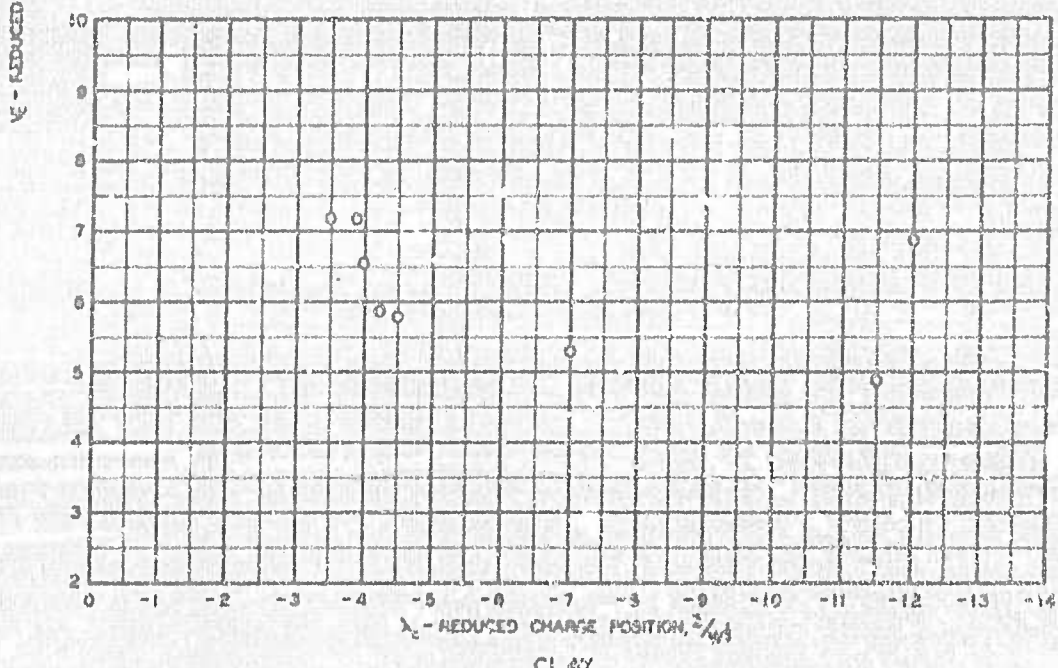
VARIATION OF w_t WITH λ_c IN LOESS AND CLAY



CONFIDENTIAL



LOESS



CLAY

VARIATION OF V' WITH x_c
IN LOESS AND CLAY

PLATE 47

CONFIDENTIAL

NOTIFICATION OF MISSING PAGES

INSTRUCTIONS: THIS FORM IS INSERTED INTO ASTIA CATALOGUED DOCUMENTS TO DENOTE
RECORDED PAGES.

DOCUMENT	CLASSIFICATION (check one)		
	UNCLASSIFIED	CONFIDENTIAL	SECRET
AD 301367		✓	
ATI			

THE PAGES, FIGURES, CHARTS, PHOTOGRAPHS, ETC., MISSING FROM THIS DOCUMENT ARE: BLANK

DO NOT REMOVE